Reliability-Based Assessment for Fender Systems

Final report master thesis

Felix Orlin

Department of Hydraulic Engineering
Faculty of Civil Engineering & Geosciences

TU Delft

Port of Rotterdam

RELIABILITY-BASED ASSESSMENT FOR FENDER SYSTEMS

A thesis submitted to the Delft University of Technology in partial fulfillment of the requirements for the degree of Master of Science in Hydraulic Engineering

by

Felix Orlin

November 2020

Felix Orlin: *Reliability-Based Assessment for Fender Systems* (2020)

The work in this thesis was made in cooperation with:

Port of Rotterdam

Chairman	Dr. ir. O. Morales Napoles (*TU Delft*)
Committees	Dr. ir. R. C. Lanzafame (*TU Delft*)
	Dr. ir. A. A. Roubos (*Port of Rotterdam*)
	Bross, E.J. (*Port of Rotterdam*)

ABSTRACT

PIANC has published several working group reports related to the design of fender systems. The work of PIANC WG33 is widely accepted by the industry and has been used to design marine structures worldwide. However, the existing design approach does not distinguish uncertainties in fender engineering, e.g. uncertainties related to vessel sizes, berthing velocities, and berthing angles. This paper aims to show how to take into account some of these uncertainties into fender design using a reliability-based approach. The influence of multiple fenders contact and multivariate dependence between vessel size, berthing velocity, and berthing angle on the failure probability of a fender system was analyzed. These correlations were modelled using a Vine-Copula, while the contribution of multiple fenders contact was investigated by performing simulation. Furthermore, the failure probability of the fender system was determined using the First Order Reliability Method and Monte Carlo simulation. The results show that uncertainty in berthing velocity, the effect of multiple fenders contact, and dependence between design variables largely influence the reliability of a fender system. It is highly recommended to incorporate all these aspects into the design approach to accomplish a cost-effective design solution. The key findings of this study can be used to update the existing design approach of fender systems and help to interpret the berthing records collected by Port Authorities.

Keywords: Fender systems, Berthing velocity, Reliability-based design, FORM, Vine-Copula

ACKNOWLEDGEMENTS

This chapter is devoted to those who have supported my study at TU Delft and also my master thesis. First of all, I would like to express my gratitude to Jesus since it is only by His grace that I can finish my master study. I would also especially thank the Indonesia Endowment Fund for Education (LPDP-RI) that has fully funded my master study. I hope I can contribute my knowledge to the development of my beloved country Indonesia. Furthermore, I would like to thank Port of Rotterdam for all the supports and the opportunity to have my final graduation project there.

Next, I would like to express my sincere thanks to all of my thesis committees: Oswaldo Morales, Robert Lanzafame, Alfred Roubos, and Erik Broos. First, I want to thank Oswaldo for being a very supportive chairman, especially for his guidance and expertise that helped me when I was working on my thesis. His office has always been open for me when I was in confusion and needed for advice. Second, I would also like to thank my daily supervisor, Robert Lanzafame, especially for his time, patience, and valuable inputs. I don't know how many e-mails I sent to him and how many meetings I had with him, asking for help and advice when encountering problems during my thesis. He always helped me to find the right solution for those problems and taught me patiently. Therefore, without his help, this thesis could not be completed.

Further, I am indebted to Alfred Roubos and Erik Bross. Alfred's feedback, inputs, and experience have been a great help for my thesis. His knowledge, especially with fender engineering and probabilistic design, was beneficial for the improvement of my thesis. Moreover, Alfred has provided all the necessary data for this thesis. Without him, this thesis will also not be completed. For Erik Broos, I still remember how he welcomed me so warmly when I first came to the Port of Rotterdam's office. As a chairman of PIANC WG211, Erik has introduced me to his networks and even invited me to participate in the PIANC group meeting, which was a gratifying experience for me. He also has always been my go-to supervisor when I needed advice, inputs, or when I had to make a difficult decision.

This 2-years of studying abroad has been very challenging for me, especially with the COVID-19 pandemic now. However, I manage to survive due to the supports and prayers of my family (especially Papa, Mama, and my sister) in Indonesia. Also, to my fellow Indonesian students in Delft who has made Delft feels like home. I will remember all the laughter and tears that we shared during these 2-years periods in the Netherlands. Also, Jessica, who has always been very supportive of me when I was stressful and tired.

I hope that this thesis could contribute academically and industrially. Finally, I would like to say that I am truly grateful for this journey.

Delft, November 2020

Felix Orlin

CONTENTS

LIST OF FIGURES

LIST OF TABLES

NOMENCLATURE

α	Berthing angle	$[^o]$
α	Sensitivity factor	[-]
β	Reliability Level	[-]
β_t	Reliability target indices	[-]
γ	Importance factor	[-]
$\gamma_{E_{Fender}}$	Partial safety factor of fender absorption capacity	[-]
γ_{E_k}	Partial safety factor of kinetic energy	[-]
γ_F	Partial safety factor of reaction force	[-]
AF	Angular factor	[-]
B	Beam of vessel	$[m]$
C_{ab}	Abnormal berthing coefficient	[-]
C_b	Block coefficient	[-]
C_c	Berth configuration coefficient	[-]
C_e	Eccentricity coefficient	[-]
C_i	Investment cost	[€]
C_m	Virtual mass coefficient	[-]
C_R	Capitalized risk cost	[€]
C_s	Softness coefficient	[-]
C_{tot}	Total cost	[€]
D	Draft of the vessel	$[m]$
E_{cv}	Rated energy capacity	$[kN \cdot m]$
$E_{F;d}$	Design value of reaction force	$[kN \cdot m]$
$E_{F;kar}$	Characteristic value of reaction force	$[kN \cdot m]$
$E_{Fender;d}$	Design value of fender capacity	$[kN \cdot m]$
$E_{Fender;kar}$	Characteristic value of fender capacity	$[kN \cdot m]$
E_{Fender}	Fender energy absorption (capacity)	$[kN \cdot m]$
$E_{k;d}$	Design value of kinetic energy	$[kN \cdot m]$
$E_{k;kar}$	Characteristic value of kinetic energy	$[kN \cdot m]$
E_k	Kinetic energy (load)	$[kN \cdot m]$
F	Reaction force	$[kN]$
F_d	Design reaction force	$[kN]$
F_{kar}	Characteristic reaction force	$[kN]$

K	Radius of gyration of the vessel	$[m]$
K_c	Keel under clearance	$[m]$
L_{oa}	Length overall	$[m]$
L_{pp}	Length between perpendiculars	$[m]$
M	Displacement mass of a vessel	$[ton]$
MF	Manufacturing tolerance	[-]
$n_{multiple}$	Energy multiplication factor	[-]
r	Interest rate	[%]
R_B	Bow radius	$[m]$
R_{cv}	Rated reaction force	$[kN]$
TF	Temperature factor	[-]
v	Berthing approach velocity	$[m/s]$
VF	Velocity factor	[-]
U-space	Standard normal space	[-]
X-space	Physical space	[-]

1 INTRODUCTION

This chapter discusses the background, the objectives, and also the general outline of the thesis.

1.1 BACKGROUND

Marine structures such as quay walls, flexible dolphins, and jetties are often equipped with fenders (Figure 1.1) to avoid damage to vessels and the berthing facility. The primary function of a fender is to absorb the kinetic energy induced by vessels during berthing or mooring operations. When fenders are not able to absorb this energy, financial losses for a terminal or port might occur. Consequently, it is crucial to ensure that fenders are sufficiently reliable. Engineers usually select an appropriate fender size based on design codes and guidelines. One of the most recognized and widely used guidelines for fender design is the work of PIANC WG33 entitled 'Guidelines for the Design of Fender Systems,' which was published in 2002. This guideline recommends applying an abnormal berthing factor (C_{ab}), which could be seen as a global safety factor, to the normal berthing energy to select a suitable fender.

Figure 1.1: Fender Structures Trelleborg [2018]

However, recent studies argue that the existing design method for fenders can be improved. Firstly, the derivation of the abnormal berthing factor (C_{ab}) is fairly unclear, leading to an imprecise reliability level of fenders Iversen et al. [2019]. Secondly, the input values suggested for fender design often differ significantly from field observations. For instance, field measurements in several ports show that the measured berthing velocities do not always align with fender design guidelines and that the actual berthing angles of large sea-going container vessels are generally much lower (Yamase et al. [2010]; Hein [2014]; Roubos et al. [2018]). Lastly, the existing design approach does not clearly distinguish uncertainties in fender engineering, e.g., uncertainties related to berthing frequency, vessel sizes, berthing velocities, and berthing angles. Consequently, the members of PIANC WG211 sug-

gested performing a reliability-based study to verify and improve the existing design approach.

Although the application of the reliability-based design approach has started becoming more prevalent nowadays, it is not implemented in the existing design approach. Since 2002, some studies have been conducted regarding the reliability of fender systems to verify the failure probability of a fender system and to determine factors that influence fender reliability. Among them are studies performed by Ueda et al. [2003], Yamase et al. [2010], and Versteegt [2013]. However, these studies often assume that vessel sizes, berthing velocities, and berthing angles are uncorrelated and that a single fender absorbs all kinetic energy.

In reality, dependency may exist between vessel size and other design variables such as berthing velocity and berthing angle. For instance, larger vessels might perform a more controlled maneuver and tend to have a lower berthing speed and berthing angle than smaller vessels. Roubos et al. [2016] studied the factors that influence berthing velocity. Based on the measurement data collected in the Port of Rotterdam and Bremerhaven, this study examined the correlation between berthing velocity and other variables such as vessels' dimensions, environmental factors, berthing policy, and type of fender system. This study shows that the vessels' size generally does not have a strong negative correlation with berthing velocity as what has been historically assumed by Brolsma et al. [1977]. However, the absence of a strong correlation does not always imply independence. It might be the case that random variables that appear to exhibit no correlation have a non-linear dependency or only show correlation during extreme events, which could not be captured by the linear correlation coefficient.

Also, when multiple fenders are installed on a marine structure, it is unlikely that vessels will contact only one fender during normal berthing conditions. Single fender contact usually only occurs in the event of a reasonably high berthing angle. Depending on their size, berthing angle, and fender spacing, vessels may contact several fenders during berthing. If this happens, each fender's respective deflection will determine the total berthing energy absorbed by the fender system. The fender system can then absorb higher kinetic energy than that of a single fender contact, thus increasing its reliability. Nevertheless, despite its importance, the underlying theory and calculation method of multiple fender contact is still limited. As a result, no studies on the probabilistic design of a fender system have yet taken into account this factor.

Furthermore, the importance of the design variables was also of interest to this thesis. This information is valuable since it can help us to allocate more resources to focus on the critical variables. The studies of Ueda et al. [2003] and Versteegt [2013] show that the uncertainty of berthing velocity has the most substantial contribution to the failure of a fender system. The question, however, arises, "Is the velocity still the most dominant variable when a vessel contacts multiple fenders simultaneously?". In that case, other variables might become more critical. For instance, the influence of vessels' size and berthing angle is critical in the event of multiple fender contact as they determine the number of fenders activated during berthing impact.

This study aims to determine the reliability level of fender systems taking into account the influence of dependence between design variables and multiple fender contact. The results of this reliability-based assessment will be used to determine partial factors of safety to be implemented in fender engineering and to reach a cost-effective fender size.

1.2 OBJECTIVES AND RESEARCH QUESTIONS

1.2.1 Objectives

Based on the knowledge gaps presented in the previous section, the objectives of this thesis are formulated which are shown below:

1. Define the reliability level (β) and probability of failure of fender system designed using older PIANC standard taking into account the effect of multiple fender contact and dependence between variables.
   a) Investigate and model the dependency between each of the variables
   b) Investigate how the effect of multiple fender contact could be integrated into the limit state function
   c) Perform reliability analysis for the fender system while taking into account the effect of dependent variables and multiple fender contact
   d) Assess what effects both factors have on the reliability level of the fender system
2. Determine which variable has the most influence on the failure of a fender system.
   a) Derive the sensitivity factor (α) to find dominant variables from the Probabilistic level II analysis using FORM.
   b) Assess the effect of dependency and multiple fender contact on the sensitivity factors
3. Calculate the partial safety factors (γ) for the load, resistance, and reaction force.
   a) Based on the design points obtained from level II analysis, derive the partial safety factor for kinetic energy, fender performance and reaction force
4. Evaluate the target reliability levels for the design of new fenders according to the reliability framework on EN1990 by means of economic optimization.
   a) Using Cost Benefit Analysis to find the optimum target reliability levels of fender system considering the consequences caused by the failure of fender system and also the investment cost of fender system.

1.2.2 Research Questions

The main research question of this thesis is:

"How can the existing fender design approach be improved using the reliability-based design approach and what aspects need to be considered?"

The main research question then could be divided into the following sub-questions:

1. What are the reliability levels of the fender systems designed using the current PIANC fender design guidelines?
2. Do those fender designs meet the reliability targets proposed by PIANC WG211?
3. How could the dependence between the load variables be modelled?
4. What influence does the dependence have on the reliability of a fender system?

5. How could the influence of multiple fender contact be included in the limit-state function?
6. How significant is the influence of the multiple fender contact on the reliability of a fender system?
7. Which random variable has the most dominant influence on the failure of a fender system?
8. What is the optimum reliability target (β_t) for a fender system?
9. What are the appropriate partial safety factors for the kinetic energy, fender capacity, and reaction force?

1.3 THESIS OUTLINE

This thesis comprises 7 chapters which are organized as follows:

- Chapter 1: Introduction
- Chapter 2: Theoretical Framework
- Chapter 3: Deterministic Method
- Chapter 4: Reliability-based Assessment
- Chapter 5: Derivation of Partial Safety Factor
- Chapter 6: Optimum Reliability Index
- Chapter 7: Conclusion and Recommendation

The first chapter highlights the current knowledge gaps in the field of fender engineering and also how this thesis can address those gaps. The second chapter elaborates all relevant theories of the methods used for the analysis in this thesis. In the third chapter, fender designs were made for a container berth in Port of Rotterdam using the deterministic method implemented in the existing PIANC guidelines. The reliability of the fender designs was then assessed using Monte Carlo simulation and the First Order Reliability Method in Chapter 4. Chapter 5 shows how partial safety factors could be derived using the results of the reliability-based assessment. The optimum reliability index for a fender system was derived in Chapter 6 based on cost-benefit analysis. Finally, the last chapter (Chapter 7) concludes the main findings of this thesis. Furthermore, recommendations are given for future research related to the fender design.

2 THEORETICAL FRAMEWORK

This chapter presents an overview of the underlying theory of the methods used in this thesis. The first section starts with the basics of the fender design, including how to calculate berthing energy and what factors influence the performance of a fender. The chapter then continues with the basic theory of statistical inference, where the readers can find an explanation about the basic concept of the maximum likelihood estimation and goodness-of-fit tests. Section 3, 4, and 5 of this chapter addresses the concept of dependence, Copula, and Vine-copula, respectively. The fundamental of the probabilistic-based design, including the concept of partial safety factor (level I), First Order Reliability Method (level II), and Monte Carlo (level III) are presented in section 6. Finally, the last section presents the concept of economic optimization, which is often used to find the optimum reliability indices of a structure.

2.1 FENDER SYSTEM

2.1.1 Berthing Energy

As a vessel approaches a marine structure, it possesses kinetic energy whose magnitude is proportional to its mass and the square of its berthing velocity. This kinetic energy is basically the load acting on a fender system. During the berthing impact (Figure 2.1), a massive mass of a vessel will cause deformation to the fenders. Through this deformation, the kinetic energy is then absorbed by the fenders.

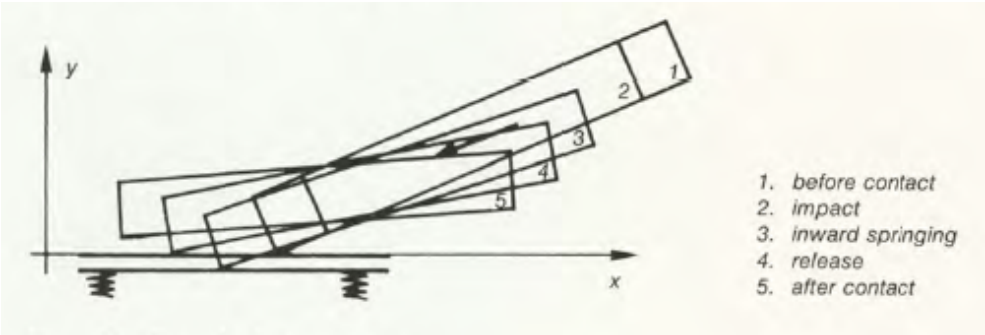

Figure 2.1: Illustration of a vessel berthing process Vrijburcht [1991]

In the case of rigid dolphins as shown in Figure 2.2, the deflection of the fenders absorbs most of the kinetic energy. Whereas, in the case of flexible dolphins, the deformation of the piles will also contribute to absorbing the energy. A fender system is considered safe when its absorption capacity is higher than the kinetic energy working on it.

The amount of kinetic energy acting on the fenders is influenced by some factors, such as initial contact position between the vessel and the fenders, and the move-

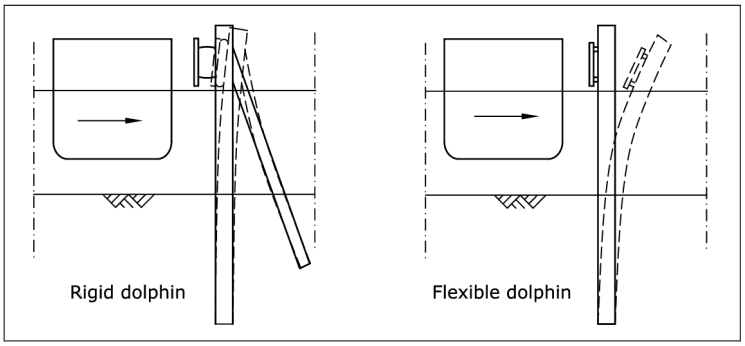

Figure 2.2: Illustration of flexible and rigid dolphin (E Bruijns, 2005)

ment of water around the vessel during the berthing process. PIANC [2002] gives the following simplified formula to compute the actual kinetic energy:

$$E_k = \frac{1}{2} * M * v^2 * C_e * C_m * C_s * C_c \tag{2.1}$$

where:

E_k = Berthing kinetic energy (kNm)
M = Displacement of water caused by the mass of a vessel (ton)
v = Berthing approach velocity (m/s)
C_e = Eccentricity coefficient
C_m = Virtual mass coefficient
C_s = Softness coefficient
C_c = Berth configuration coefficient

Furthermore, PIANC [2002] guideline also introduces what is known as an abnormal berthing coefficient (C_{ab}). This coefficient is used to take into account the unfavourable deviation of the kinetic energy, which might be caused by mishandling, malfunction, or extreme weather condition. It could also be seen as a global safety factor assigned directly to the computed normal kinetic energy (Equation 2.1). The abnormal berthing energy E_{ab} is computed as:

$$E_{ab} = E_k * C_{ab} \tag{2.2}$$

Table 2.1 presents the abnormal berthing coefficients for different types and sizes of vessels recommended by PIANC [2002]. The table suggests higher safety factors for smaller vessels.

Table 2.1: Abnormal berthing coefficient recommended by PIANC (2002)

Type of vessels	Size	C_{ab}
Tanker and Bulk Cargo	Largest	1.25
	Smallest	1.75
Container	Largest	1.50
	Smallest	2.00
General Cargo	-	1.75
Ro-Ro and Ferries	-	2.00 or higher
Tugs, Work, Boats	-	2.00

The variables and coefficients associated with Equation 2.1 are elaborated below. Furthermore, the dimensions of the container vessels used in this thesis are presented in Appendix D.

Displacement (M)

The mass of a vessel is equivalent to the mass of the water displaced by its hull when loaded to the stated draft. In most cases, the vessel's fully loaded displacement is used to compute kinetic energy PIANC [2002].

$$M = C_B * L_{PP} * D * B * \rho_{sw} \tag{2.3}$$

where:

C_B = Block coefficient
L_{PP} = Length between perpendiculars (m)
D = Vessel draught (m)
B = Beam of vessel (m), distance between hulls
ρ_{sw} = Sea water density (kg/m^3)

In this thesis, the maximum displacement of a vessel and its associated dimensions are based on the PIANC's report from working group 121 "Harbor approach channels design guidelines (2014)". The report contains very useful tables with design information on vessels and considered as the latest available design information Trelleborg [2018].

Berthing velocity (v)

Ueda et al. [2003] defined the berthing velocity as the speed just before a vessel touches the fender with the speed element perpendicular to the face line of mooring facility. The berthing velocity of a vessel depends on several factors such as the weather condition during berthing, size of the vessel, and berthing location. Consequently, it is necessary to use the berthing record data to derive design velocity when designing a fender. However, such data is often unavailable. PIANC guideline, therefore, suggests using the design berthing velocity derived by Brolsma et al. [1977] (Figure 2.3) when no berthing records are available. Brolsma, in his paper, recommended design berthing velocities for different navigation conditions and vessel sizes. Roubos et al. [2016] later found that the values recommended by Brolsma were the berthing velocity with an exceedance probability of 5% in a reference period of 30 years.

Eccentricity coefficient (C_e)

If the ship's velocity vector does not pass through the point of contact with the fender then the ship will rotate about its point of contact. This will allow some dissipation of the kinetic energy which is taken into account into the calculation by the presence of C_e. The eccentricity coefficient is largely influenced by the berthing angle, point of contact and also how the vessel approach the fender. For container vessels, there are usually two cases of berthing. The first one is side berthing where velocity vector is approximately perpendicular to berthing line and the ship is parallel or at a small angle to the berthing line. The second case is mid-ship berthing where the centre of gravity of the vessel is align with the point of contact with fender. The difference is illustrated in Figure 2.4.

According to Trelleborg [2018], the eccentricity coefficient can be calculated using the formula below:

$$C_e = \frac{K^2 + K^2 * cos^2\phi}{K^2 + R^2} \tag{2.4}$$

$$K = (0.19 * C_B + 0.11) * L_{PP} \tag{2.5}$$

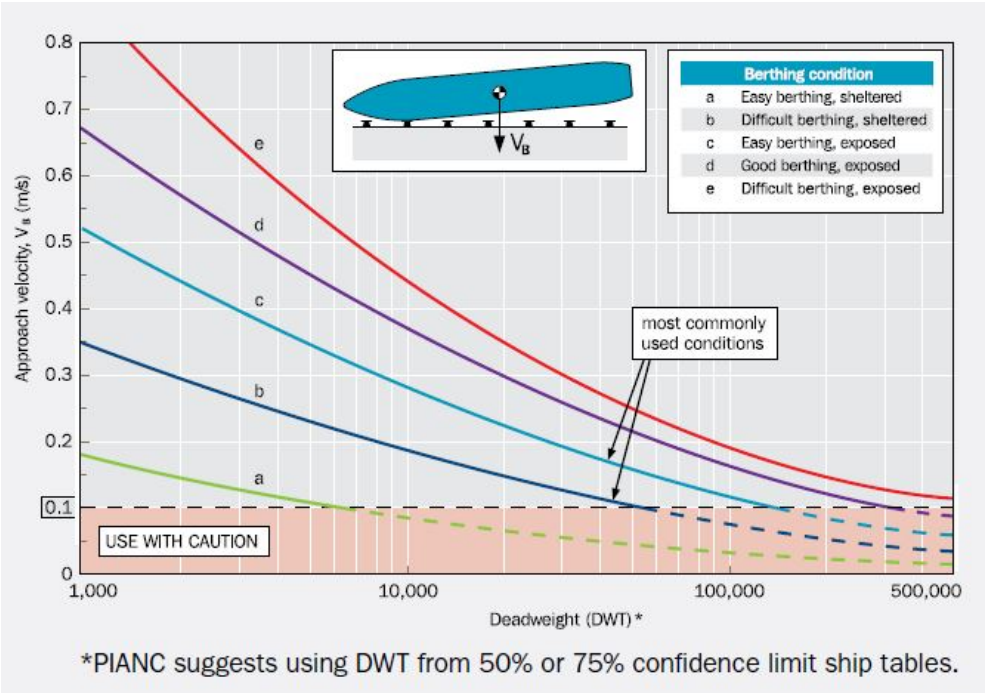

Figure 2.3: Brolsma velocity curve Trelleborg [2018]

$$R = \sqrt{(\frac{L_{PP}}{2} - x)^2 + (\frac{B}{2})^2} \tag{2.6}$$

$$\phi = 90 - \alpha - asin(\frac{B}{2R}) \tag{2.7}$$

where:

K = radius of gyration of the vessel (depending on block coefficient) (m)
R = distance of point of contact to the center of the mass (m)
ϕ = angle between velocity vector and the line between the point of contact
= and the center of mass (degree)
x = Distance from bow to the point of contact with fender (m)

While x depends on how pilots choose to berth their vessels. The common berthing cases are:

- Quarter-point berthing
  $x = L_{PP}/4 \longrightarrow C_E = 0.4 - 0.6$
- Third-point berthing
  $x = L_{PP}/3 \longrightarrow C_E = 0.6 - 0.8$
- Midships berthing
  $x = L_{PP}/2 \longrightarrow C_E = 1$

Figure 2.5 illustrates the geometric of a vessel and fenders during berthing process and gives a clear explanation on how to use the formulas that are given above.

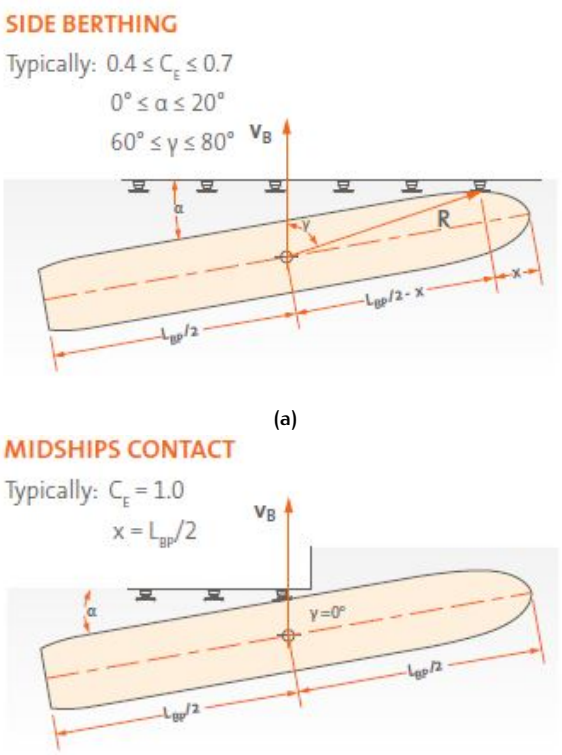

Figure 2.4: Berthing type (a) Side berthing (b) Mid-ship berthing Shibata [2017]

Virtual Mass Coefficient (C_m)

As the body of vessel approaches the berthing structure, a body of water carried along with the vessel as it moves sideways through the water and as the ship is stopped by the fender, the entrained water continues to push against the ships increasing the overall mass of the ships. This factor is taken into account by the coefficient of virtual mass (C_m). There are 3 widely used method to determine the added mass coefficient which are PIANC 2002, Shigeru Ueda (1981) and Vasco Costa (1964).

The three formulas are presented in Table 2.2. In this thesis, the formula by PIANC(2002) will be used for the analysis. The Vasco Costa method is only valid where $V_B \geq 0.08m/s$ and $K_c \geq 0.1D$.

Table 2.2: Virtual mass coefficient

PIANC (2002)		Shigeru Ueda (1981)	Vasco Costa (1964)
for $\frac{K_c}{D} \leq 0.1$	$C_m = 1.8$	$C_M = 1 + \frac{\pi * D}{2 * C_B * B}$	$C_M = 1 + \frac{2 * D}{B}$
for $0.1 \leq \frac{K_c}{D} \leq 0.5$	$C_m = 1.875 - 0.75\frac{K_c}{D}$		
for $\frac{K_c}{D} \geq 0.5$	$C_m = 1.5$		

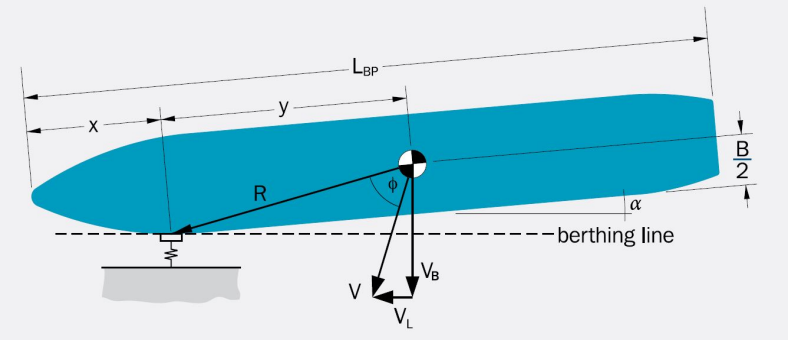

Figure 2.5: Illustration of fenders and vessel geometric Trelleborg [2018]

Softness coefficient (C_s)

If fender is harder than the vessel's hull, part of the kinetic energy will be absorbed by the elastic deformation of the hull and thus, a softness coefficient C_s is used to take into account this reduction. The recommended value for this coefficient usually is 0.9 and 1 for hard fender and soft fender, respectively PIANC [2002]. The British Standard Code of Practice for Maritime Structures (BS 6349) defines hard fenders as fenders where the designed deformation is less or equal to 150 mm while soft fenders are fenders with a deformation larger than 150 mm.

Table 2.3: Softness coefficient Trelleborg [2018]

$C_s = 1$	Soft fenders ($\delta_F > 150$mm)
$C_s = 0.9$	Hard fenders ($\delta_F \leq 150$mm)

Berth configuration coefficient (C_c)

The berth configuration coefficient is the coefficient that takes into account the cushion effect of water between hull and quay structure that contributes to the dissipation of berthing energy absorbed by fender system. This coefficient depends on some factors such as the design of quay wall, under keel clearance, velocity and angle of approach and also the shape of the vessel hull.The difference between closed and open berth configuration could be seen in Figure 2.6. PIANC [2002] recommends the following values for the coefficient:

Table 2.4: Berth Configuration Coefficient

$C_c = 1$	- Open structures including berth corners - Berthing angle $> 5^o$ - Very low berthing velocities - Large under keel clearance
$C_c = 0.9$	Solid quay walls under parallel approach (berthing angle $< 5^o$) and under keel clearance less than 15% of the vessel draught

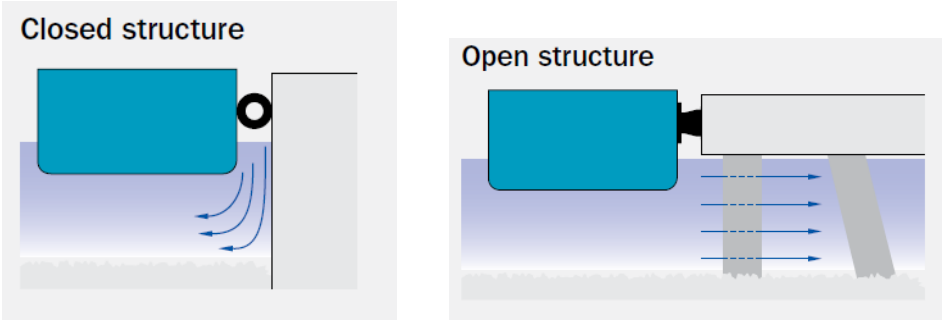

Figure 2.6: (a) Closed structure (b) Open structure Trelleborg [2018]

2.1.2 Reaction Force

Fenders generate reaction force during the compression process. This reaction force will act as a load to berthing structures. Moreover, it is also important for the design of fender components such as panel and chains. The amount of reaction force generated by a fender is the function of its deflection, where higher deflection results in a higher reaction force. Figure 2.7 is known as the performance curve. This curve shows the amount of energy absorbed and the reaction force generated by a fender as a function of deflection.

Figure 2.7 shows performance curves for two different types of fenders, SCN and Cylindrical, manufactured by Trelleborg. It could be seen from the figure that SCN and Cylindrical fenders behave differently under compression. For the SCN fenders, the rated or design force peaks twice, at 35% and 72% deflection, respectively. Whereas, for the Cylindrical fenders, the rated force only occurs at the rated deflection (100% deflection). Beyond its rated deflection, fenders will still absorb kinetic energy. However, the reaction force will increase exponentially due to the behaviour of rubber PIANC [2002].

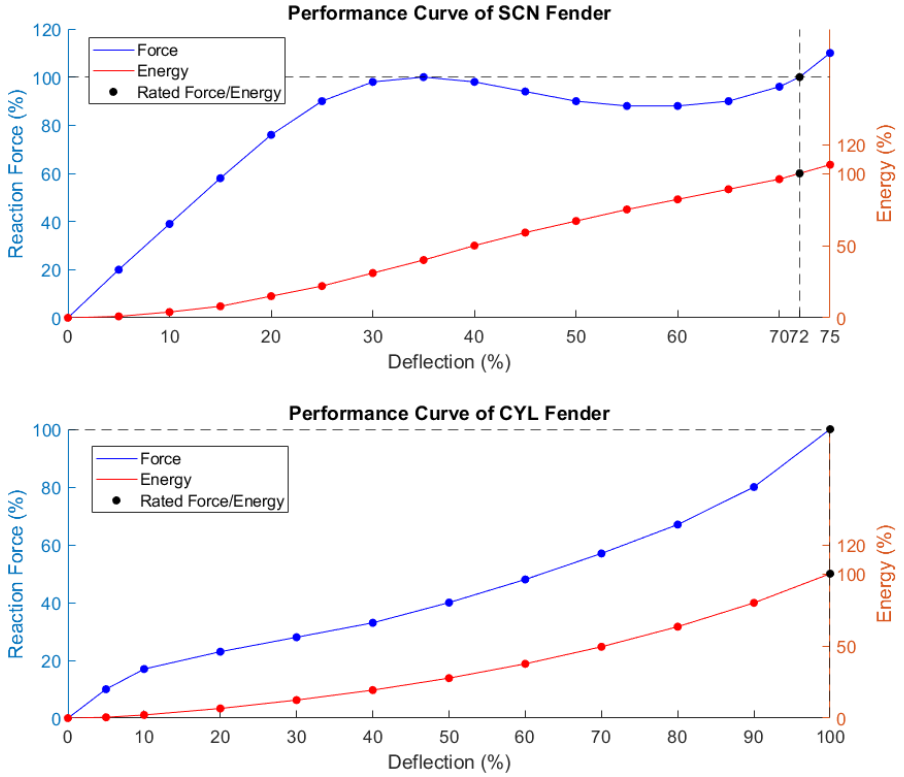

Figure 2.7: Performance curve of SCN and Cylindrical fender Trelleborg [2018]

Furthermore, since energy and reaction force are both the function of deflection, it is possible to translate from one to another. In other words, the reaction force could be determined when the energy absorbed by a fender is known and vice versa.

2.1.3 Energy absorption capacity of a fender system (E_{Fender})

The actual berthing energy absorbed by a fender is often different from the rated energy specified in fender catalogues. The rated energy in the catalogue is known as the constant velocity performance (E_{cv}), which is the energy absorbed by a fender measured at a standard test condition (e.g. slow speed constant velocity (2-8

cm/min), temperature equals to 23±5^{o}C, and 0^o compression angle). Consequently, adjustment factors taking into account the influence of temperature, manufacturing tolerance, compression rate, and compression angle have to be applied to the rated energy (E_{cv}) when the actual berthing condition is different from the standard test condition. The actual energy capacity of a fender can be calculated using the following formula:

$$E_{Fender} = E_{cv} * MF * VF * TF * AF \tag{2.8}$$

where:

E_{Fender} = Energy absorption capacity of a fender (kNm)
E_{cv} = Rated energy capacity of a fender (e.g. at 72% deflection) (kNm)
MF = Manufacturing tolerance (-)
VF = Velocity Factor (-)
TF = Temperature Factor (-)
AF = Angular Factor (-)

Equation 2.8 is valid when a vessel only contacts one fender during berthing impact. In reality, multiple fenders are often activated during the impact. Hence, energy multiplication factor ($n_{multiple}$) is introduced to incorporate the contribution of multiple fender contact to the total energy capacity of a fender system. In the event of multiple fender contact, Equation 2.8 is written as:

$$E_{Fender} = n_{multiple} * E_{cv} * MF * VF * TF * AF \tag{2.9}$$

In the deterministic approach adopted by PIANC [2002], a fender system is designed to absorb the abnormal berthing energy (E_{ab}). Consequently, the following condition has to be fulfilled:

$$E_{Fender} > E_{ab} \tag{2.10}$$

The energy multiplication factor and the influence factors (e.g. MF, TF, AF, VF) are further explained below.

Energy multiplication factor ($n_{multiple}$)

The contribution of multiple fender contact is taken into account via energy multiplication factor, denoted by $n_{multiple}$. During the berthing impact, a vessel might activate multiple fenders. In that instance, the total absorption capacity of the fender system is determined according to the maximum allowable deflection of each fender. In other words, the determination of absorption capacity in the event of multiple fender contact should not be based on the rated capacity of the individual fender (e.g. the number of fenders activated multiplied by their rated energy) as it is not always the case. In most cases, the deflection of some fenders is limited, as illustrated in Figure 2.8.

The first figure of Figure 2.8 shows a case of multiple fender contact where the middle fender is fully compressed to its rated deflection, whereas two fenders on its sides are not. On the other hand, the second figure shows what would happen if the adjacent fenders were also fully compressed. The second condition should be avoided when possible. The first reason is that the forces to be resisted by the berth structures will increase excessively when the rated deflection is exceeded as explained in Section 2.1.2. Another reason is that the distance between the berthing structure and the vessel will be to narrow, increasing the risk of collision. Therefore, in this thesis, the fender system is designed such that no rated deflection is exceeded.

Consequently, the absorption capacity of a fender system should be determined based on the maximum allowable deflection (δ_{F_i}) of each fender. Usually, one fender is designed to be fully deflected, while the deflection of the other fenders is adjusted accordingly. The ratio of the total energy that these multiple fenders can absorb (computed based on the respective maximum allowable deflection of each fender) to the rated energy capacity of a single fender is then defined as the energy multiplication factor:

$$n_{multiple} = \frac{\sum_{i=1}^{m} E_i}{E_{cv}} \tag{2.11}$$

where E_i is the total energy that can be absorbed by fender i based on its maximum allowable deflection (δ_{F_i}), and m is the number of fenders activated during berthing impact. Theoretically, this factor is mainly influenced by vessel size, the distance between fenders, and berthing angle Shibata [2017].

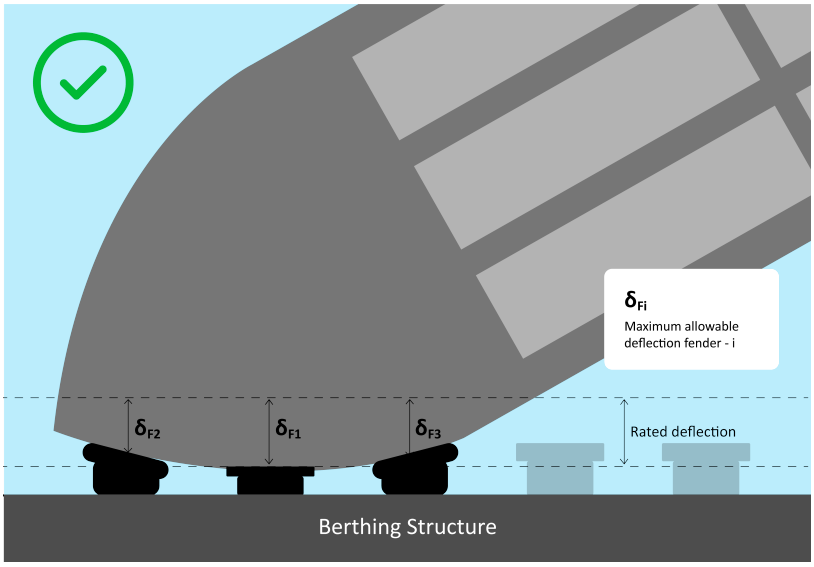

(a)

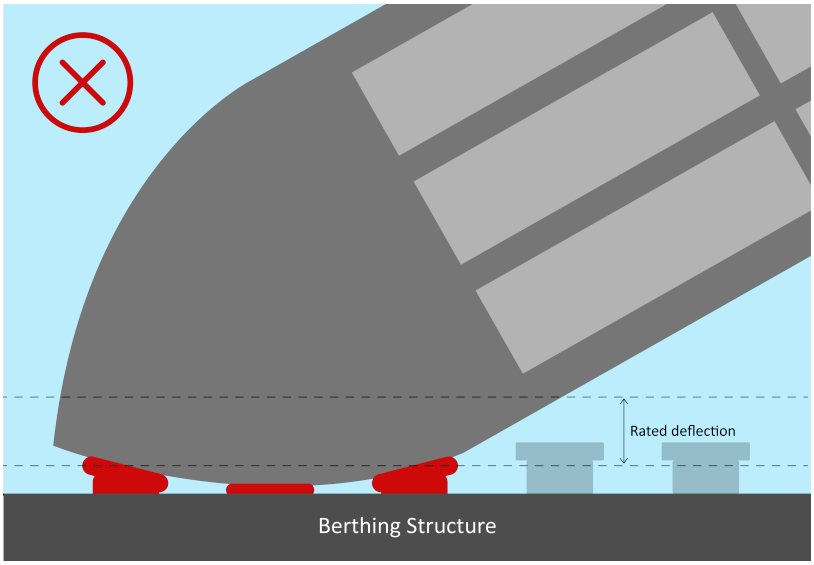

(b)

Figure 2.8: (a) The middle fender is compressed to its rated deflection (b) The adjacent fenders are compressed to the rated deflection

Velocity Factor (VF)

Rubber behaves uniquely under compression stress. The reaction force produced by rubber fender during compression not only depends on strain level but also strain rate. In other words, how fast the fenders compressed will influence the amount of the reaction force they generate. According to Trelleborg [2018], the resultant reaction force and energy absorption are higher when fenders are compressed with a higher speed (e.g. higher berthing velocity). Therefore, a velocity factor (VF) is introduced to take into account the influence of the compression rate on the fender absorption capacity. This compression rate is often represented as compression time (t):

$$t = \frac{d}{f * V_d} \tag{2.12}$$

where:

t = compression time (seconds)
d = rated deflection (mm)
V_d = initial berthing velocity (mm/s)
f = 0.74 deceleration factor (Peak reaction force occurs between 30% - 40% deflection

The corresponding velocity factor then could be determined based on the compression time. For instance, Figure 2.9 shows the velocity factor as a function of compression time for a buckling SCN fender manufactured by Trelleborg, which was used in this study. It could be seen from the figure that the velocity factor (VF) decreases as the compression time increases. However, it is important to note that the chemical composition of the rubber compound is different for different manufactures; consequently, the velocity factors are also different for different manufactures.

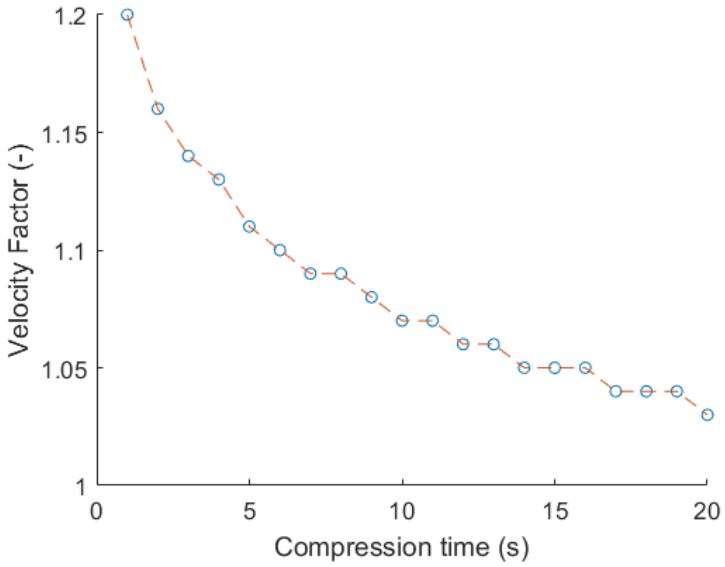

Figure 2.9: Velocity factor as a function of compression time, for buckling SCN fender Trelleborg [2018]

Manufacturing Tolerance (MF)

The production tolerance is the ratio of static compression test results of an individual fender to the standard performance or the value in the catalogue. Most of

the fender manufacture (e.g. such as Trelleborg and Shibata) agree that production tolerance is ±10%. Furthermore, the result of the study by Coastal Development Institute of Technology [2019], as shown in Figure 2.10, also confirms the value of ±10% for production tolerance. In practice, fender designers often do not want to take a risk and thus use $MF = 0.9$ in their design calculations.

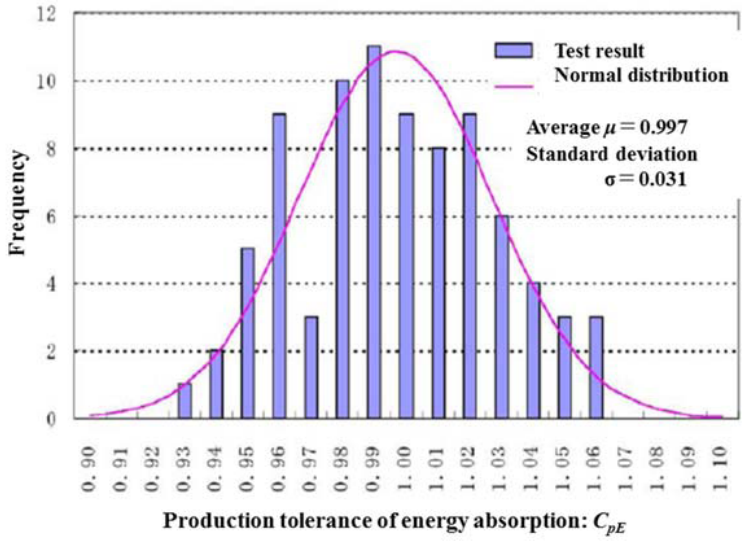

Figure 2.10: Histogram of production tolerance Coastal Development Institute of Technology [2019]

Temperature Factor (TF)

The temperature will influence the stiffness of the rubber and thus has to be taken into consideration during the fender design calculation. The effect of temperature is included in the calculation through the temperature factor (TF). In general, the engineering design will review possible minimum and maximum temperature that is likely to be experienced by a fender. At high temperatures, fenders will become softer and thus, will have a lower energy absorption capacity. Whereas, at low temperatures, fenders become harder and thus, have higher reaction forces. Therefore, a lower temperature is favourable in the sense that fenders can absorb more energy. However, at the same time, the reaction force experienced by berthing structures will also be higher. Figure 2.11 gives an example of the temperature factor for a buckling SCN fender manufactured by Trelleborg.

Angular Factor (AF)

When a vessel berths with a certain angle, some areas of the rubber or foam are more compressed than others and therefore, the reaction force generated by the fender will also be influenced. The fender's minimum energy will occur at the largest compression angle. Angular factor should be determined using the compound (vertical and horizontal) angle for cone and cell fenders while angular factor should be determined using the individual vertical and horizontal factors for linear types of fender like cylindrical and foam fenders. In practice, for berthing angle lower than 10^0, angular factor equals 1 is recommended to use. Trelleborg [2018].

2.2 CLASSICAL STATISTICAL INFERENCE

The general problem of statistical inference is how to make an inference about the probability distribution that could describe some available observed data Bedford

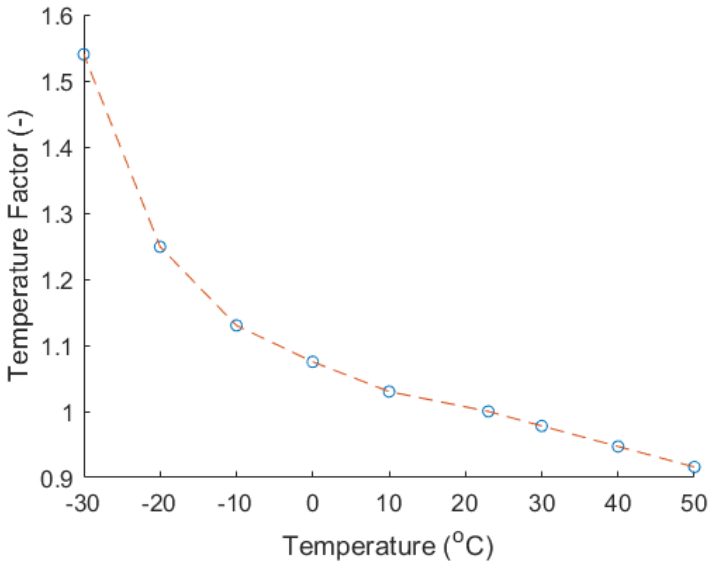

Figure 2.11: Temperature factor for buckling SCN fender Trelleborg [2018]

and Cooke [2001]. Choosing inaccurate distribution functions for the basic stochastic variables will inevitably lead to incorrect results as well. First Order Reliability Method (FORM) and Monte Carlo, for example, require distribution functions of all stochastic variables as the inputs to compute the probability of failure. Thus, the distribution of the stochastic input variables will directly influence the result of the probabilistic analysis.

Firstly, one must be aware of the difference between the maximum likelihood estimation method and the goodness-of-fit test. The maximum likelihood function is best for estimating the parameters of a certain distribution function based on the available observed data. On the other hand, the goodness-of-fit test is done to see how well a certain distribution function fits the empirical distribution. Therefore, the process of statistical inference usually starts with estimating parameters for some candidate distribution families using the maximum likelihood method. Then, the goodness-of-fit tests are performed to find which distribution candidate is the best fit for the empirical data. It is worth noting that a distribution function with the largest likelihood value is not always the best distribution to model the observed data. In the end, the chosen distribution is the one that, according to goodness-of-fit tests, fits the observed data best. This procedure is illustrated in Figure 2.12.

2.2.1 Maximum Likelihood Estimation

According to Bedford and Cooke [2001], likelihood principle is the best basis for statistical inference. The main idea of the maximum likelihood is to estimate parameters of a distribution function in which the observed data has the highest probability.

The maximum likelihood function is given below:

$$L(\hat{\theta}|\mathbf{X}) = \prod_{i=1}^{n} f(x_i|\hat{\theta}) \tag{2.13}$$

Where:

$L(\hat{\theta}|X)$ = Likelihood function
$\hat{\theta}$ = Estimated parameter
$\mathbf{X}$ = Observed data
$f(X_i|\hat{\theta})$ = probability density function of X_i given $\hat{\theta}$

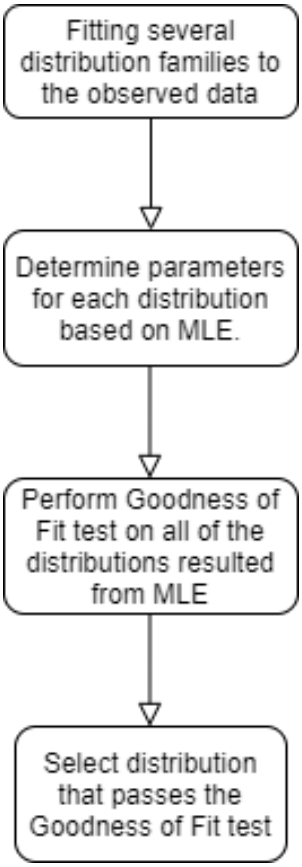

Figure 2.12: Procedure of selecting distribution for a stochastic variable

In the manual calculation, the parameters could be found by setting the partial derivative of $L(\hat{\theta}|X)$ or its log with respect to the parameter(s) to zero and solve the equation. Log of the likelihood function is often used to ease the calculation.

2.2.2 Goodness-of-Fit

While the general idea of maximum likelihood is to estimate parameter(s) of a certain distribution function given observed data, the goodness of fit test is also very important to check whether the observed data comes from a certain distribution family or not. In general, the main idea of this test is to test whether the observed data represents the expected data in the actual population or not. The Kolmogorov-Smirnov and Chi-square test are often used for the goodness of fit test for the univariate distribution.

Kolmogorov-Smirnov test

The test statistic for Kolmogorov-Smirnov is the maximum absolute difference between the empirical cumulative distribution of the observed data and the hypothesized cumulative distribution as shown below:

$$D^* = max(|\hat{F}(x) - G(x)|) \tag{2.14}$$

Where:

$\hat{F}(x)$ = the empirical CDF
$G(x)$ = the CDF of the hypothesized distribution

In KS test, when a sample comes from the hypothesized distribution then the D^* will converge to 0.

Chi-square test

While, the formula for Chi-Square is:

$$X_c = \sum_{i=1}^{k} \frac{(O_i - E_i)^2}{E_i} \tag{2.15}$$

Where:

c = Degrees of freedom (k-1)
O_i = the observed value based on the actual data
E_i = the expected value based on the hypothesized distribution

Akaike Information Criterion

The Akaike information criterion (AIC) is a handy equation used to compare statistical models based on the trade-off between number of estimated parameters and the log-likelihood value. Basically, the greater value of likelihood and fewer parameters are desired since it indicates that the selected distribution function is both simple and good fit for the observed data. Thus, the result of MLE will be used as the input for the AIC, the basic formula of AIC is defined as:

$$AIC = 2k - 2 * ln(L) \tag{2.16}$$

Where:

k = Number of parameters
$\ln(L)$ = Maximum value of the log likelihood function for the model

Small AIC value indicates that the relative amount of information lost by a given model is small implying that the model has a high quality.

2.3 DEPENDENCE

Two events are statistically dependent when one event's occurrence probability influences the probability of the other event. P(A|B) in Equation 2.17 is known as the conditional probability, and we can define it as the probability of event A happens when we know the probability of B happens equals P(B), for which P(B)>0.

$$P(A|B) = \frac{P(A \cap B)}{P(B)} \tag{2.17}$$

When A and B are statistically independent, the joint probability of A and B equal to the product of P(A) and P(B) and thus, Equation 2.17 can be written as:

$$P(A|B) = \frac{P(A).\cancel{P(B)}}{\cancel{P(B)}} \tag{2.18}$$

As given in the above equation, knowing information about B will not alter our uncertainty about the truth of A when A is independent of B.

2.3.1 Correlation coefficients

A popular way to measure dependence between two random variables is by using the Pearson's correlation coefficient. Using this method, one can measure the linear relationship between two random variables. Pearson's correlation coefficient can be calculated using the equation below:

$$\rho_{XY} = \frac{\text{cov}(XY)}{\sigma_X \sigma_Y} = E\left\{\frac{X - E(X)}{\sigma_X} . \frac{Y - E(Y)}{\sigma_Y}\right\} \in [-1, 1] \tag{2.19}$$

where:

$cov(XY)$ = Covariance between X and Y
σ_X = Standard deviation of random variable X
σ_Y = Standard deviation of random variable Y
$E(X)$ = Expected value of X
$E(Y)$ = Expected value of Y

However, one limitation of the Pearson's coefficient of correlation is that it could not identify non-linear dependence. In that sense, uncorrelated random variables do not always mean independence since it might be the case that the variables have a non-linear relationship. Bedford and Cooke [2001] gives an example in which two variables are functionally related, but the correlation coefficient is minimal, as demonstrated in the case of Y = x^{11}. In this example, the Pearson's correlation coefficient will be zero even though Y is a direct function of X.

Alternatively, a dependence between variables could also be evaluated through rank-correlation. One advantage of the rank-correlation is that it is a non-parametric measure. Thus, it does not depend on the marginal behaviour of the random variables. The rank correlation measures the monotone relationship between two random variables. Two most commonly used non-parametric measures of dependence are Spearman's rank correlation or Kendall's tau. The Spearman's rank correlation (r) could be expressed as:

$$r(X, Y) = \rho(F_X(X), F_Y(Y)) \in [-1, 1] \tag{2.20}$$

In which, $F_x(X)$ and $F_Y(Y)$ are the empirical cumulative distribution of data X and Y, respectively. At the same time, the empirical formula of Kendall's tau is:

$$\tau_n = \frac{P_n - Q_n}{\binom{n}{2}} = \frac{4}{n(n-1)} P_n - 1 \tag{2.21}$$

Where P_n and Q_n are number of concordant and discordant pairs, respectively and n is the number of observations. A pair (x_i, y_i) is said to be in concordant if either one of the following conditions holds: $x_i > x_{i-1}$ while $y_i > y_{i-1}$ or $x_i < x_{i-1}$ while $y_i < y_{i-1}$. The opposite is known as discordant. Based on the Kendall's tau, one can also perform a hypothesis test of independence. Under the null hypothesis of independence, the test statistic of independence test is close to normal distribution with zero mean and variance $2(2n+5)/9n(n-1)$. Therefore, the null hypothesis would be rejected at approximate level α=5% if:

$$\sqrt{\frac{9n(n-1)}{2(2n+5)}} |\tau_n| > 1.96 \tag{2.22}$$

Later on, this thesis will use the Kendall's tau independence test to prove dependency between the load variables.

2.4 BIVARIATE COPULAS

In the past, the dependence between two random variables is usually modeled using classical families of bivariate distribution such as bivariate normal or log-normal distribution. However, this approach is only applicable to modeling the dependency between two random variables that come from the same distribution family. Due to this limitation, most statisticians thus prefer to use copula to model a bivariate joint distribution. With the use of a copula, the modeling of the dependence structure does not depend on the marginal distribution of the basic variables Genest and Favre [2007]. Due to this feature, copula can provide more flexibility compared to other bivariate dependence modeling methods.

Jonkman et al. [2017] gives an easy-to-understand definition of the copula, where they define copula as the bivariate cumulative distribution corresponding to the "ranks" of the original variables. According to the Sklar's theorem, random variables X and Y with marginal cumulative distribution $F_X(X)$ and $F_Y(Y)$ are joined by a copula C if their joint cumulative distribution function $F_{XY}(X, Y)$ could be written as:

$$F_{XY}(X, Y) = C(F_X(X), F_Y(Y)) \tag{2.23}$$

If the cumulative distribution $F_X(X)$ and $F_Y(Y)$ are denoted as u and v, respectively, the joint probability density of a copula C can be written as follow:

$$c(u, v) = \frac{\delta^2}{\delta u \delta v} C(u, v) \tag{2.24}$$

Since u and v are the cumulative distribution of variables x and y, consequently, u and $v \in$ [0,1]. Bivariate copula $C(u, v)$, therefore, is defined on the unit square $[0,1]^2$. Furthermore, the bivariate joint density function can be obtained by multiplying the copula density $c(u, v)$ with the marginal density functions of the random variables X and Y, as given in the equation below:

$$f_{XY}(X, Y) = c(u, v).f_X(X).f_Y(Y) \tag{2.25}$$

According to Sklar, every continuous distribution can be represented in terms of a copula. Given a pair of random variables X and Y, we can always derive an empirical copula by ranking the data and re-scaling them into the unit square [0,1]:

$$C_n(u, v) = \frac{1}{n} \sum_{i=1}^{n} \left(\frac{R_i}{n+1} \leq u, \frac{S_i}{n+1} \leq v \right) \tag{2.26}$$

Where:

R_i & S_i = Pairs of ranked transformed data
C_n = Empirical copula

Figure 2.13 illustrates some bivariate copulas that are often used to model dependence structures, while the corresponding Copula functions are described in Table 2.5. The copula fitting principle is similar to the univariate statistical inference, in which we aim to select a copula function that can adequately describe the dependence structures of the observed data.

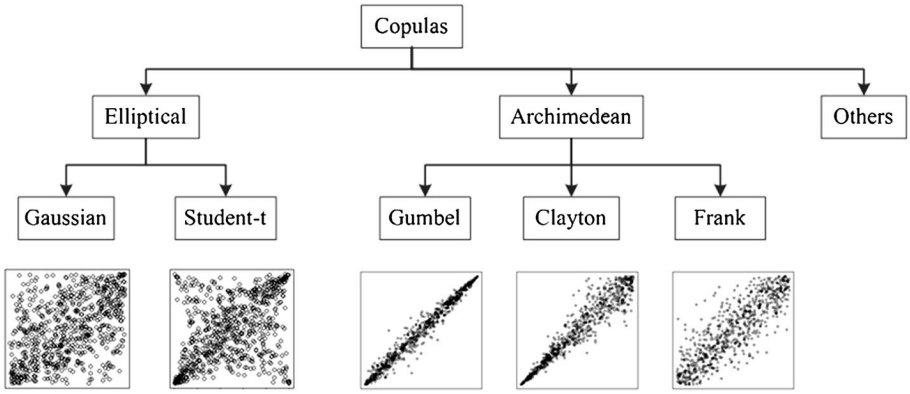

Figure 2.13: Different copulas in the classes of elliptical and Archimedean copula families Jianping et al. [2015]

Table 2.5 presents the copula functions used in this thesis.

Table 2.5: Commonly used copula functions

Name	Copula function	Parameter
Independent	$C_{uv} = uv$	[-]
Gaussian	$C_\theta(u,v) = \int_{-\infty}^{\phi^{-1}(u)} \int_{-\infty}^{\phi^{-1}(v)} \frac{1}{2\pi(1-\theta^2)^{\frac{1}{2}}} \exp\left\{-\frac{x^2-2\theta xy+y^2}{2(1-\theta^2)}\right\} dxdy$	$-1 \leq \theta \leq 1$
Clayton	$C_\theta(u,v) = \max([u^{-\theta}+v^{-\theta}-1]^{-\frac{1}{\theta}}, 0)$	$\theta \in [-1,\infty)\backslash\{0\}$
Gumbel	$C_\theta(u,v) = \exp\left\{-[(-\ln u)^\theta + (-\ln v)^\theta]^{\frac{1}{\theta}}\right\}$	$\theta \in [1,\infty)$
Frank	$C_\theta(u,v) = -\frac{1}{\theta}\ln\left(1+\frac{(e^{-\theta u}-1)(e^{-\theta v}-1)}{e^{-\theta}-1}\right)$	$\theta \in [-\infty,\infty)\backslash\{0\}$

The Archimedean copulas can only be used to model positive correlation. However, one can rotate the bivariate copulas by replacing variable u or v or both of them to 1-u and 1-v, thus allowing us to model negative correlation by rotating the copula 90° or 270°. As an example, Figure 2.14 illustrates the rotated Clayton copula. One can compute the cumulative rotated copula distribution using the following equation:

$$\begin{aligned} C_{90}(u,v) &= v - C(1-u,v) \\ C_{180}(u,v) &= u + v - 1 + C(1-u,1-v) \\ C_{270}(u,v) &= u - C(u,1-v) \end{aligned} \tag{2.27}$$

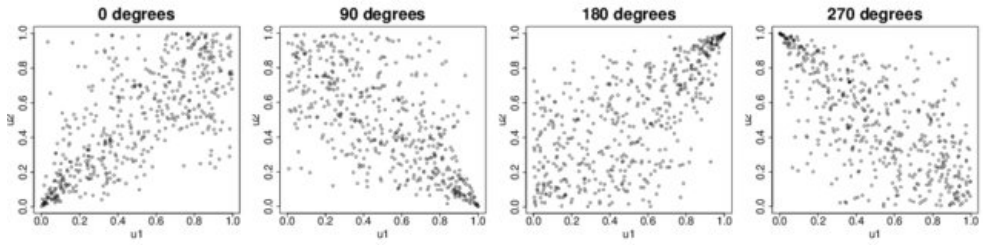

Figure 2.14: Illustration of rotated Clayton copulas

2.4.1 Goodness-of-fit tests

Goodness-of-fit tests are essential to assess a particular copula's adequacy in modeling the empirical copula. Several methods are available, including Akaike Information Criterion (AIC), Cramer-von Mises statistic, and Semi-correlation analysis.

Akaike Information Criterion

The concept of the Akaike Information Criterion has been explained in Equation 2.2.2. Many studies, such as those done by Kooij [2020] and Valls [2019], used AIC as the basis to find the most optimum theoretical copula to describe the observed data.

Cramér-Von Mises

The Cramer von Mises (CvM) statistic is basically based on the squared differences between the selected theoretical copula and the empirical copula. The smaller the differences, the better a certain copula family in describing the empirical copula.

The basic formula of CvM is:

$$CM_n = n * \sum_{i=1}^{n} \left\{ C_n \left(\frac{R_i}{n+1}, \frac{S_i}{n+1} \right) - C_{\theta_n} \left(\frac{R_i}{n+1}, \frac{S_i}{n+1} \right) \right\}^2 \tag{2.28}$$

Where:

R_i & S_i = Pairs of ranked transformed data
C_n = Empirical copula (Equation 2.26)
C_θ = Parametric estimator
CM_n = Cramer von Mises value

Semi Correlation

Semi correlation could help identify tail dependence in the empirical copula. The conversion of the marginal variables from the standard uniform space to the standard normal space enables us to compare the empirical copula with the bivariate normal density. The normal copula does not have tail dependence and thus, the semi correlation plot will be symmetry while in case of tail dependence, the plot of the semi-correlation will be asymmetry.

This information could be helpful when choosing a copula family to represent the empirical joint distribution, for instance, Gumbel copula is chosen when the semi-correlation plot shows that the observed data has a sharper right upper corners (relative to the ellipse) and Clayton copula might be an option to represent joint empirical distribution with stronger tail dependence on the bottom-left quadrant. The illustration of the semi correlation coefficients is given in Figure 2.15.

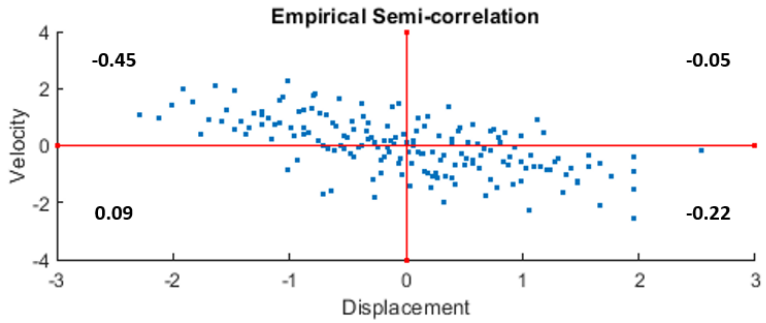

Figure 2.15: An example of the semi-correlation between the vessel displacement and berthing velocity

2.5 VINE COPULA

We often have to model dependence between multiple random variables (e.g. more than 2 variables). One way to model multivariate dependence is by using multivariate copulas as some bivariate copulas can be extended into multidimensional copulas. However, only a few multivariate copulas have been developed so far, and some multivariate dependence structures are just too complex to be modelled using these available multivariate copulas.

Therefore, Cooke [1997] developed a new method called vines, which is more flexible to model multivariate dependence structures. The formal definition of vine copula is given in the book written by Kurowicka and Cooke [2006], "A vine on n variables is a nested set of trees, where the edges of the tree j are the nodes of the tree j + 1 where j = 1,...,n-2, and each tree has the maximum number of edges". There are two types of vines, a regular and irregular vine. The vine with n-nodes is regular when two edges in tree j that are joined by an edge in tree j+1, share a common node in tree j. While if this is not the case, the vine is called irregular. Figure 2.16 shows an example of regular and irregular vines.

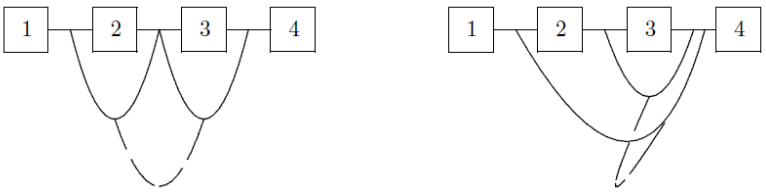

Figure 2.16: Illustration of regular (left) and irregular vines (right) Kurowicka and Cooke [2006]

The regular vine copulas are further divided into several categories, amongst them are the canonical vines (C-vines) and the drawable vines (D-vines). According to Kurowicka and Cooke [2006], a regular vine is called a D-vine if each node in the first tree (T_1) has a degree of at most 2. Whereas, it is called C-Vine if each tree (T_i) has a unique node of degree $n - i$. The node with maximal degree in T_1 is the root. In this thesis, we will deal with a three divisional probability distributions. For three random variables, there are no difference between C-vines and D-vines copulas.

2.5.1 Trivariate vine copula

This sub-section will specifically discuss the concept of regular vines, particularly for trivariate cases, as this is what was used for the analysis. The application of vine copula to model trivariate dependence structures has found a wide application in

the field of hydrology. For example, Gräler et al. [2013] used vine copula to construct dependence structures between peak discharge, duration, and rain volume.

The main idea of vine copulas is to construct a multi-dimensional copula based on the bivariate copulas' stage-wise mixing. This is illustrated in Figure 2.17. There are a total of 3 bivariate copulas in the vine structure, two capturing dependence between U with V and V with W, and the other one used to join the conditional cumulative distribution of the variables U and W to V. Therefore, the variables U and W are connected through the copula $C_{UW|V}$.

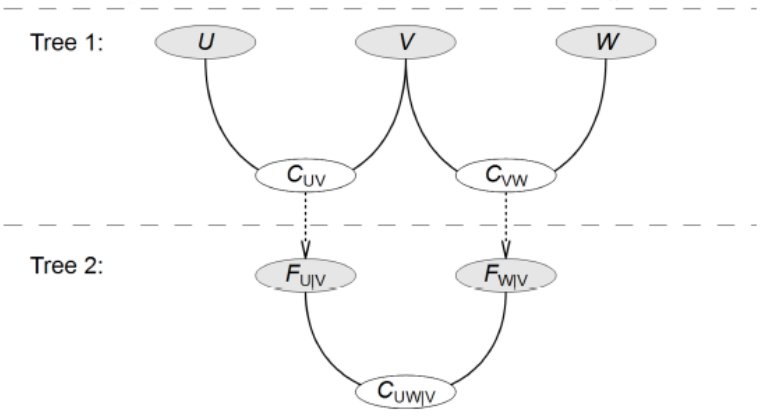

Figure 2.17: Illustration of hierarchical nesting of bivariate copulas in the construction of a 3-D vine copula Gräler et al. [2013]

Figure 2.17 shows that we need the conditional cumulative distribution functions $F_{U|V}$ and $F_{W|V}$ in order to find the bivariate copula $C_{UW|V}$. These conditional cumulative distributions $F_{U|V}$ and $F_{W|V}$ can be obtained through partial differentiation of the bivariate copulas C_{UV} and C_{VW} with respect to the variable V, respectively. This conditional distribution is also commonly known as **h-function** and generally formulated as:

$$F(x_i|x_j) = h_{ij}(u_i, u_j) = \frac{\delta C(u_i, u_j)}{\delta u_j} \tag{2.29}$$

For which u_i and u_j are the cumulative distribution of the variables x_i and x_j. Given the conditional distributions of $F_{U|V}$ and $F_{W|V}$, the full density function c_{UVW} of the 3-D copula can be written as:

$$c_{UVW}(u, v, w) = c_{UW|V}(F_{U|V}(u|v), F_{W|V}(w|v)).c_{UV}(u, v).c_{VW}(v, w) \tag{2.30}$$

Considering the random vector $\mathbf{X} = (x_1, x_2, ..., x_n)$, its joint density function $f(x_1, x_2, ..., x_n)$ could be decomposed as:

$$f(x_1, x_2, ..., x_n) = f_1(x_1).f_{2|1}(x_2|x_1).f_{3|1,2}(x_3|x_1, x_2)...f_{n|1,2,..,n-1}(x_n|x_1, x_2, ..., x_{n-1}) \tag{2.31}$$

In a case of three variables, the joint pdf simplifies to:

$$\begin{aligned} f(x_1, x_2, x_3) &= f_1(x_1).f_{2|1}(x_2|x_1).f_{3|1,2}(x_3|x_1, x_2) \\ &= f_1(x_1)f_2(x_2)f_3(x_3)c_{12}(F_1(x_1), F_2(x_2))c_{23}(F_2(x_2), F_3(x_3))c_{13|2}(F_{1|2}(x_{1|2}), F_{3|2}(x_{3|2})) \end{aligned} \tag{2.32}$$

Furthermore, it is also important to note that the choice of the conditioning variable (i.e. V) is not unique, and different choices might lead to different outcomes. In practice, the conditioning variable is often selected based on the result of the vine copula fitting, for instance based on the smallest AIC value.

2.6 RELIABILITY-BASED DESIGN

The reliability of a structure could be defined as its capability to fulfil its function. In this study, fender reliability is described as a function of the energy absorption capacity of a fender system (E_{Fender}) and the kinetic energy (E_k). At the same time, E_{Fender} and E_k are also functions of stochastic and deterministic variables. Therefore, there might exist a combination of the variables that leads to a failure of the fender system. In this study, a reliability of fender system is expressed using failure probability, which is the probability of the kinetic energy is higher than the fender capacity:

$$P_f = P[E_{Fender} \leq E_k] \tag{2.33}$$

Furthermore, a limit-state function is formulated. This function is used in the reliability-based computation to separate the failure region and safe region ($g = 0$). In this study, this function is composed as:

$$g = E_{Fender} - E_k = 0 \tag{2.34}$$

Figure 2.18 illustrates the general concept of failure probability and limit-state function. The figure shows the joint probability distribution of the kinetic energy and fender capacity, and how the failure probability could be derived from the joint distribution.

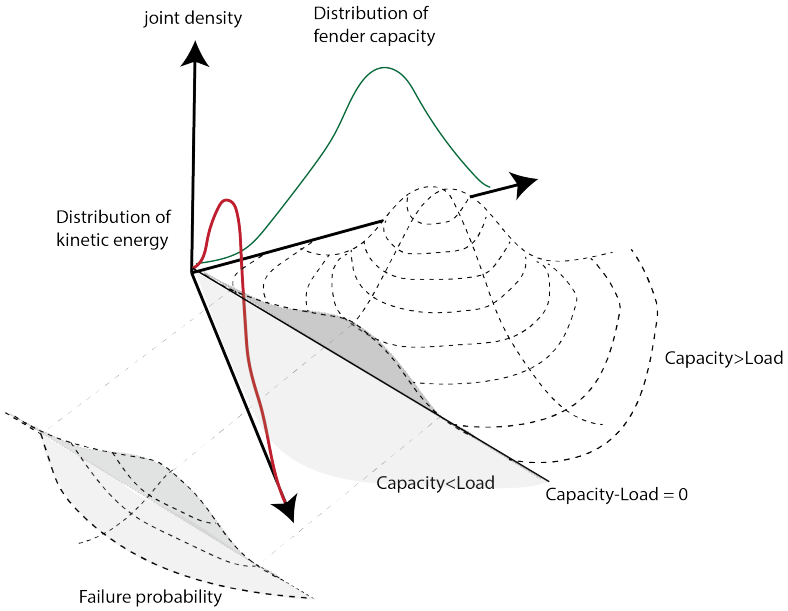

Figure 2.18: Conceptual illustration of probability of failure (Author's illustration)

In the figure, the failure probability is depicted as the volume of the joint probability density in the unsafe region (Fender capacity≤Kinetic energy). The failure probability then could be found directly by using numerical integration:

$$P_f = \iint_{g<0} f_{E_k E_{fender}}(E_k, E_{fender}) d_{E_k} d_{E_{Fender}} \tag{2.35}$$

However, since the kinetic energy and fender capacity are also functions of several stochastic variables, it is difficult to compute the probability of failure analytically (e.g.using a direct integral as done in Equation 2.35). Therefore, several methods such as Monte Carlo and FORM are often used to estimate the probability of failure.

2.7 MONTE CARLO

This section presents the application of Monte Carlo simulation for independent variables case and also for the case when the variables are dependent on each other. For the latter case, this section demonstrates how the Vine Copula could be incorporated into the Monte Carlo simulation.

2.7.1 Independent Variables case

When level III reliability method is applied, the probabilistic formulation for P_f is approximated using either numerical integration or Monte Carlo simulation. Monte Carlo simulation is a broad class of computational algorithms that rely on random sampling to obtain probability of failure. This method allows a practical and easier computation for the probability of failure in case it is impossible to obtain a closed-form expression for the LSF or it is not feasible to apply a deterministic algorithm.

The principle of Monte Carlo simulation is actually quite straight forward. Given that the distribution functions of all of the random variables are known, a standard random uniform number $\in$[0,1] is generated and we treat the generated random number as a cumulative distribution value of the variables and thus, the random number then can be inverted into the distribution of the variables using the inverse of already known cumulative distribution functions.

Monte Carlo simulation could be explained mathematically using formula below:

$$\begin{aligned} u_i &= F_X(x_i) \\ x_i &= F_X^{-1}(u_i) \end{aligned} \tag{2.36}$$

Where:

u_i = a random generated standard uniform number [0,1]
$F_X(x_i)$ = a cumulative distribution function of variable X_i
x_i = the value of random generated variable in the original space

By taking n realizations of the uniform probability distribution between zero and one, a value can be determined for ever x_i. By inserting the randomly simulated values obtained from Equation 2.36 for each of the variables to the limit state function, one can check whether the load is greater or not compared to the resistance. By repeating this procedure a large number of times, according to the Central Limit Theorem, the probability of failure could be approached with:

$$P_f = \frac{n_f}{n} \tag{2.37}$$

in which:

n = the total number of simulations
n_f = number of times that LSF<0

2.7.2 Dependent Variables case

This part presents the algorithm which was developed by Jiang et al. [2015] to incorporate the dependence between variables (e.g. modelled using a Vine Copula) into Monte Carlo simulation. The following algorithm is used when there are three dependent variables (x_1, x_2, and x_3):

Step 1 Select the best Vine copula structure to model the dependence between the variables. For three dependent variables, the following bivariate Copulas have to be defined:
$C_{12}(F_1(x_1), F_2(x_2))$, $C_{23}(F_2(x_2), F_3(x_3))$, and $C_{13|2}(F_{3|2}(x_3|x_2), F_{1|2}(x_1|x_2))$

Iteration 1
a) Generate a random uniform number $r_1 \in [0\ 1]$, where $r_1 = F_1(x_1)$
b) Find the corresponding random variable in the physical space $x_1 = F_1^{-1}(x_1)$

Iteration 2
a) Generate a random uniform number r_2, where $r_2 = F_{2|1}(x_2|x_1)$
b) Find the cumulative distribution function of the second variable $F_2(x_2)$ by solving the following equation:

$$r_2 = \frac{\delta C_{12}(F_1(x_1), F_2(x_2))}{\delta(F_1(x_1))}$$

c) Find x_2 by solving $x_2 = F_2^{-1}(x_2)$

Iteration 3
a) Generate a random uniform number r_3, where $r_3 = F_{3|12}(x_3|x_1, x_2)$
b) Solve for the conditional distribution of x_3 on x_2, which is $F_{3|2}(x_3|x_2)$, by solving:

$$r_3 = \frac{\delta C_{13|2}(F_{3|2}(x_3|x_2), F_{1|2}(x_1|x_2))}{\delta(F_{1|2}(x_1|x_2))}$$

c) Solve for $F_3(x_3)$, by solving:

$$F_{3|2}(x_3|x_2) = \frac{\delta C_{32}(F_2(x_2), F_3(x_3))}{\delta(F_2(x_2))}$$

d) Find x_3 by solving $x_3 = F_3^{-1}(x_3)$

Step 2 Repeat iteration 1 to iteration 3 to generate n number of samples.

Step 3 Substitute all the generated samples to the limit-state function and use Equation 2.37 to approximate the failure probability.

The only difference between the Monte Carlo simulation for the independent variables and dependent variables lies on the method used to generate the random vector **X**. For the independent variables case, Equation 2.36 is used. Whereas, when the variables are dependent on each other, the transformation from the standard uniform generated sample r_i to its corresponding value in the physical space x_i is based on the selected Vine copula structure.

2.8 FIRST ORDER RELIABILITY METHOD (FORM)

This section presents the basic concept of FORM and the implementation of the Vine Copula FORM algorithm which was developed by Jiang et al. [2015].

2.8.1 Independent Variables case

In the First Order Reliability Method (FORM), all the basic variables in the original X-space are transformed into the independent standard normal U-space, and all calculations are done in this U-space. The primary goal of FORM is to find a design point in the standard normal U-space. The design point is defined as the point located on the limit state function whose distance from the origin is the shortest. One of the properties of a multivariate standard normal distribution is that it has concentric circles joint density contour which implies that this design point **u*** also has the highest probability density in the failure region as it is located closest to the centre of the circles. This is illustrated in Figure 2.19.

Another important feature of FORM is the linearization of the limit state function at the design point, for which the perpendicular distance from this linearized limit state function to the centre of the circles is defined as **reliability level (β)**. The

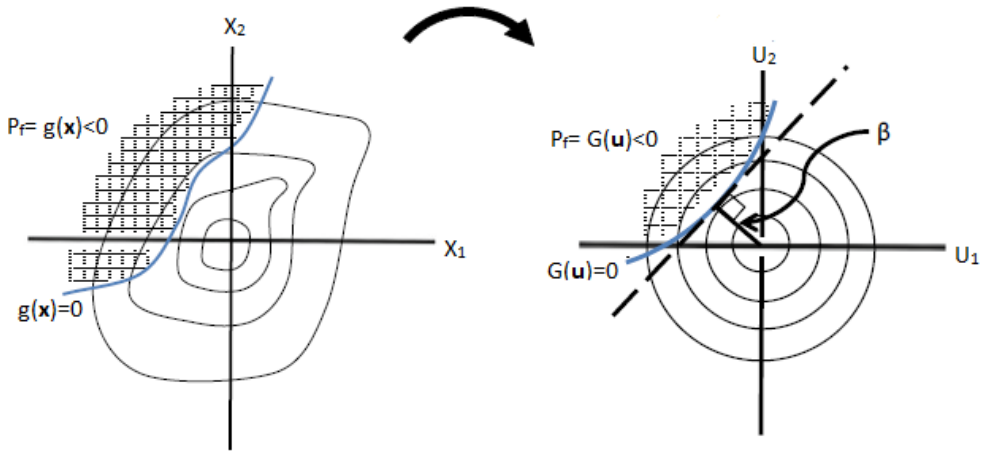

Figure 2.19: Limit state function is transformed from the original space (left figure) to the standard normal space (right figure) Moss [2020]

probability of failure is then approximated as the area behind this linearized limit state function ($G_{\mathbf{u}} < 0$), whose value equals to:

$$p_f = \phi(-\beta) \tag{2.38}$$

While the linearized limit-state function could be expressed as:

$$G(\mathbf{u}) = \|G(\mathbf{u}^*)\| \, (\beta - \alpha \mathbf{u}) \tag{2.39}$$

Kiureghian [2005] gives the following optimization problem to solve for the design point ($\mathbf{u}^*$):

$$\mathbf{u}^* = argmin\{\|u\| \, |G(\mathbf{u} = 0)\} \tag{2.40}$$

While the "arg min" denotes the argument of the minimum of a function. Basically, the main computational effort in FORM is to solve the optimization problem above and FORM usually requires some iterations in order to converge and find the design point. In this thesis, the improved Hasofer-Lind Rackwitz-Fiessler (i HL-RF) algorithm is used to solve the optimization problem.

One must be aware of the fact that the design points ($\mathbf{u}^*$) is solved in the standard normal U-space, implying that $\mathbf{u}^*$ are the most likely failure point in the U-space. However, it does not directly imply that the corresponding design points in the original X-space ($\mathbf{x}^*$) are also the most likely failure points. Citing Lemaire [2005], "Nothing enables us to affirm that the design point $\mathbf{x}^*$ in physical space is the maximum likelihood point," which occurs if the transformation between the U-space and X-space is non-linear. However, in the case of linear transformations, $\mathbf{x}^*$ are also the most probable failure point as the Jacobian is constant. The values of the design point in the X-space (and their associated α values) are usually used to calibrate partial safety factors in the semi-probabilistic method, which implies that the design points in the U- and X-space are comparable.

Finally, Kiureghian [2005] also explains some conditions under which the results obtained from FORM fails to give a good approximation of probability of failure. The first case is when the surface of the limit state function in the U-space ($G_{\mathbf{u}}$) is highly non-linear, this is because FORM performs linearization of the limit state function at the design point. The second case is when the optimization problem has multiple local or global solutions. Therefore, one should always interpret the FORM result with caution.

Sensitivity factors (α)

One of the advantages of FORM compared to the Monte Carlo is that besides the probability of failure, it also gives the sensitivity factors ($\boldsymbol{\alpha}$) which could be interpreted as the relative contribution of each random variable to the total variance of the limit-state function. Alpha could be computed as:

$$\boldsymbol{\alpha} = -\frac{\bigtriangledown G(\mathbf{u}^*)}{\|\bigtriangledown G(\mathbf{u}^*)\|} \tag{2.41}$$

Where $\bigtriangledown G(\mathbf{u}^*)$ is the partial derivative of limit-state function with respect to the random variables $\mathbf{x}$. A positive alpha value indicates that a variable is a load variable where negative alpha value indicates a capacity variable. Moreover, the absolute value of alpha indicates the relative influence of the variables to the limit state function.

Furthermore, if from the analysis it is known that a variable is not too important which is indicated by a very low sensitivity factor value, this variable could be replaced with a deterministic value in order to reduce the effort needs for probabilistic calculation.

2.8.2 Dependent Variables case

This sub-section presents how Vine Copula could be incorporated in FORM using the VC-FORM algorithm developed by Jiang et al. [2015]. This algorithm itself adopts the improved HL-RF algorithm (iHL-RF) of Kiureghian [2005] and therefore, the objective function Equation 2.40 still holds.

The iteration steps for the VC-FORM algorithm are:

Step 1 Find the most optimum Vine copula structure to describe the observed data, based on the results of goodness-of-fit.

Step 2 Given the first iteration step (k=0), select iterative points for each random variable ($x_{i_{k=0}}$).

Iteration 1 Convert variables $\mathbf{x_k}$ to standard normal variables $\mathbf{u_k}$ using the **Rosenblatt transformation**, as shown in the following equation:

$$\begin{aligned}
u_1 &= \phi^{-1}[F_1(x_1)] \\
u_2 &= \phi^{-1}[F_{2|1}(x_2|x_1)] \\
&= \phi^{-1}(h_{21}(u_2, u_1)) \\
&= \phi^{-1}(\frac{\delta C_{12}(F_1(x_1), F_2(x_2))}{\delta F_1}) \\
u_3 &= \phi^{-1}[F_{3|12}(x_3|x_1, x_2)] \\
&= \phi^{-1}(h_{3|2,1|2}(h_{32}(u_3, u_2), h_{12}(u_1, u_2))) \\
&= \phi^{-1}(\frac{\delta C_{13|2}(F_{3|2}(x_3|x_2), F_{1|2}(x_1|x_2))}{\delta F_{1|2}(x_1|x_2)})
\end{aligned} \tag{2.42}$$

Iteration 2 After obtaining $\mathbf{u_k}$, the next step is to compute the gradient of the linearized limit-state function $\nabla G(\mathbf{u_k})$:

$$\nabla G(\mathbf{u}_k) = \mathbf{J}^T_{\mathbf{x},\mathbf{u}} \nabla g(\mathbf{x}_k) \tag{2.43}$$

where $\nabla g(x_{\mathbf{k}})$ is the partial derivation of the limit-state function in the original space with respect to $\mathbf{x_k}$, and $\mathbf{J_{x,u}}$ is the Jacobian of the transformation from X-

to U-space. However, the common practice is to compute $\mathbf{J_{x,u}}$ through $\mathbf{J_{u,x}}$, as $\mathbf{J_{x,u}}$ is equivalent to $\mathbf{J_{u,x}^{-1}}$. The Jacobian $\mathbf{J_{u,x}}$ is formulated as:

$$\mathbf{J_{u,x}} = \left[\frac{\delta u_i}{\delta x_i}\right]_{n\times n} \tag{2.44}$$

with

$$\left[\frac{\delta u_i}{\delta x_i}\right]_{n\times n} = \begin{cases} 0 & \text{i} < \text{j} \\ \frac{1}{\varphi(u_i)} f_{i|1,2,\ldots,i-1}(x_i|x_1, x_2, \ldots, x_{i-1}) & \text{i} = \text{j} \\ \frac{1}{\varphi(u_j)} \frac{\delta F_{i|1,2,\ldots,i-1}(u_i|u_1,u_2,\ldots,u_{i-1})}{\delta u_i} & \text{i} > \text{j} \end{cases} \tag{2.45}$$

Iteration 3 Find the sensitivity factors ($\boldsymbol{\alpha_k}$) using Equation 2.41.

Iteration 4 Find the search direction ($\boldsymbol{d_k}$) using the following:

$$\mathbf{d_k} = \left[\frac{G(\mathbf{u_k})}{\|\nabla G(\mathbf{u_k})\|} + \boldsymbol{\alpha_k}\mathbf{u_k}\right]\boldsymbol{\alpha}_\mathbf{k}^T - \mathbf{u_k} \tag{2.46}$$

Iteration 5 The new iterative point $\mathbf{u_{k+1}}$ is then found using the following equation:

$$\mathbf{u_{k+1}} = \mathbf{u}_k + \lambda_k \mathbf{d_k} \tag{2.47}$$

where λ_k is the step size of the iteration. It is important to ensure that the step size λ_k leads to a convergence. According to Kiureghian [2005], an optimal step size satisfies the following merit functions:

$$\begin{aligned} m(\mathbf{u_k}) &= \frac{1}{2}\|\mathbf{u_k}\|^2 + c\,|G(\mathbf{u_k})| \\ c &> \frac{\|\mathbf{u_k}\|}{\|\nabla G(\mathbf{u_k})\|} \end{aligned} \tag{2.48}$$

A step size $\lambda_k \in (0, 1]$ then has to be selected such that:

$$m(\mathbf{u_k} + \lambda_k \mathbf{d_k}) < m(\mathbf{u_k}) \tag{2.49}$$

Iteration 6 Convert the new iteration point $\mathbf{u_{k+1}}$ back to $\mathbf{x_{k+1}}$, using the inverse of Equation 2.42

Iteration 7 Check whether the following criterion is met:

$$\begin{aligned} |G(\mathbf{u_{k+1}})/G(\mathbf{u_k})| &\leq 10^{-3} \\ \|\mathbf{u_{k+1}} - \boldsymbol{\alpha_{k+1}}\mathbf{u_{k+1}}\boldsymbol{\alpha_{k+1}}\| &\leq 10^{-3} \end{aligned} \tag{2.50}$$

If the above criterion is met, then the iteration stops. Otherwise, repeat the iteration from iteration 1 using $\mathbf{x_{k+1}}$ as the input for the iterative points.

Step 3 Compute the reliability level (β):

$$\beta = \|\mathbf{u}_k\| \tag{2.51}$$

The outputs of the algorithm above is the reliability level (β) and the design points ($\mathbf{x_i^*}$). In this thesis, the above algorithm was implemented in 'R'.

Importance Factor (γ)

In case of independent variables, the standard normal random variables u_i have one-to-one correspondence with the random variable x_i in the original space and therefore, the sensitivity factor in the U-space equals to the sensitivity factor in the X-space. However, it is not the case for the dependent variables, particularly with the lower triangular-type transformation such as Rosenblatt transformation, where the standard normal random variable u_i is the function of x_1, x_2,..., x_i. This implies that the sensitivity factors for the standard normal variables u_i do not provide the same information about the sensitivity factors of the variables x_1, x_2,..., x_i in the original space.

In case of dependent random variables, therefore,a new measure that describes the relative importance of random variables in the original space is needed. These importance factors could be found by correcting the sensitivity factors (α) obtained in the U-space as elaborated by Kiureghian [2005] and Lemaire [2005]. The derivation of this importance factor (γ) starts with the isoprobabilistic transformation (transformation between physical and standardized random variables) **u=T(x)** which is linearised at the design points:

$$\mathbf{u} \cong \mathbf{u}^* + J_{u,x}(\boldsymbol{x} - \boldsymbol{x}^*) \tag{2.52}$$

We then could replace the coordinate $\mathbf{x}$ with a vector $\hat{\mathbf{x}}$ (defined below), that differs only slightly from $\mathbf{x}$, allowing the approximation sign to be replaced with an equality:

$$\mathbf{u} = \mathbf{u}^* + J_{u,x}(\hat{\boldsymbol{x}} - \boldsymbol{x}^*) \tag{2.53}$$

Alternatively, Equation 2.53 can also be written as:

$$\hat{\mathbf{x}} = J_{x,u}(\mathbf{u} - \mathbf{u}^*) + \mathbf{x}^* \tag{2.54}$$

Since $\hat{\mathbf{x}}$ is a linear function of $\mathbf{u}$ and given that $\mathbf{u}$ has a standard normal distribution, $\hat{\mathbf{x}}$ consequently will also have a standard normal distribution with moments (mean and covariance):

$$\begin{aligned} \mathbf{M}_{\hat{X}} &= \boldsymbol{x}^* - J_{x,u}\boldsymbol{u}^* \\ \mathbf{cov}_{\hat{X}\hat{X}} &= J_{x,u} \cdot {J_{x,u}}^{\mathrm{T}} \end{aligned} \tag{2.55}$$

Using these moments based on the linear approximation of $\mathbf{u}$ is the reason $\hat{\mathbf{x}}$ is known as the "equivalent normal" of $\mathbf{x}$ at the design point. By normalizing the linearized limit-state function in Equation 2.39 and substituting the $\mathbf{u}$ from Equation 2.53 to the equation, we then obtain a linearized and normalized version of the limit-state function:

$$\frac{G(\mathbf{u})}{\|G(\mathbf{u}^*)\|} = -\hat{\boldsymbol{\alpha}} J_{u,x}(\hat{\boldsymbol{x}} - \boldsymbol{x}^*) \tag{2.56}$$

It can be shown that the above formulation has expectation β and variance 1, which is consistent with the original FORM solution and allows the variance and covariance matrix of the linearized and normalized limit-state function to be written as:

$$\mathbf{Var}\left[\frac{G(\mathbf{u})}{\|G(\mathbf{u}^*)\|}\right] \cong -J_{u,x}\hat{\boldsymbol{\alpha}}\mathbf{cov}_{\hat{X}\hat{X}}\hat{\boldsymbol{\alpha}}^T {J_{u,x}}^T = 1 \tag{2.57}$$

Expanding the covariance matrix ($\mathbf{cov}_{\hat{X}\hat{X}}$) to:

$$\mathbf{cov}_{\hat{X}\hat{X}} = \boldsymbol{D}_{\hat{X}}\boldsymbol{D}_{\hat{X}} + (\mathbf{cov}_{\hat{X}\hat{X}} - \boldsymbol{D}_{\hat{X}}\boldsymbol{D}_{\hat{X}}) \tag{2.58}$$

and substituting into Equation 2.57 results in the following expression:

$$\mathbf{Var}\left[\frac{G(\mathbf{u})}{\|G(\mathbf{u}^*)\|}\right] = \boldsymbol{J}_{u,x}\boldsymbol{\alpha}\boldsymbol{D}_{\hat{X}}\boldsymbol{D}_{\hat{X}}{}^{\mathrm{T}}\boldsymbol{J}_{u,x}{}^{\mathrm{T}}\boldsymbol{\alpha}^{\mathrm{T}} + \boldsymbol{J}_{u,x}\boldsymbol{\alpha}(\mathbf{cov}_{\hat{X}\hat{X}}\text{-}\boldsymbol{D}_{\hat{X}}\boldsymbol{D}_{\hat{X}}{}^{\mathrm{T}})\boldsymbol{J}_{u,x}{}^{\mathrm{T}}\boldsymbol{\alpha}^{\mathrm{T}} = 1 \tag{2.59}$$

It is clear from the equation that $\boldsymbol{\alpha}\boldsymbol{J}_{u,x}\hat{\boldsymbol{D}}$ in the first term represents the contributions of the variance of the individual variables $\hat{\boldsymbol{x}}$ to the variance of the linearized limit-state function and thus, the elements of this vector can be considered as indicators of the importance of the elements of $\mathbf{x}$ on the original X-space. Because of the covariance term, the sum of the individual contribution does not equal to unity and therefore it has to be normalized. The normalized vector of this individual contribution is called γ which is defined as the importance factor of variables in the original space.

$$\gamma = \frac{\boldsymbol{\alpha}.\boldsymbol{J}_{u,x}.\boldsymbol{D}_{\hat{X}}}{\left\|\boldsymbol{\alpha}.\boldsymbol{J}_{u,x}.\boldsymbol{D}_{\hat{X}}\right\|} \tag{2.60}$$

Where:

$\boldsymbol{J}_{u,x}$ = Jacobian of the transformation from U- to X-space at the design point
$\boldsymbol{\alpha}$ = Sensitivity factor at the design points
$\boldsymbol{D}_{\hat{X}}$ = Diagonal matrix of standard deviations of $\mathbf{x}^*$
$\mathbf{cov}_{\hat{X}\hat{X}}$ = Covariance matrix of $\mathbf{x}^*$

Finally, it is important to recall once again that $\boldsymbol{D}_{\hat{X}}$ and $\mathbf{cov}_{\hat{X}\hat{X}}$ are the approximation of those of $\mathbf{x}$.

2.9 PARTIAL SAFETY FACTOR

This section explains how partial safety factors could be derived for the case of independent and dependent variables.

2.9.1 Independent Variables case

The essence of the semi-probabilistic calculation is to find the design points of load (S_d) and resistance (R_d) by assigning the partial safety factors to the characteristic values of load (S_{kar}) and resistance (R_{kar}), respectively. Figure 2.20 demonstrates the concept of the partial safety factor. Eurocode 1990 defines characteristic value as the representative value of load or resistance variable with a certain probability of being exceeded by unfavorable values during some reference period. On the other hand, the design value is the value with the highest joint probability density in the failure region in a standard normal space.

Based on the their definition in the previous paragraph, the partial safety factors for the load (γ_S) and resistance (γ_R) thus can be written as:

$$\begin{aligned}\gamma_S &= \frac{S_d}{S_{kar}} \\ \gamma_R &= \frac{R_{kar}}{R_d}\end{aligned} \tag{2.61}$$

The partial safety factors obtained from Equation 2.61 are usually greater than 1. However, if a fairly high characteristic value is selected, it is possible that the associated coefficient is less than 1. Eurocode 1990 recommends using 95-quantile and

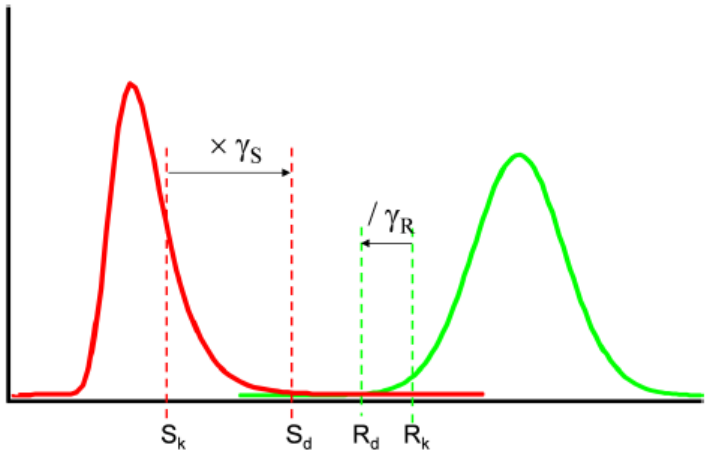

Figure 2.20: Probability density functions showing the variation in load (red) and resistance (green). The design values are derived in such a way that the structure meets a certain reliability target prescribed in the relevant standard. Jonkman et al. [2017]

5-quantile of the distribution under consideration as the characteristic values for load effect and resistance, respectively. If the values recommended by the Eurocode are used, the characteristic values could be computed as:

$$\begin{aligned} P(S \leq S_{kar}) = 0.95 \longrightarrow S_{kar} &= F_S^{-1}(0.95) \\ P(R \leq R_{kar}) = 0.05 \longrightarrow R_{kar} &= F_R^{-1}(0.05) \end{aligned} \tag{2.62}$$

As an alternative, a nominal value could also be used for the characteristic value as long as it is practical, easy to understand, and approved by the engineers who are going to use it. On the other hand, The design values of load effects (S_d) and resistance (R_d) are determined such that the probability of having a more unfavourable values equal to:

$$\begin{aligned} P(S > S_d) = \phi(\alpha_S * -\beta_t) \longrightarrow S_d &= F_S^{-1}(\phi(\alpha_S * -\beta_t)) \\ P(R \leq R_d) = \phi(\alpha_R * -\beta_t) \longrightarrow R_d &= F_R^{-1}(\phi(\alpha_R * -\beta_t)) \end{aligned} \tag{2.63}$$

where:

α_S = sensitivity factors for load variables, values are negative
α_R = sensitivity factors for resistance variables, values are positive
$F_S(s)$ = distribution function of the load variable
$F_R(r)$ = distribution function of the resistance variable
β_t = prescribed target reliability index

Combining Equation 2.61, Equation 2.62, and Equation 2.63, we come up with:

$$\begin{aligned} \gamma_S &= \frac{F_S^{-1}(\phi(\alpha_S * -\beta_t))}{F_S^{-1}(0.95)} \\ \gamma_R &= \frac{F_R^{-1}(0.05)}{F_R^{-1}(\phi(\alpha_R * -\beta_t))} \end{aligned} \tag{2.64}$$

The α-values used for partial safety factor calculation should be determined using FORM analysis. Alternatively, Eurocode 1990 provides standardized α-values for the load effects and resistances, for which these values are considered independent of an arbitrary specific case Jonkman et al. [2017]. The values are -0.7 and 0.8 for load and resistance variables, respectively. Moreover, the target reliability index should be set such that a structure is adequately safe. Table 2.6 shows the target reliability index for a general structure recommended by Eurocode 1990.

Table 2.6: Recommended minimum values for reliability index (ultimate limit states) (Eurocode 1990)

Reliability Class	t_{ref} = 1 year	t_{ref} = 50 years
RC3	5.2	4.3
RC2	4.7	3.8
RC1	4.2	3.3

When the main source of uncertainty is independent, the following equation can be used to convert the reliability target for t_{ref}=1 year (β_1) to different reference periods:

$$\phi(\beta_n) = [\phi(\beta_1)]^n \tag{2.65}$$

where β_n is the reliability index for t_{ref}= n years. Finally, a structure is designed such that the design value of resistance is larger than the design value of the load in the semi-probabilistic design. Therefore, the following requirement should be checked at the end of the design calculation:

$$\frac{R_k}{\gamma_R} \leq \gamma_S S_k \tag{2.66}$$

2.9.2 Dependent Variables Case

The Equation 2.63 is valid only for the independent variables case. According to Lemaire [2005], in the event of dependent variables, the Rosenblatt transformation has to be used to find the design points ($\boldsymbol{x}^*$). Let x_1, x_2, and x_2 be three dependent variables connected through a Vine Copula. The design values of those variables ($\boldsymbol{x}^*$) then could be computed as:

$$\begin{aligned}
F_1(x_1^*) &= \phi(-\alpha_1 * \beta_t) \\
x_1 &= F_1^{-1}(F_1(x_1^*)) \\
F_{2|1}(x_2^*|x_1^*) &= \phi(-\alpha_2 * \beta_t) \\
F_2(x_2^*) &= h_{12}^{-1}(F_{2|1}(x_2^*|x_1^*)|F_1(x_1^*)) \\
x_2^* &= F_2^{-1}(F_2(x_2^*)) \\
F_{3|21}(x_3^*|x_2^*, x_1^*) &= \phi(-\alpha_3 * \beta_t) \\
F_{3|2}(x_3^*|x_2^*) &= h_{31|2}^{-1}(F_{3|21}(x_3^*|x_2^*, x_1^*)|F_{1|2}(x_1^*|x_2^*)) \\
F_3(x_3^*) &= h_{23}^{-1}(F_{3|2}(x_3^*|x_2^*)|F_2(x_2^*)) \\
x_3^* &= F_3^{-1}(F_3(x_3^*))
\end{aligned} \tag{2.67}$$

Recall that the h-function is defined as the conditional distribution function of a bivariate copula, such that:

$$\begin{aligned}
h_1(F_2(x_2)|F_1(x_1)) &= P(X_2 < x_2|X_1 < x_1) = \frac{\delta C(F_1(x_1), F_2(x_2))}{\delta F_1(x_1)} \\
h_2(F_1(x_1)|F_2(x_2)) &= P(X_1 < x_1|X_2 < x_2) = \frac{\delta C(F_1(x_1), F_2(x_2))}{\delta F_2(x_2)}
\end{aligned} \tag{2.68}$$

It should be noted that Equation 2.67 needs to be solved from top to bottom. Consequently, the order of the variables in Rosenblatt transformation will influence the design points.

Finally, after the design values are obtained, the partial factors for load (S) and resistance (R) could be determined using the following:

$$\gamma_S = \frac{S(x^*)}{S(x_{kar})}$$
$$\gamma_R = \frac{R(x^*)}{R(x_{kar})} \tag{2.69}$$

2.10 ECONOMIC OPTIMISATION

We can always invest more in the structure to reduce failure probability. However, the question is, "How much do we need to spend to have a safe enough structure?". One way to answer the question is by performing economic optimization calculation. Van Dantzig developed this method in 1956 when he tried to determine the most optimum dike's height for South Holland after a storm surge disaster occurred in 1953.

Figure 2.21 illustrates the basic concept of economic optimization. From the figure, it is evident that the efficiency of safety investments and the failure consequences influence the optimum reliability level of a structure. Logically, if the failure of a structure leads to catastrophic consequences, a high investment cost might be worth it to prevent failure to happen. Conversely, a high investment cost is not needed when the consequences of failure are negligible.

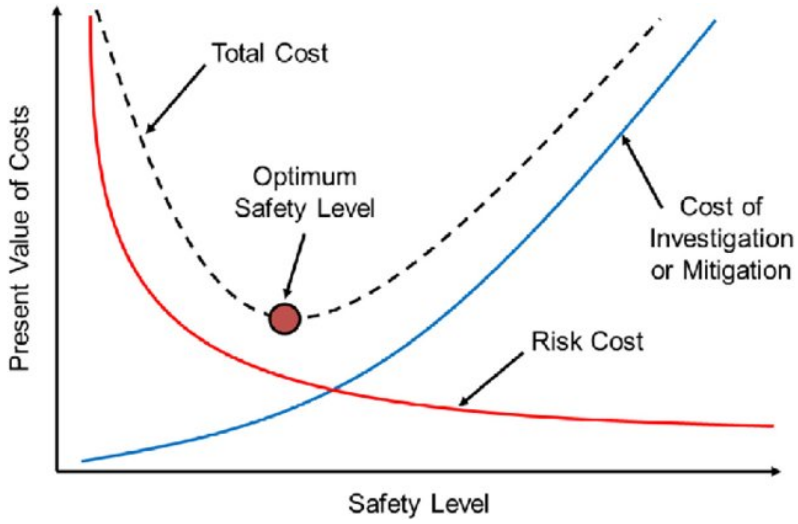

Figure 2.21: Economic optimisation, costs, risks and total costs as a function of the failure probability of the system

In the economic optimisation method, a total cost (C_{tot}) is calculated. This total cost basically is the sum of the present value of the risk (C_R) and also, the cost of safety investment measures (C_i) . This can be formulated as follow:

$$C_{tot} = C_i + C_R$$
$$C_R = \sum_{t=1}^{T} \frac{C_f}{(1+r)^t} \Delta P_{f(t)} \tag{2.70}$$

Where:

C_{tot} = Total cost (€)
C_i = Mitigation or safety investment cost (€)
C_R = Capitalized risk cost (€)
C_f = Failure consequence (€)
$P_{f(t)}$ = Probability of failure at year t
r = Interest rate (%)
T = Reference period

The total cost function in Equation 2.70 implicitly is the function of the fender's reliability level, as the investment and the capitalized risk cost are both dependent on the fender's reliability level. The investment cost (C_i) will become a function of the failure probability of the system since increasing the safety will lead to an increase of cost. Conversely, increasing the safety of system will reduce the risk cost (C_R). Therefore, our aim to find the optimum reliability target (β*), where the total cost of investment and risk cost is minimum. This can be formulated as:

$$\min \{C_{tot}(\beta^*) = C_i(\beta^*) + C_R(\beta^*)\} \tag{2.71}$$

At the optimum reliability target (β*), the following condition is valid:

$$\frac{dC_{tot}}{dP_f} = 0 \tag{2.72}$$

3 DETERMINISTIC METHOD

In this chapter, two fender designs were made for a container berth at Port of Rotterdam, which was used as the study case in this thesis. The first design was made assuming a single fender contact, while the second was assuming multiple fender contact. Both designs were made in accordance with the deterministic method adopted in PIANC [2002]. Later in Chapter 4, the reliability of the selected fenders were assessed.

3.1 METHOD

The design method adopted by PIANC guidelines is already described in the first section of Section 2.1. In essence, PIANC [2002] recommends appropriate design values of the variables (e.g. displacement, berthing velocity, angle) for the calculation of the berthing energy. Subsequently, an abnormal berthing coefficient (C_{ab}) is applied to the computed berthing energy. Finally, the appropriate fender size and absorption capacity are determined based on the abnormal berthing energy, for which the absorption capacity of the selected fenders has to be higher than the abnormal berthing energy. The design process is summarized in Figure 3.1.

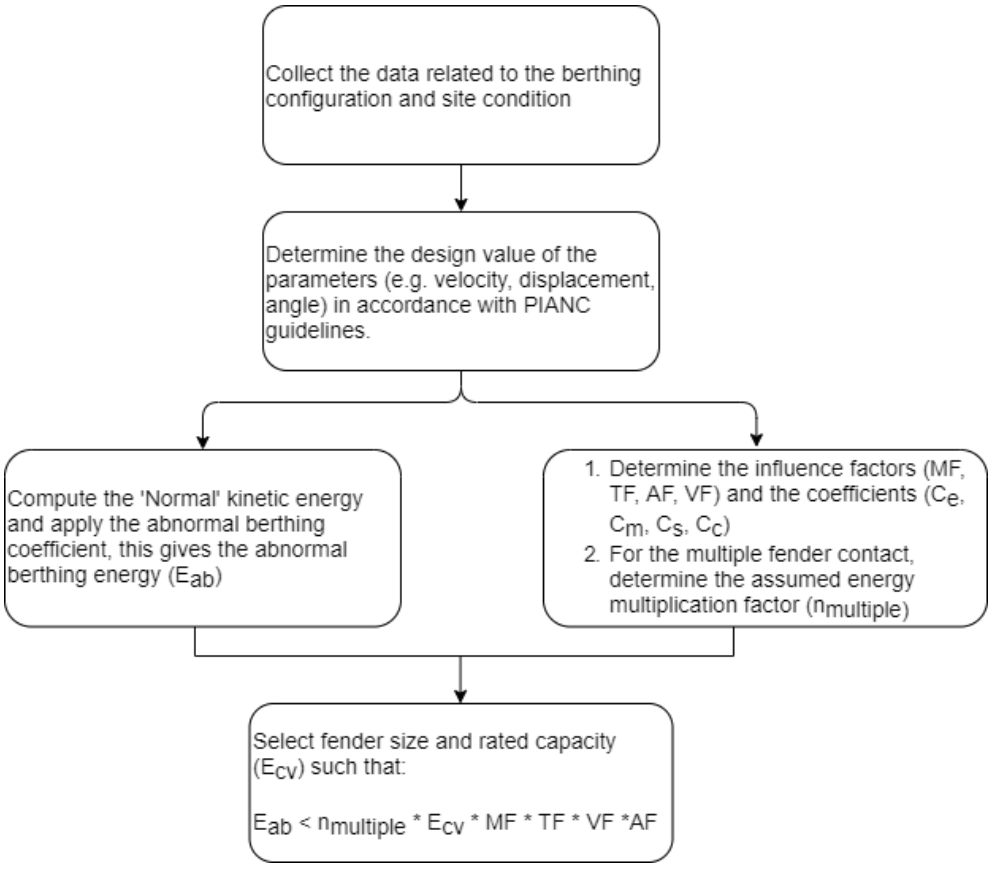

Figure 3.1: Flow chart of fender designs based on deterministic approach

3.2 DATA COLLECTION

This study used the field measurement data to derive insight into the uncertainties of stochastic variables. From October to December 2011, Port of Rotterdam Authority collected berthing records of large sea-going vessels. Figure 3.2 shows the location of the measurement. As could be seen from the layout, the navigation conditions are relatively sheltered, e.g. low tidal current, low wind speed, and small waves.

The type of berthing in these berths is a parallel landing procedure, e.g. the vessels is stopped 20-30 m in front of the fender line and then gently pushed towards the marine structure using tug boats. Furthermore, it is known that the nautical depth at the container berths is approximately 17 m. The marine structure is generally a rigid quay wall, equipped with buckling fenders having a fender pitch of approximately 14 m.

Figure 3.2: The location of the measurement in Port of Rotterdam Roubos et al. [2016]

The berthing operations were recorded using a technology developed by Trelleborg Marine Systems, 'SmartDock laser LITE.' This technology utilizes a portable laser to measure the data, as illustrated in Figure 3.3. A more detailed information regarding the technology could be found in Roubos et al. [2016].

There are 177 berthing record data of large container vessels collected by Port of Rotterdam's authority during the measurement period. The observed data is presented in Figure 3.4 and described in Table 3.1. The data shows that the displacement of the container vessel is varying from 8000 ton to approximately 260,000 ton. Moreover, it is observed that in general, the berthing angle is fairly low, with an average of 0.3^o.

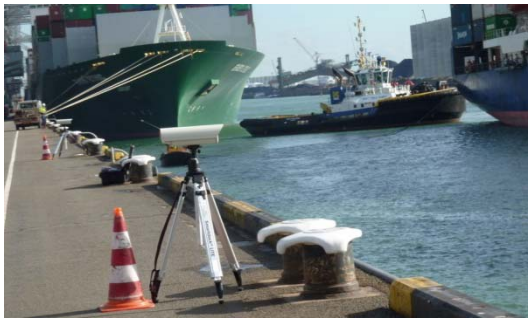

(a)

(b)

Figure 3.3: (a) Smartdock laser lite system (b) Software interface

Table 3.1: Description of the collected data

Variables	Unit	Mean	Std. deviation	Max	Min
Displacement	ton	85,414	58,453	260,000	8000
Velocity	cm/s	3.9	2.3	10.6	0.1
Angle	degree	0.3	0.3	1.5	0

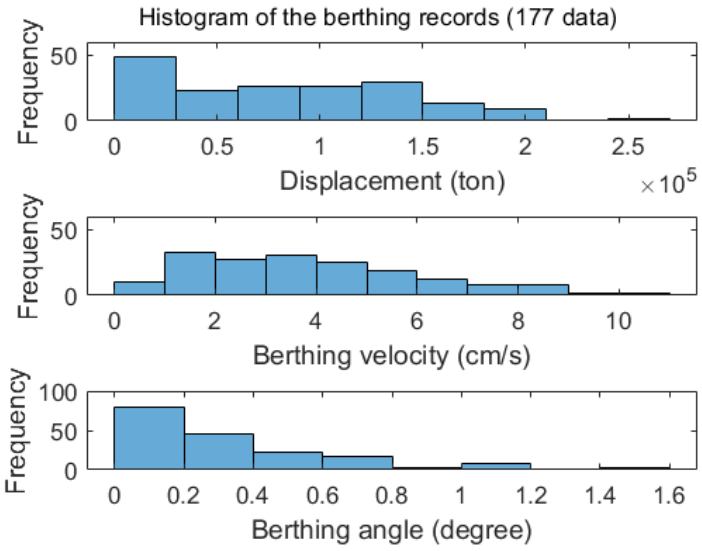

Figure 3.4: Histogram of the observed data

3.3 DETERMINATION OF FENDER SIZE AND CAPACITY BASED ON PIANC 2002

3.3.1 Design Values

Based on the available information provided in Section 3.2, the design values for the parameters could be determined. Subsequently, the associated coefficients and influence factors were computed based on the PIANC [2002] guideline and the fender design manual published by Trelleborg [2018]. In the deterministic method, the design is often made considering the most unfavourable condition. For instance, the maximum value is used for the load variables, whereas minimum value is used for the resistance variables. The values used for the design calculation are presented in Table 3.2.

Table 3.2: Input parameters for the deterministic design

Parameters	Unit	Design Value	Source
Velocity	cm/s	10	Figure 2.3 (sheltered berthing condition)
Displacement	ton	260,000	Table 3.1 (The maximum value)
Berthing angle	degree	1.5	Table 3.1 (The maximum value)
Temperature	^oC	30	Based on the local information
Nautical depth	m	17	Section 3.2
Fender pitch	m	14	Section 3.2

Coefficients	Unit	Design Value	Source
C_e	[-]	0.51	Equation 2.4
C_m	[-]	1.8	Table 2.2 (PIANC method)
C_s	[-]	1	Table 2.3
C_c	[-]	1	Table 2.4
C_{ab}	[-]	1.5	Table 2.1 (for largest container vessel)

Influence Factors	Unit	Design Value	Source
VF	[-]	1.05	Figure 2.9
TF	[-]	0.98	Figure 2.11
MF	[-]	0.9	Section 2.1.3
AF	[-]	1	Section 2.1.3

3.3.2 Fender Selection

Based on the design parameters in Table 3.2, the kinetic and abnormal berthing energy were computed, and two fenders were subsequently selected. One fender was selected based on the assumption of single fender contact, whereas the other fender was chosen, taking into account the effect of multiple fender contact. In the second case, it was considered that three fenders absorb the berthing energy, in which the ship hits the middle fender first and that the adjacent fenders do not completely deflect Figure 3.5. This assumption of 3-fenders contact can be the worst-case scenario of multiple fender contact, where the minimum value of energy multiplication factor ($n_{multiple}$) was found, which equals to 1.76.

The results are then summarized in Table 3.3. The result shows that the abnormal berthing energy (E_{ab}) equals to 1790 kNm. Therefore, a fender with a height of 1.6 m and rated capacity (E_{cv}) of 1950 kNm was selected for a single fender contact assumption. Whereas, a smaller fender with a height of 1.4 m and rated capacity of 1140 kNm was chosen for multiple fender contact. It should be noted that the energy absorption capacity (E_{Fender}) for multiple fender contact is higher since three fenders contribute to absorbing the berthing energy. Furthermore, the result shows

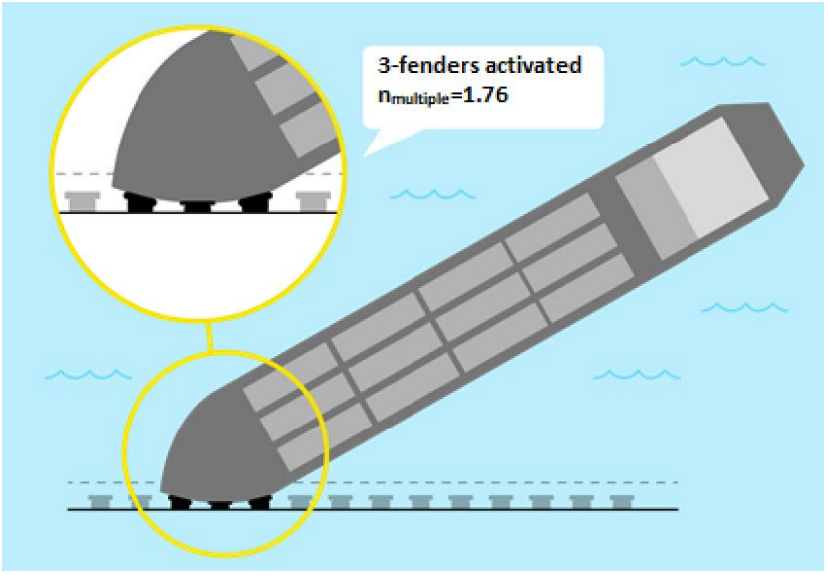

Figure 3.5: Assumption used for multiple fender contact calculation (3 fender contact)

that the absorption capacity of the selected fenders is higher than the abnormal berthing energy and thus, meeting the requirement prescribed in Equation 2.10.

Table 3.3: The design load and the capacity of selected buckling SCN fenders

Cases	Berthing Energy (kNm)		Selected Fenders			
	E_k	E_{ab}	Type	Height (m)	E_{cv} (kNm)	E_{Fender} (kNm)
Single Fender Contact	1193	1790	SCN1600	1.6	1950	1809
Multiple Fender Contact			SCN1400	1.4	1140	1861

The associated dimensions of the selected buckling fenders are then presented in Table 3.4 and illustrated in Figure 3.6.

Table 3.4: Dimensions of the selected fenders (Trelleborg [2018])

Type	SCN1600 F2.0	SCN1400 F1.4
H	1600 mm	1400 mm
⌀ W	2560 mm	2240 mm
⌀ U	1570 mm	1370 mm
⌀ B	2335 mm	2040 mm
⌀ S	1365 mm	1195 mm
Weight	4645 kg	3105 kg

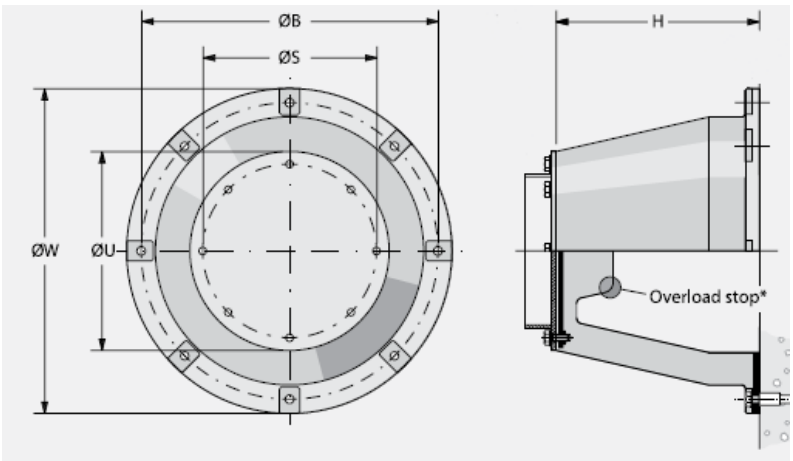

Figure 3.6: Dimension of super cone fender

3.4 SUMMARY

This chapter shows how fender size is determined based on the deterministic method of PIANC [2002]. Two fender designs were made for a container berth in Port of Rotterdam. This berthing facility was designed to be able to accommodate container vessels with the maximum displacement of 260,000 ton. The type of berthing in this berth is a parallel landing procedure with a reasonably low berthing angle (e.g. $< 1.5^o$). The first design was made assuming single fender contact, while the second assuming multiple fender contact. The field measurement data was used to derive the design values of the parameters. Moreover, a super cone fender (SCN) manufactured by Trelleborg was chosen for the designs.

Based on the deterministic method, the following fenders were selected:

Single Fender Contact	=	SCN1600 F2.0 (E_{cv}= 1950 kNm)
Multiple Fender Contact	=	SCN1400 F1.4 (E_{cv}= 1140 kNm)

It could be seen that a smaller fender size could be used when the contribution of multiple fender contact is taken into account.

4 RELIABILITY-BASED ASSESSMENT

This chapter aims to answer these following questions:

1. Is there a dependency between load variables? If yes, how could this be modelled?
2. How reliable is the fender designed following the PIANC guideline?
3. What and how significant is the influence of multiple fender contact and dependence between variables on the reliability of a fender system?
4. Which variables whose uncertainties have a dominant contribution to the uncertainty of the limit-state function?
5. What are the distributions of the kinetic energy and fender capacity?

The first section of this method discusses the method used to answer the questions above. Whereas, the results are presented in the subsequent sections.

4.1 METHOD

4.1.1 Reliability-based assessment

Figure 4.1 shows a step-by-step analysis of the method used to assess the reliability of the fenders selected in Chapter 3. In the reliability-based design, the uncertainties of design variables were taken into account and described using parametric distribution functions. In this thesis, the field measurement data was used to derive insight into the uncertainties of stochastic variables in this study. Therefore, the first step of the analysis was to select parametric distribution functions that can describe the observed data the best, based on the maximum-likelihood and the goodness-of-fit tests.

Kendall's tau independence test was performed to confirm the dependence between the load variables (e.g. berthing velocity, berthing angle, and vessel displacement). The dependence structure between those variables was then modelled using a Vine copula. Moreover, a berthing simulation was done in order to include the influence of multiple fender contact into the limit-state function.

Subsequently, the reliability of the fenders was estimated using FORM, and Monte Carlo simulation, where the solution algorithms proposed by Jiang et al. [2015] for Monte Carlo (Section 2.7.2) and FORM (Section 2.8.2) were used to take into account the dependence between the variables. The outputs of the reliability-based assessment are the reliability level of the fender system and the sensitivity factors of the design variables.

FORM is a faster method than Monte Carlo as it requires less computational effort. In addition to that, FORM also provides sensitivity factors of the random variables. However, FORM does not come without disadvantages. The probability of failure resulting from FORM could be inaccurate for a strongly non-linear limit-state function and a very low failure probability. Therefore, Monte Carlo simulation was performed to confirm the validity of the results of FORM. Furthermore, the influence of dependence and multiple fender contact was studied by comparing the results of the reliability-based assessment for the following four cases:

- Single fender contact & Independent variables
- Single fender contact & Dependent variables
- Multiple fender contact & Independent variables
- Multiple fender contact & Dependent variables

In the last section, the distributions of the berthing energy and fender absorption capacity were derived using Monte Carlo simulation.

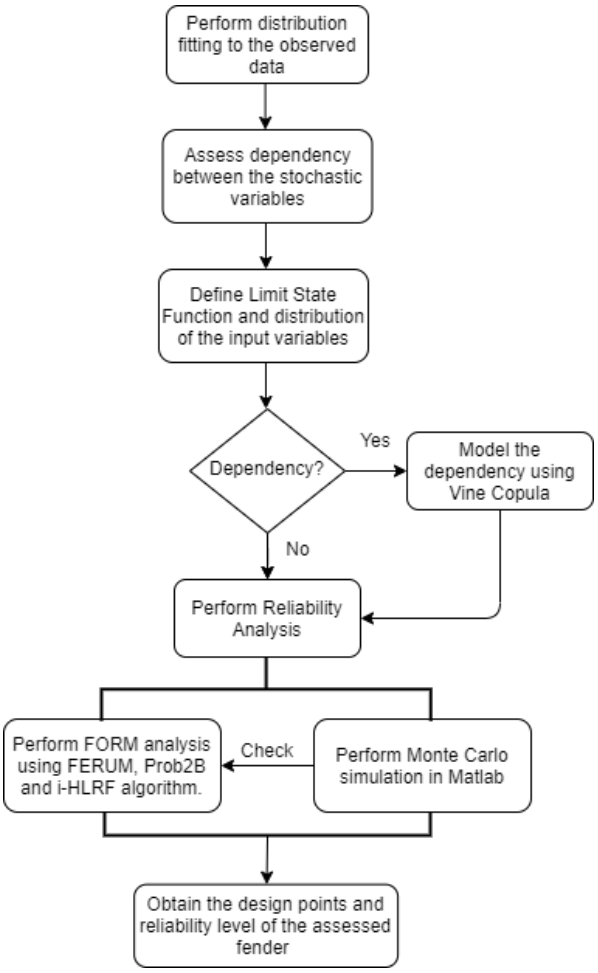

Figure 4.1: Flowchart of reliability analysis

4.1.2 Multiple Fender Contact Simulation

The energy absorption capacity of a fender system in the event of multiple fender contact depends on several factors such as berthing angle, bow radius, and fender spacing. This thesis derived the empirical relationship between the energy absorption capacity of a fender system with berthing angles and vessel sizes assuming a constant fender spacing of 14 m.

The simulation was done by simulating many berthing manoeuvres, each with different vessel size and berthing angle. For every berthing manoeuvre, the number of the fenders in contact with the vessel during berthing impact and the associated fender deflection were computed. Using the energy-deflection curve in Figure 2.7, the total energy that the fender system can absorb was determined. Figure 4.2 illustrates how the berthing simulation works and, what the inputs and outputs of the simulation are. Based on the simulation results, an empirical relationship was found between the energy multiplication factor, vessels' size, and berthing angle.

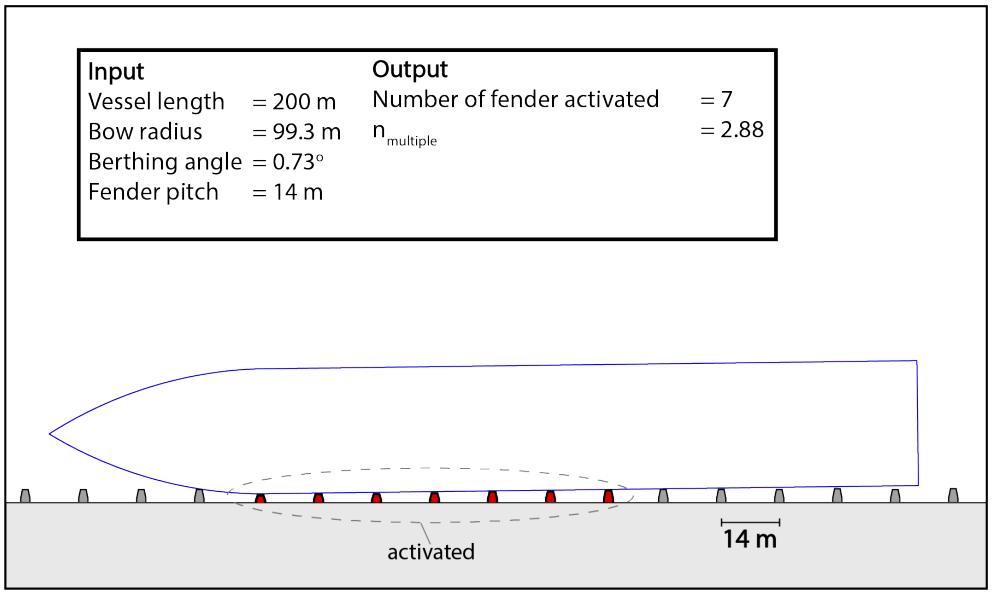

Figure 4.2: An illustration of the berthing simulation

The simulation was done based on these following assumptions:

1. The distance between fender is 14 m.
2. A super cone fender (SCN) with a height of 1.4 m was used in the simulation.
3. The maximum allowable deflection of the fender equals to the associated rated deflection of an SCN fender (72%).
4. Quarter point berthing was assumed.

4.1.3 Analysis Software

FORM calculation for the independent case was performed in Prob2B and FERUM. Prob2B is a probabilistic numerical toolbox developed by TNO Built Environment and Geo-sciences, while FERUM (Finite Element Reliability Using MATLAB) is an open-source MATLAB toolbox developed by researchers in UC Berkeley. Both tools can perform Monte Carlo simulation and FORM analysis. However, they are not yet capable of modelling asymmetric dependence structures such as those represented by Archimedean Copula. Therefore, the Vine Copula-FORM Solution Algorithm

developed by Jiang et al. [2015] was used in this thesis to incorporate the multivariate dependence into FORM. This algorithm was implemented in R as it already has Vine-Copula package that is built for dependence modelling.

4.2 RESULT OF DISTRIBUTION FITTING

Distribution fitting was performed for the 177 data collected from the measurement of berthing activities in Port of Rotterdam. The purpose of this distribution fitting is to select the most appropriate distribution family to describe the observed data. The maximum likelihood method was used to estimate the parameters of several candidate distribution functions, while the best candidate was determined based on the results of goodness-of-fit tests. There are five stochastic variables which were considered in this thesis; they are berthing velocity, displacement, berthing angle, manufacturing tolerance, and temperature.

4.2.1 Berthing velocity

Figure 4.3 shows the Log-normal, Weibull, Gamma, and Normal distribution fitted to the empirical probability density of the berthing velocity and Table 4.1 gives us the log-likelihood and also AIC value for each distribution function. It is found that the AIC value is the smallest for Weibull distribution. Moreover, the null hypothesis of the Kolmogorov-Smirnoff test is not rejected for the Weibull distribution. It is thus concluded that the distribution of the berthing velocity follows Weibull distribution with scale and shape parameters of 4.38 and 1.70, respectively.

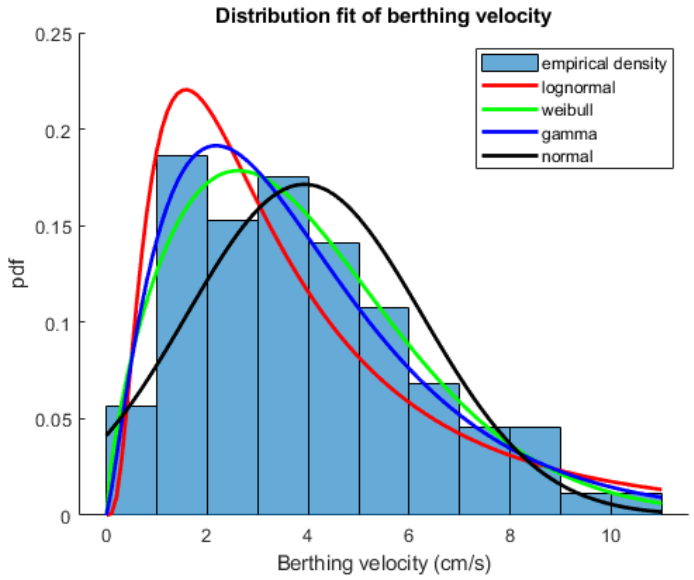

Figure 4.3: Berthing velocity distribution fit

Table 4.1: Akaike Information Criterion for Berthing Velocity

Distribution type	Parameters		ln (L)	Number of parameters (k)	AIC
	$\hat{P}_1$	$\hat{P}_2$			
Log-Normal	1.12	0.82	-415.25	2	834.50
Weibull	4.38	1.70	-387.88	2	779.76
Gamma	2.23	1.75	-392.34	2	788.68
Normal	3.92	2.32	-400.18	2	804.36

4.2.2 Berthing angle

Figure 4.4 shows several distribution functions fitted to the empirical density of the berthing angle. While the corresponding AIC and the log-likelihood values are given in Table 4.2.

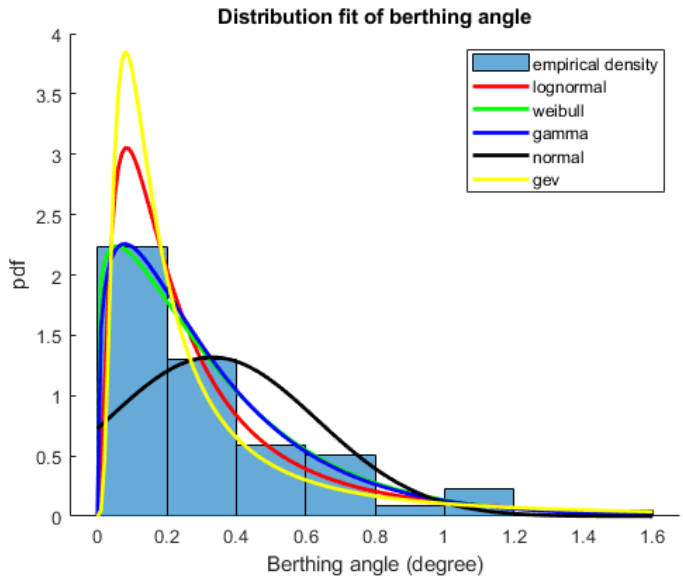

Figure 4.4: Berthing angle distribution fit

Table 4.2: AIC for the berthing angle

Distribution type	Parameters			ln (L)	(k)	AIC
	$\hat{P}_1$	$\hat{P}_2$	$\hat{P}_3$			
Log-Normal	-1.61	1.04	-	-27.79	2	59.58
Weibull	0.33	1.08	-	-25.40	2	54.80
Gamma	1.19	0.27	-	-26.02	2	56.04
Normal	0.32	0.30	-	-74.29	2	152.58
Generalized Extreme Value	0.79	0.123	0.128	-18.70	3	43.40

The Kolmogorov-Smirnoff and Chi-squared tests were performed to check which distribution fits the berthing angle data the best. Table 4.3 shows the result of this goodness of fit tests where 0 means the null hypothesis that the observed data comes from a specific distribution family is approved, whereas one is rejected. According to the test results, it is thus concluded that the observed data comes from the gamma distribution.

Table 4.3: The result of goodness of fit test

Test	Distribution			
	GEV	Log normal	Weibull	Gamma
KS test	1	1	1	0
Chi squared test	1	0	0	0

4.2.3 Displacement

In this thesis, the distribution of displacement was described using the uniform distribution (Figure 4.5) with lower and upper boundaries of 8000 ton and 260,000 ton, respectively.

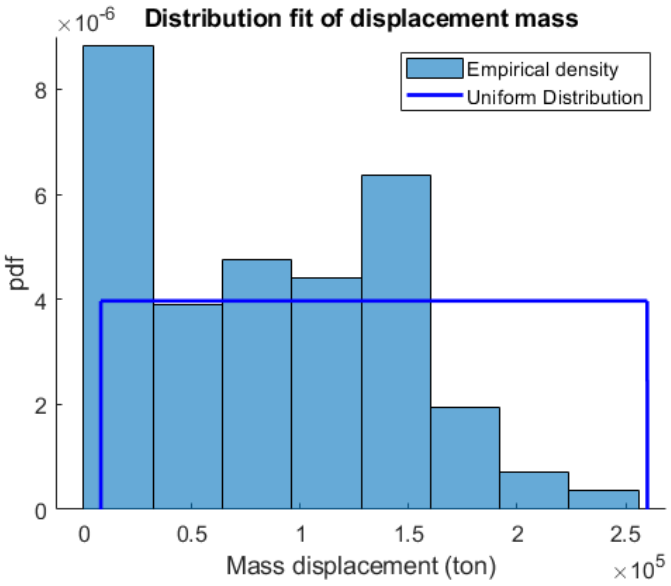

Figure 4.5: Displacement distribution fit

4.2.4 Temperature and Manufacturing tolerance

Figure 4.6 shows the distribution families used to describe temperature and manufacturing tolerance. Both variables were described using the normal distribution. The temperature was assumed to have a mean value of 15^{o} with a standard deviation of 5^{o}, based on the local information. On the other hand, the distribution of manufacturing tolerance was obtained from test results provided by one of the fender suppliers.

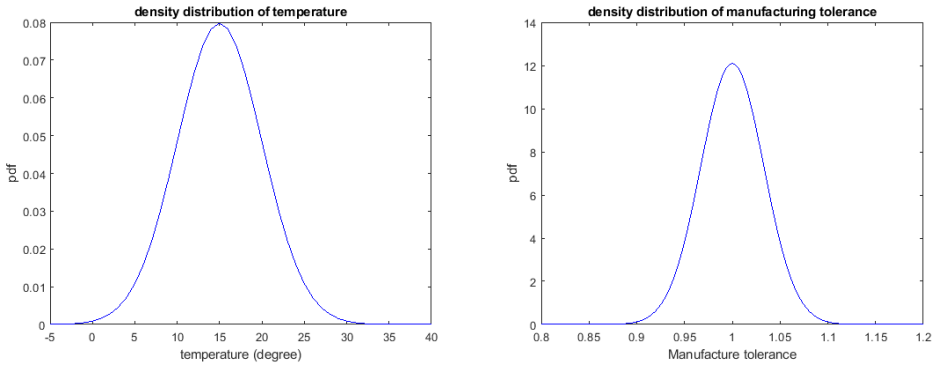

(a) (b)

Figure 4.6: Marginal distribution of (a) temperature (b) manufacturing tolerance

4.3 RESULT OF DEPENDENCE ANALYSIS

Figure 4.7 presents the bivariate plots of the design variables (berthing angle, velocity, and displacement) and also their associated Pearson's correlation coefficients. The figure shows that berthing velocity, berthing angle, and displacement are, to some extent, correlated. It could be seen that the larger vessels tend to have a lower berthing angle and berthing velocity. Moreover, it is observed that the dependence structures between the variables are not entirely linear.

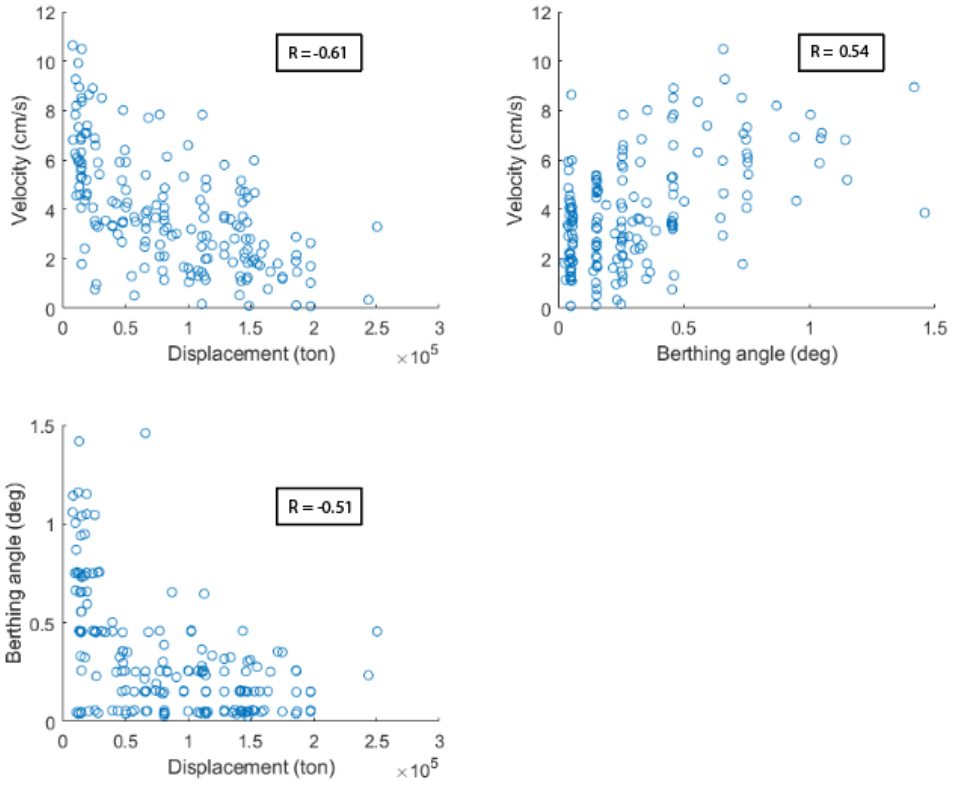

Figure 4.7: Bivariate plots of the observed data

In order to confirm whether or not the monotonous relationship exists between the variables, Kendall's tau independence test was performed for the empirical copula shown in Figure 4.8. The result of the independence test is presented in Table 4.4. The result shows that all of the p-values equal to 0. Given the results, the null hypothesis of independence was therefore rejected, and the dependence between variables was confirmed.

Table 4.4: Result of independence test based on Kendall's tau

Variables		Statistic Value	p-value
Displacement	Angle	7.21	$5.4*10^{-13}$
Displacement	Velocity	8.52	0
Angle	Velocity	5.95	$2.59*10^{-9}$

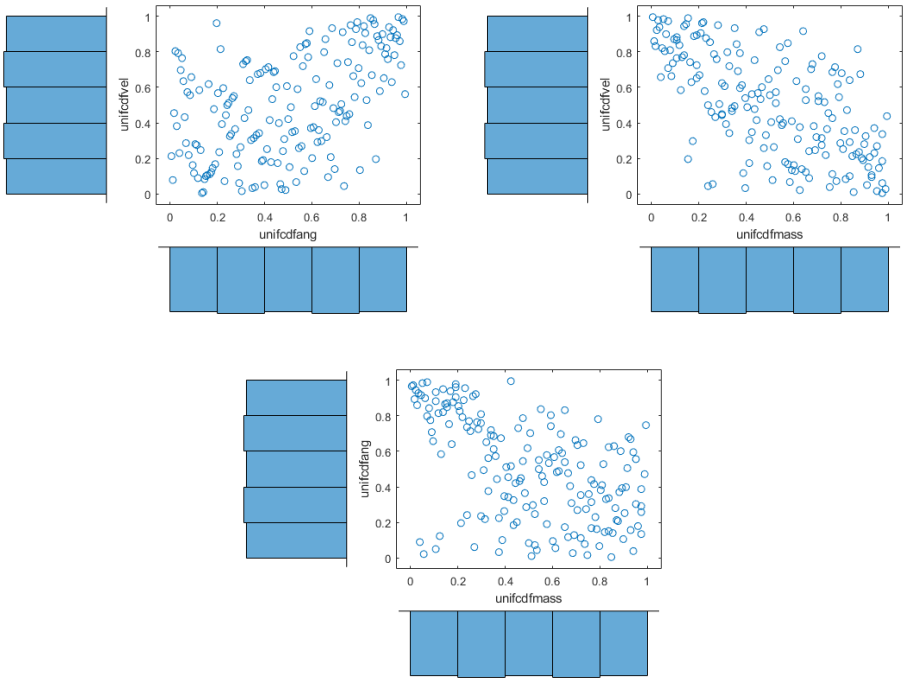

Figure 4.8: Empirical Copula

4.3.1 Vine Copula

Since the berthing velocity, berthing angle, and displacement, are to some extent correlated, a Vine-Copula structure was constructed to the model dependency between the variables. The first step in constructing the Vine copula model was to find the bivariate theoretical copulas that can adequately describe the empirical copula of the observed data (Figure 4.8), for which the Akaike Information Criterion was used as the main criteria in this thesis.

Figure 4.9 shows the Vine copula structure that has the smallest AIC value. The selected bivariate copulas and their associated parameters are presented in Table 4.5. All analysis was done in 'R' using the 'BiCopVineSelect' function.

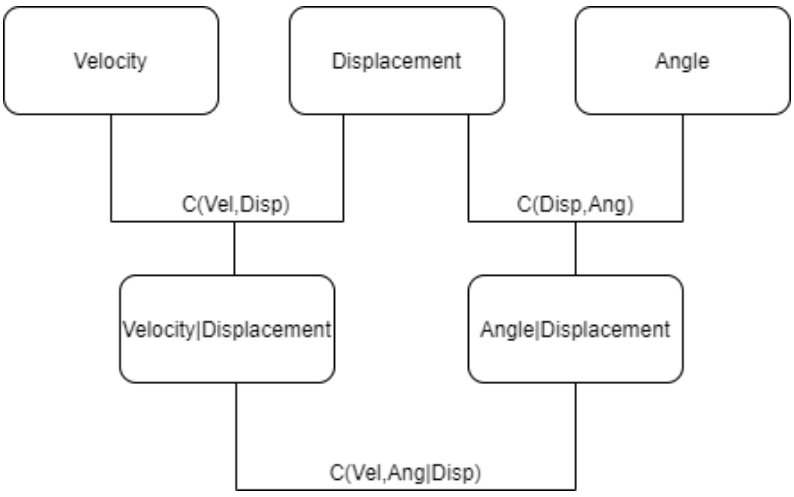

Figure 4.9: Selected Vine Copula structure based on the AIC value

Table 4.5: Summary of the most optimum Vine Copula tree structure

Variables	Copula	Parameter
Displacement-Angle	Clayton 270°	1.12
Velocity-Displacement	Gumbel 270°	1.69
Velocity-Angle | Displacement	Frank	1.35
log-Likelihood: 80.93	AIC: -155.86	

The goodness-of-fit of this Vine copula structure is presented in Appendix A. In general, it is found that the selected Vine copula could adequately describe the dependence structures between the variables. However, it should be noted that there are only 177 data, which is considered limited to derive Vine copula. Therefore, it was challenging to find Copula families that perfectly fits the data.

4.4 SIMULATION OF MULTIPLE FENDER CONTACT

Since the observed berthing angles are relatively low, the effect of multiple fender contact was taken into account via simulation (Figure 4.10). The result shows that in the event of low berthing angles, more fenders are activated. Hence, the energy absorption capacity of the fender system is much higher for low berthing angles. For high berthing angles (e.g.$> 1.5^o$), the energy multiplication factor ($n_{multiple}$) seems to reach a minimum value of approximately 2.8. Therefore, in the event of low berthing angle, it seems reasonable to use $n_{multiple}$=2.5-3 in the design calculation.

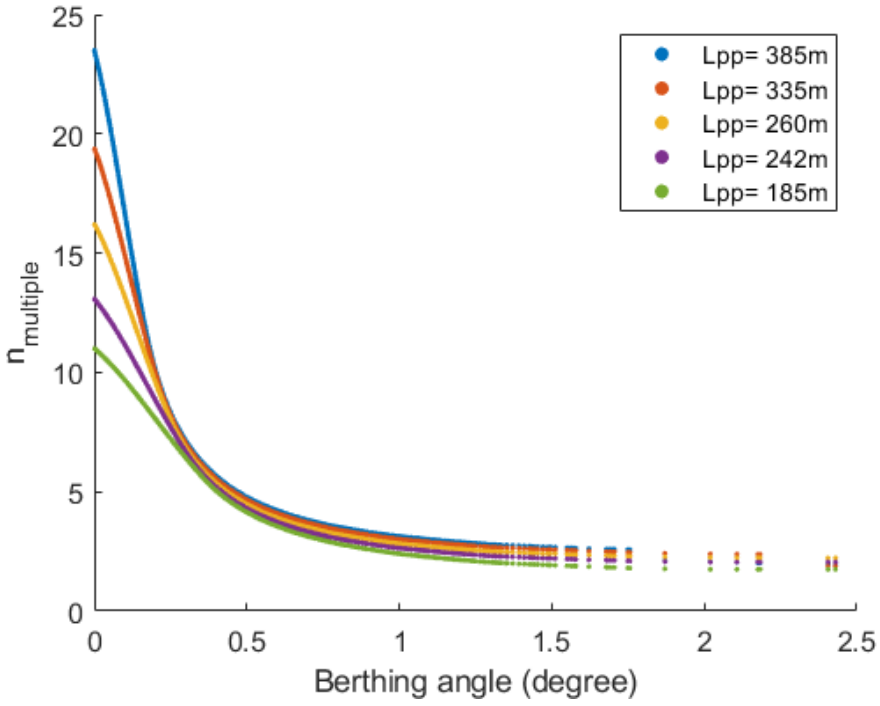

Figure 4.10: Scatter plot of the energy multiplication factor as a function of berthing angle for different vessel lengths (Pitch = 14 m)

Furthermore, the result shows that almost all fenders along a vessel's body are activated during parallel berthing. Consequently, longer vessels activate more fenders. While for high berthing angles, the number of fenders activated is influenced mainly by the bow radius, whose size difference is much smaller compared to the difference of vessel length, which explains why the values of $n_{multiple}$ are similar for high berthing angle. This is illustrated in Figure 4.11

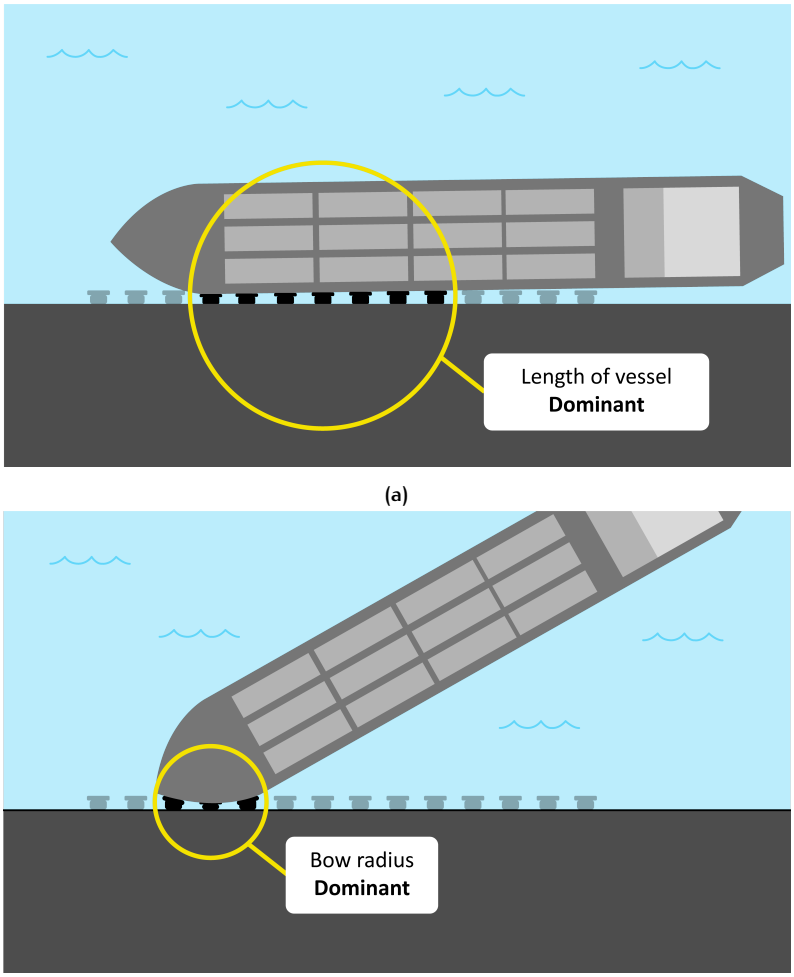

Figure 4.11: Multiple fender contact in the event of a (a) low berthing angle (b) high berthing angle

Based on the result of the simulation above, an empirical copula could be derived to approximate the energy factor:

$$
\begin{aligned}
n_{multiple} &= a * exp(-b * \alpha) + c \\
a &= \frac{(0.75 * Lpp)}{P} + 1 \\
b &= 2.85 * ln(Lpp) - 11.97 \\
c &= 1.43 * ln(Lpp) - 5.76
\end{aligned}
\tag{4.1}
$$

where:

$n_{multiple}$ = Energy multiplication factor
L_{PP} = Length between perpendiculars (m)
P = Fender pitch or distance between fenders (m)
α = Berthing angle in degree
b = Parameter estimated by curve fitting, function of Lpp
c = Parameter estimated by curve fitting, function of Lpp

4.5 RESULT OF RELIABILITY ANALYSIS

This section presents the results of the reliability-based assessment, e.g. failure probability and to what extent the design variables influence the fender reliability. The reliability level of the fenders selected according to the deterministic approach (Table 3.3) was assessed using FORM and Monte Carlo. The following equation gives the limit-state function, which was used for the reliability assessment:

$$G = n_{multiple} * E_{cv} * MF * VF * TF - 1/2 * M * v^2 * C_e * C_m \tag{4.2}$$

Table 4.6 summarizes the distribution families used to describe the uncertainties of the design variables. Other necessary information, such as selected fenders, nautical depth and distance between fenders, are described in Chapter 3.

Table 4.6: Distribution of the stochastic variables

Variables	Distribution	Parameters			
Velocity	Weibull	4.38 cm/s	Scale	1.7 cm/s	Shape
Displacement	Uniform	8000 ton	Lower bound	260,000 ton	Upper bound
Angle	Gamma	1.19^o	Scale	0.27^o	Shape
MF	Normal	1	Mean	0.033	Std dev
Temperature	Normal	15^oC	Mean	5^oC	Std dev

4.5.1 Single Fender Contact

A super cone fender with a rated energy capacity of 1950 kNm and a height 1.6 m was selected based on the deterministic approach. The reliability levels of this fender based on the FORM and Monte Carlo analysis are presented in Table 4.7. It could be seen that for the single fender contact scenario and independent variables, the approximate reliability level is 3.64. Whereas, when the variables are negatively correlated, the reliability level increases to 4.88.

The result, therefore, shows that the failure probability decreases significantly when the dependency between design variables is taken into account. This decrease is due to the lower likelihood of having a large vessel with a high berthing velocity when both variables are negatively correlated. Furthermore, as can be seen in Table 4.7, the FORM results from three different tools produce the same value. On the other hand, it appears that the failure probability of FORM is slightly higher compared to the Monte Carlo result. This slight difference is due to the slight outward curvature of the limit state function in the standard normal space that is linearized in FORM analysis.

Table 4.7: Probability of failure of a single fender per arrival (E_{cv}=1950 kNm)

Method	Independent		Dependent	
	P_f	β	P_f	β
Monte Carlo*	$(1.06 \pm 0.19) * 10^{-4}$	3.70	$(1.56 \pm 0.23) * 10^{-7}$	5.06
FORM (FERUM)	$1.35 * 10^{-4}$	3.64	-	-
FORM (Prob2B)	$1.35 * 10^{-4}$	3.64	-	-
FORM (i HL-RF)	$1.35 * 10^{-4}$	3.64	$5.30 * 10^{-7}$	4.88

*) Confidence interval of 95%

Sensitivity factors and design points

Table 4.8 and Table 4.9 show the sensitivity factors and design points for the independent and dependent cases, respectively. For the independent case, the sensitivity factor is the largest for the velocity (0.94), indicating that the uncertainty of berthing

velocity largely dominates the uncertainty of the limit-state function. This finding is consistent with the findings of Versteegt [2013] and Yamase et al. [2010].

Table 4.8: Sensitivity factors α and design points for independent case (single fender contact)

Variables	Independent		unit
	α	Design point	
Velocity	0.94	15.07	cm/s
Displacement	0.32	228,600	ton
Angle	$1.85*10^{-4}$	0.24	^{o}
Manufacturing tolerance	-0.057	0.99	[-]
Temperature	0.014	15.27	^{o}C

The sensitivity factors for the dependent case is given in Table 4.9. For the case of dependent variables, the importance factor (γ) is used instead of the sensitivity factor (α) to represent the contribution of each stochastic variable in the original space. When the design variables are uncorrelated, the value of γ equals to α. The value differs when the variables are dependent since the effect of dependence might amplify or reduce the contribution of the variables in the original space. The result shows that the γ-value of the velocity is the highest compared to other design variables, followed by the displacement in the second place.

Table 4.9: Sensitivity factors α and design points for dependent case (single fender contact)

Variables	Dependent			unit
	α	γ	Design point	
Velocity	0.70	0.83	14.97	cm/s
Displacement	0.71	0.55	230,530	ton
Angle	0.0001	$8.68*10^{-5}$	0.20	^{o}
Manufacturing tolerance	-0.068	-0.053	0.99	[-]
Temperature	0.018	0.014	15.44	^{o}C

The use of Vine-copula might cause unexpected local minima or maxima in the joint probability density, which is the condition where the neighbourhood of the design point does not significantly contribute to the failure probability Kiureghian [2005]. Therefore, besides performing Monte Carlo to confirm the FORM result, it is also suggested to check the results by plotting the joint distribution and the limit state function to ensure that the design points are the global solution, not the local one. Figure 4.12 shows the joint distributions plotted for each pair of the dependent variables. The figure shows that the design points are not located in the local maxima or minima since its neighbourhood contributes to the probability of failure.

In conclusion, berthing velocity is the most governing variable for single fender contact. Another variable with a substantial contribution to the variance of the limit-state function is displacement. The sensitivity factors for other variables are close to zero, indicating their negligible contributions to the limit-state function's uncertainty.

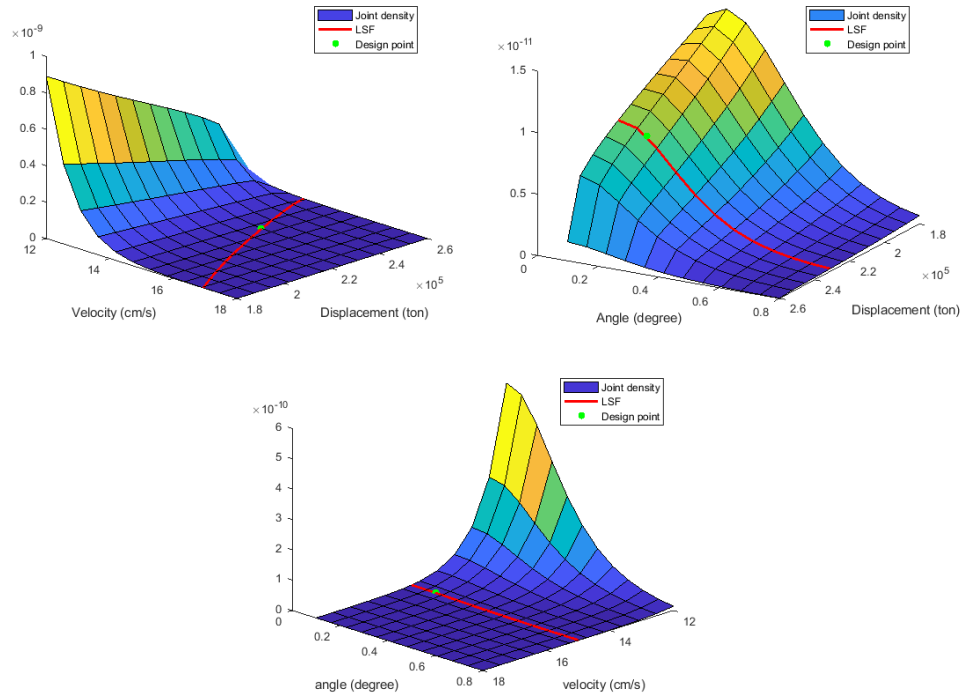

Figure 4.12: The joint probability density of the dependent variables around design points for single fender contact

4.5.2 Multiple Fender Contact

The deterministic approach results in the selection of a fender with a rated energy capacity of 1140.4 kNm and a height of 1.4 m in the event of multiple fender contact. Table 4.10 gives the result of the reliability assessment of this selected fender. The result shows that the failure probability of this fender is much lower than that of single fender contact, even though this fender has a smaller size and rated energy capacity. This is because, in the case of multiple fender contact, several fenders work together to absorb kinetic energy, providing higher energy absorption capacity and, thus, increasing the reliability of the fender system. The failure probability drops to 2.10^{-7} for the independent case and decreases, even more, to order of magnitude 10^{-12} when the effect of dependence is taken into account.

Table 4.10: Probability of failure per arrival for multiple fender contact case (E_{cv}=1140.4 kNm)

Method	Independent		Dependent	
	P_f	β	P_f	β
Monte Carlo*	$(4.30 \pm 1.33) * 10^{-8}$	5.20	$(1.62 \pm 1.27) * 10^{-12}$	6.96
FORM (FERUM)	$2.09 * 10^{-7}$	5.06	-	-
FORM (Prob2B)	$1.94 * 10^{-7}$	5.07	-	-
FORM (i HL-RF)	$2.20 * 10^{-7}$	5.05	$2.99 * 10^{-12}$	6.88

*) Confidence interval of 95%

Sensitivity factors and design points

Table 4.11 presents the sensitivity factors and design point for the independent case. The result shows that the berthing angle is still the most dominant variable. However, the result shows that now the contribution of berthing angle becomes much more important in the event of multiple fender contact as its sensitivity factor increases to 0.33. This increase is related to the fact that the number of fenders in contact with vessels is influenced by the berthing angle.

Table 4.11: Sensitivity factors α and design points for independent case (multiple fender contact)

Variables	Independent		unit
	α	Design point	
Velocity	0.91	19.88	cm/s
Displacement	0.25	235,800	ton
Angle	0.33	0.91	^{o}
Manufacturing tolerance	-0.07	0.99	[-]
Temperature	0.02	15.44	^{o}C

Table 4.12 presents the importance factor (γ) for the dependent case. The berthing velocity still has the strongest influence on the variance of the limit-state function in the original space, which is followed by displacement in the second place. The joint probability density around the design points in the original space is illustrated in the Figure 4.13. It could be seen from the figure that the limit-state function in the velocity-angle space is quite non-linear. However, the reliability results presented in Table 4.10 shows this non-linearity does not significantly influence the accuracy of FORM as the difference between FORM and Monte Carlo results is fairly low.

Table 4.12: Sensitivity factors α and design points for dependent case (multiple fender contact)

Variables	Dependent			unit
	α	γ	Design point	
Velocity	0.67	0.77	20.01	cm/s
Displacement	0.64	0.57	235,766	ton
Angle	0.36	0.28	0.85	^{o}
Manufacturing tolerance	-0.0799	-0.062	0.98	[-]
Temperature	0.021	0.016	15.70	^{o}C

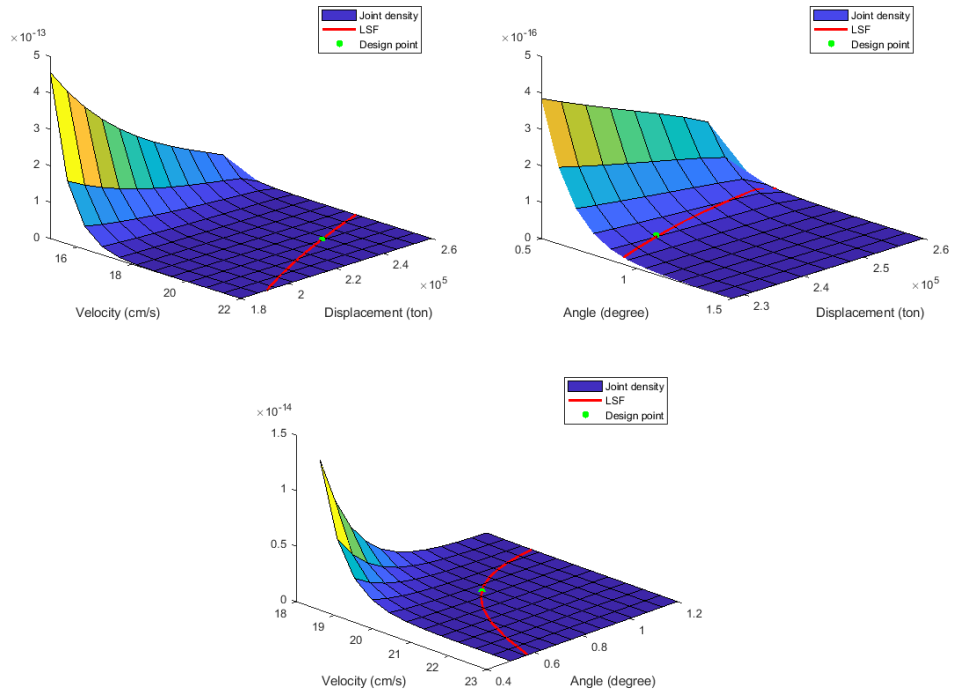

Figure 4.13: The joint probability density of the dependent variables around design points for multiple fender contact

4.6 DISTRIBUTION OF KINETIC ENERGY AND FENDER CAPACITY

This section presents the distribution of kinetic energy and fender capacity that were derived through a Monte Carlo simulation. Figure 4.14 shows distributions of the kinetic energy and fender capacity for the single fender contact berthing procedure. The figure on the left shows the distributions where the load variables are independent of each other. In comparison, the right figure shows the distributions where the load variables are negatively correlated.

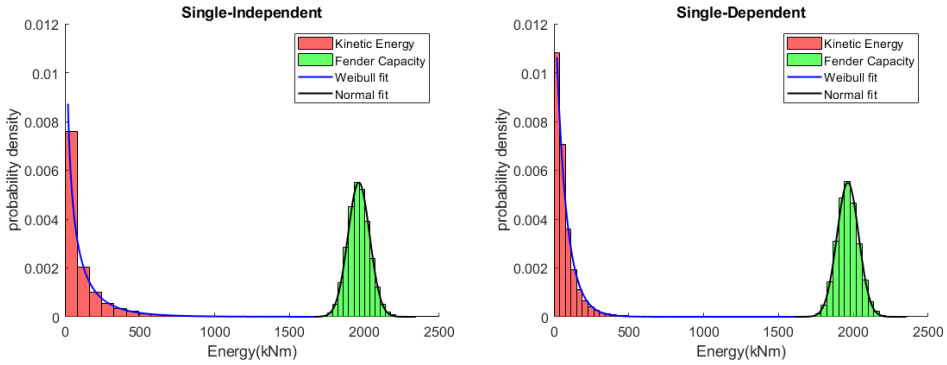

Figure 4.14: The distribution of the load and resistance for single fender case (E_{cv}=1950 kNm)

Distribution fitting was then performed for the derived distributions, for which the results are presented in Table 4.13. The kinetic energy seems to follow the same distribution as the berthing velocity, which is the Weibull distribution. On the other hand, the fender performance follows the same distribution as the manufacturing tolerance, which is the Normal distribution. The results, therefore, suggest that the distributions of kinetic energy and fender performance reflect the distribution of their basic variables.

Furthermore, the result reveals that the uncertainty of kinetic energy is much higher compared to the uncertainty of fender performance. Also, the standard deviation of the kinetic energy decreases when the negative dependence between the variables is taken into account. This decrease could be explained by the fact that the extreme kinetic energy occurs less as large vessels tend to have lower berthing velocities. According to Roubos et al. [2016], the uncertainty in kinetic energy could further be reduced by applying maxima distribution.

Table 4.13: Distribution families of the kinetic energy and fender capacity for the case of single fender contact

Independent case

Variables	Distribution	Par 1	Par 2	μ (kNm)	σ (kNm)	c.o.v
Kinetic Energy	Weibull	87.96	0.70	111.34	165.45	1.49
Fender Capacity	Normal	1962.50	72.50	1962.50	72.50	0.04

Dependent case

Variables	Distribution	Par 1	Par 2	μ (kNm)	σ (kNm)	c.o.v
Kinetic Energy	Weibull	69.96	0.98	70.79	78.42	1.10
Fender Capacity	Normal	1962.50	72.50	1962.50	72.50	0.04

Figure 4.15 presents the distribution of fender capacity for the multiple fender contact berthing procedure. It should be noted that the effect of multiple fender contact only alters the distribution of the fender capacity, whereas the distribution

of the kinetic energy remains the same. The figure shows that the distributions of the berthing angle and vessel size significantly influence the tail of fender capacity distributions. Moreover, it is found that these empirical distributions do not seem to fit any known parametric distribution families.

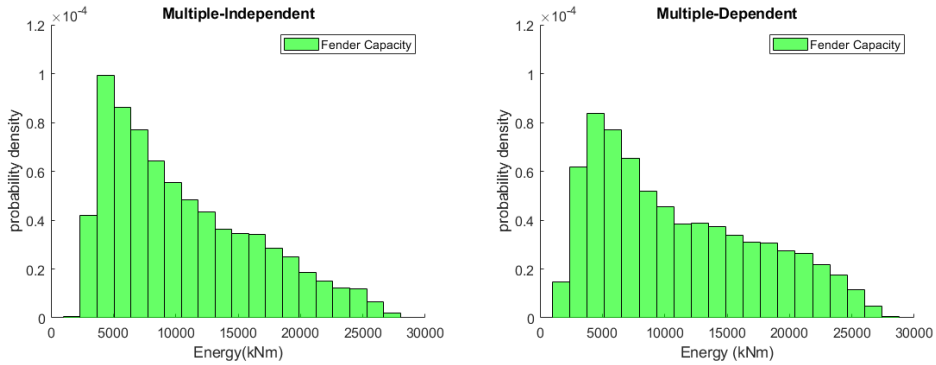

Figure 4.15: Distribution of fender capacity in the event of multiple fender contact (E_{cv}=1140.4 kNm)

4.7 DISCUSSION

4.7.1 How safe is the fender designed according to PIANC 2002 guideline?

This section discusses how safe is the fender system designed using PIANC [2002]. Figure 4.16 demonstrates the reliability of the selected fenders compared to the reliability targets proposed by a sub-group of PIANC WG211 (see Table 5.2), which is based on ISO2394 (2015).

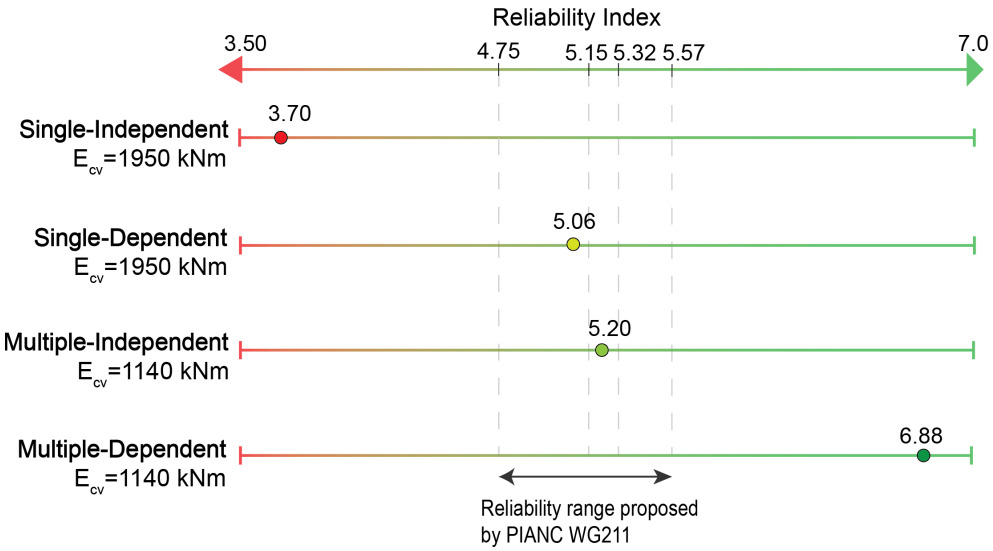

Figure 4.16: Illustration of the reliability of the selected fenders compared to the reliability targets proposed by PIANC WG211

The result shows that the reliability of the fender design is below the prescribed reliability target when the load variables are independent of each other, and only one fender absorbs the entire kinetic energy (single-independent case). The resulted fender design is safe when the effect of negative dependence between the vessel size with berthing velocity and berthing angle is taken into account. However, it should be noted that this negative dependence does not always exist, as it depends heavily

on the local port condition. In some terminals, the variables are independent of each other. Therefore, the appropriateness of the existing PIANC guidelines for a single fender contact type of berthing is still questionable.

On the other hand, for the case of multiple fender contact and independent variables case, the reliability of the selected fender is within the range of the prescribed reliability targets. For the case of Port of Rotterdam, where multiple fenders are activated during berthing, and the negative dependence exists between the variables, the reliability of the selected fender is far above the required reliability targets (over-designed).

Finally, based on the results presented in Figure 4.16 above, it could be concluded that the PIANC's method is sufficiently safe to use for the multiple fender contact berthing procedure. For the case of single fender contact, it is recommended to assign a higher safety factor or to use a higher design berthing velocity, especially when the failure of the fender results in a significant failure consequence. Furthermore, neglecting the negative dependence between variables might lead to a conservative fender design.

4.7.2 What if the Nataf transformation was used instead of the Rosenblatt?

In this study, the dependence between berthing velocity, berthing angle, and vessel displacement was modelled using the Rosenblatt transformation. Actually, besides the Rosenblatt transformation, the Nataf transformation could also be used to transform the random variables into a standard normal space and vice versa.

The Nataf transformation is considered more practical in most reliability cases. According to Kiureghian [2005], there are two reasons why: first, it only requires the correlation coefficient of the random variables and their coefficient of variation, whereas, for the Rosenblatt transformation, the joint cumulative distribution of the variables is needed. The second reason is that the transformation to the standard normal space is simple and does not depend on the ordering of the random variables. Hence, the Nataf transformation is mostly implemented in the probabilistic tools such as FERUM.

However, the Nataf transformation has several limitations. Firstly, since the Nataf transformation assumes Gaussian copula, it is therefore not able to accurately approximate non-normal marginal distributions, especially those with a large coefficient of variation (e.g. > 0.5). Moreover, the Nataf transformation is well defined if and only if the copula of the transformed random vector is Gaussian copula Lebrun and Dutfoy [2009]. In this thesis, the marginal distributions of the dependent variables are not Normal and they have a relatively high coefficient of variation (> 0.5). Moreover, the joint distributions of those variables are asymmetrical and thus, better modelled using the Archimedean copulas. Due to these reasons the Nataf transformation is not suitable for this thesis.

Table 4.14 compares the reliability of a fender system computed using the Vine Copula method with that computed using the Nataf transformation. The results are then plotted in Figure 4.17. It can be seen from the results that the reliability level of the fender computed using the Nataf transformation is slightly higher compared to the actual reliability obtained using the Vine Copula FORM algorithm. In other words, the reliability of the fender will be over-estimated when the Nataf transformation is used, particularly for the case of Port of Rotterdam.

Table 4.14: Reliability analysis results for Rosenblatt and Nataf transformations for single-dependent case

Rated capacity (E_{cv}) (kNm)	Rosenblatt transformation (Vine Copula)		Nataf transformation	
	β	P_f	β	P_f
1140	3.79	$7.53 * 10^{-5}$	4.18	$1.42 * 10^{-5}$
1300	4.04	$2.67 * 10^{-5}$	4.47	$3.89 * 10^{-6}$
1500	4.32	$7.80 * 10^{-6}$	4.80	$7.89 * 10^{-7}$
1700	4.58	$2.32 * 10^{-6}$	5.10	$1.66 * 10^{-7}$
1820	4.75	$1.01 * 10^{-6}$	5.27	$6.67 * 10^{-8}$
2175	5.15	$1.30 * 10^{-7}$	5.73	$4.81 * 10^{-9}$
2330	5.32	$5.18 * 10^{-8}$	5.92	$1.61 * 10^{-9}$
2580	5.57	$1.27 * 10^{-8}$	6.20	$2.82 * 10^{-10}$

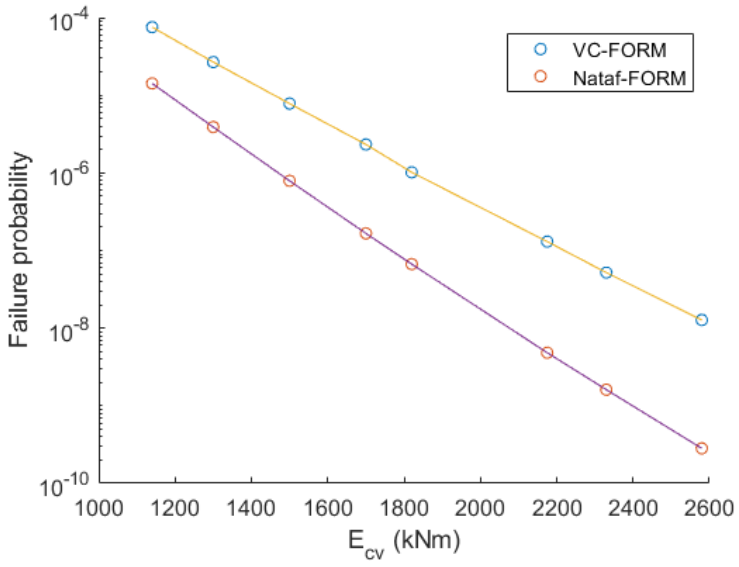

Figure 4.17: The reliability of a fender system computed using Rosenblatt and Nataf transformations

We can understand better the difference by looking at Figure 4.18. It could be seen from the figure that large vessels with high berthing velocity (shown as orange dots) were generated more for the Gumbel copula than for the Gaussian Copula, due to the tail dependence. In Gumbel copula, the dependence is stronger for one tail (Small vessels with higher velocity) than the other tail (Large vessels with lower velocity), where it is not the case for the Gaussian copula. It thus explains why the failure probability is underestimated when the Gaussian copula is assumed. Due to that reason, it is hence crucial to choose the right transformation and joint distribution when modelling dependence between the random variables; otherwise, the estimated reliability level might not be accurate.

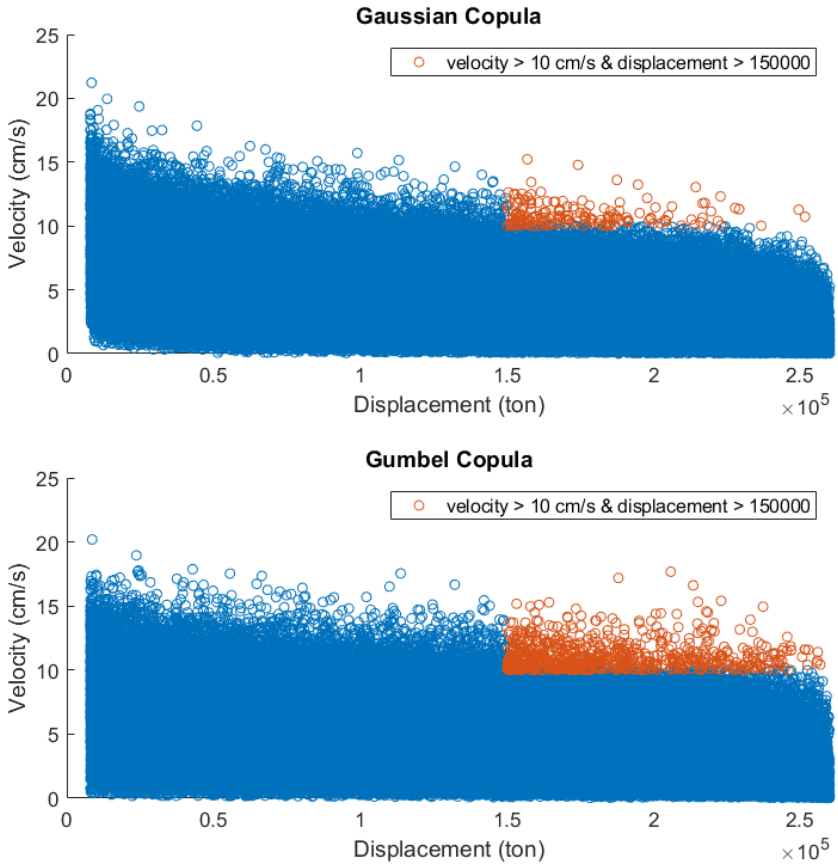

Figure 4.18: Monte Carlo simulation for Gaussian and Gumbel Copula

4.8 CONCLUSION

The following points summarize the most important findings of this chapter, which also could be used to answer the questions given at the beginning of this chapter:

- The results of the distribution fitting show that the distribution of berthing velocity follows the Weibull distribution, whereas the berthing angle follows the Gamma distribution. The results are presented in Table 4.6.
- The result of berthing simulation shows that a low berthing angle berthing procedure is favourable for a fender system as more fenders will be activated and thus, reducing the load exerted to the individual fender. In other words, taking into account the effect of multiple fender contact will increase the reliability of a fender system. Moreover, it is observed that the value of energy multiplication factor ($n_{multiple}$) is influenced mainly by the vessel length for the parallel type of berthing. Whereas, the bow radius governs the value for high berthing angles. The effect of berthing angle in governing $n_{multiple}$ is illustrated in Figure 4.11.
- The data-set of container vessels shows that vessel size is negatively correlated with berthing angle and berthing velocity (see Figure 4.7). This negative correlation significantly reduces the calculated failure probability and therefore, enhancing the computed reliability of a fender system. Consequently, a smaller fender size and capacity is required when the effect of negative correlation is taken into design consideration. It is also important to model the dependence structure between the random variables appropriately. For instance, in this

thesis, the dependence was modelled using a Vine copula. Using the Nataf distribution, on the other hand, could over-estimate the reliability of a fender system (see Table 4.14).

- The results of FORM reveal that the berthing velocity has the highest importance factor, which means that the uncertainty of berthing velocity has the highest contribution to the failure of a fender system. This finding is aligned with the findings of the earlier studies done by Ueda et al. [2003], Yamase et al. [2010], and Versteegt [2013]. Besides the berthing velocity, vessel displacement also has a substantial contribution to the uncertainty of the limit-state function. However, the contribution of the displacement is not as high as the contribution of the velocity. On the other hand, the influence of berthing angle becomes vital only in the case of multiple fender contact.

- The uncertainty of the berthing kinetic energy is far higher compared to the uncertainty of fender performance Figure 4.14. Therefore, it could be concluded that the uncertainty of the kinetic energy has the most dominant influence on the failure of a fender system. Moreover, the distribution of kinetic energy follows the same distribution as the berthing velocity, which is the Weibull distribution. Whereas, the distribution of fender performance follows the Normal distribution.

- The results of the reliability-based assessment Figure 4.16 shows that the deterministic method of PIANC guidelines is appropriate for the multiple fender contact type of berthing. Whereas, in the event of single fender contact, the reliability of the design is lower than the reliability target prescribed by PIANC WG211.

5 DERIVATION OF PARTIAL SAFETY FACTORS

One of the most common methods for designing a structure is to assign a partial safety factor to the load and resistance variables, commonly known as the semi-probabilistic method. This method allows designers to achieve the intended reliability without having to perform a complex full-probabilistic calculation such as Monte Carlo or FORM. Due to its practicality, this method will be implemented in the new fender design guidelines. This chapter shows how partial safety factors could be derived using the output of the reliability-based assessment.

5.1 METHOD

5.1.1 Partial Safety Factor for Kinetic Energy and Fender Capacity

The theoretical background of the partial safety factor is explained in Section 2.9. Essentially, the idea of this method is to design a structure such that a certain characteristic value of the capacity divided by its partial safety factor is higher than the characteristic value of the load effect multiplied by its partial factor:

$$\frac{E_{Fender;kar}}{\gamma_{E_{Fender}}} \geq \gamma_{E_k} E_{k;kar} \tag{5.1}$$

where:

$E_{Fender;kar}$ = Characteristic value of fender absorption capacity (kNm)
$\gamma_{E_{Fender}}$ = Partial safety factor for fender capacity (-)
$E_{k;kar}$ = Characteristic value of berthing kinetic energy (kNm)
γ_{E_k} = Partial safety factor for kinetic energy (-)

The question now is what are the appropriate values of partial safety factors such that the condition described in Equation 5.1 is fulfilled given the prescribed target reliability. This question was solved by finding the design values of fender capacity and kinetic energy for the target reliability at FORM design points. The partial safety factors then were determined using the following equations:

$$\begin{aligned} \gamma_{E_{Fender}} &= \frac{E_{Fender;kar}}{E_{Fender;d}} = \frac{\cancel{E_{cv}} * MF_{kar} * VF_{kar} * TF_{kar} * n_{multiple;kar}}{\cancel{E_{cv}} * MF_d * VF_d * TF_d * n_{multiple;d}} \\ \gamma_{E_k} &= \frac{E_{k;d}}{E_{k,kar}} = \frac{0.5 * M_d * v_d^2 * Cm_d * Ce_d}{0.5 * M_{kar} * v_{kar}^2 * Cm_{kar} * Ce_{kar}} \end{aligned} \tag{5.2}$$

where:

$E_{Fender;d}$ = Design value of the fender absorption capacity at FORM design points (kNm)
$E_{k;d}$ = Design value of the kinetic energy at FORM design points (kNm)

It should be noted that the fender rated capacity (E_{cv}) in Equation 5.2 is a deterministic parameter and hence, could be removed from the equation. Consequently, the value of $\gamma_{E_{Fender}}$ is only influenced by the manufacturing tolerance and uncertainties related to the rubber properties. Consequently, the partial factors derived

in this thesis are only valid if the performance of the fender aligns with the product specifications of the fender. Furthermore, the uncertainty of fender capacity also depends on the energy multiplication factor ($n_{multiple}$) for multiple fender contact berthing procedure.

Figure 5.1 presents the flow-chart of the partial safety factor derivation. The first step is to specify reliability targets for the fender system, for which the reliability targets proposed by a sub-group of PIANC WG211 was used in this thesis. The partial safety factors were then determined based on the values of the basic variables at FORM design points and the characteristic values. This calibration aims to ensure that a structure designed using the partial safety factor has a reliability level close to the prescribed target reliability. Hence, it is critical to ensure that the reliability level for the representative structure is close to the target reliability at FORM design points.

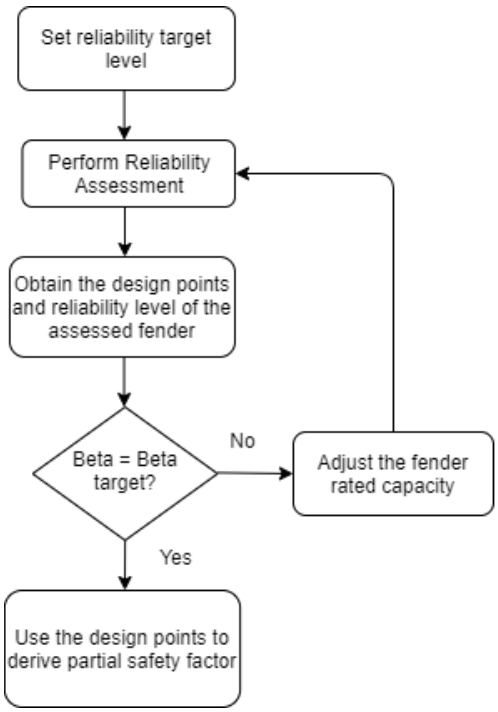

Figure 5.1: Flowchart of the derivation of partial safety factor

5.1.2 Partial Safety Factor for Reaction Force

Besides the berthing energy, the reaction force generated by fenders is also relevant for the design of berthing structures and fender system components (e.g. panel and chains). Therefore, the partial safety factors for the reaction force were derived in this thesis. Similar to Equation 5.2, the partial factors for reaction force can be determined using the following equation:

$$\gamma_F = \frac{F_d}{F_{kar}} \tag{5.3}$$

where:

γ_F = Partial safety factor for reaction force
F_d = Design value of reaction force (kN)
F_{kar} = Characteristic value of reaction force (kN)

However, the method used to determine the design value of reaction force is different from the method used for energy. As explained previously, the design

values of kinetic energy and fender capacity were obtained from FORM design points. Whereas, the design value of reaction force was derived from its distribution. Figure 5.2 shows how the safety factors for reaction force was determined in this thesis.

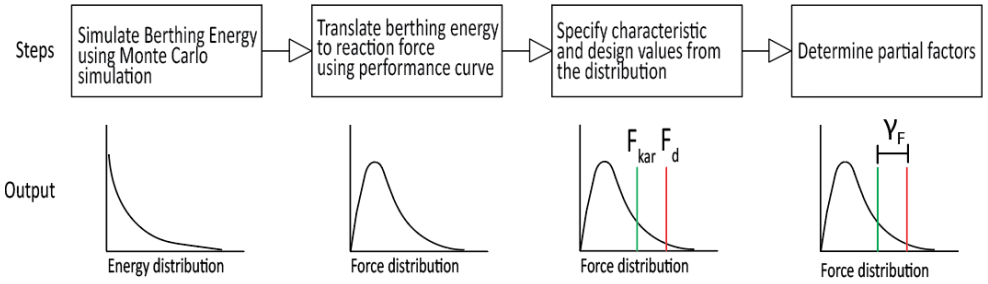

Figure 5.2: Flow-chart of the partial safety factor derivation for reaction force

This partial factor could be seen as the safety factor accounts for the uncertainty related to velocity factor, manufacturing tolerance, and the exponential increase of the reaction force when the fender rated deflection is exceeded.

Characteristic Value

For cone fenders, a small fender deflection already leads to a generation of the rated reaction force (R_{cv}) as shown in Figure 5.3. Consequently, the characteristic and maximum values of the reaction force will be more or less equal to the R_{cv}. Therefore, it is reasonable to use the rated reaction force as the characteristic value to derive partial safety factors.

However, there is another aspect that should be taken into account in determining the design reaction force, which is the possibility of having an extremely low temperature. For a rubber fender, the temperature factor will rise to 1.2-1.5 for a temperature below -10^oC. This case becomes relevant for the design of berthing structures in countries with a reasonably low temperature such as Norway. This effect, therefore, was taken into account in this thesis by adjusting the rated reaction force (R_{cv}) with a temperature factor corresponding to a characteristic temperature (t_{kar}), for which t_{kar} has an exceedance probability of 5% per year. The characteristic force thus could be written as:

$$F_{kar} = R_{cv} * TF(t_{kar}); \text{ where } P(t \leq t_{kar}) = 0.05 \tag{5.4}$$

Design Value

The design value was determined based on the Load and Resistance Factor Design approach (LRFD), therefore. the kinetic energy is considered as the dominant load for the design of berthing structure. A sensitivity factor of $\alpha = -0.7$ was therefore applied as recommended by the Eurocode 1990. The design reaction force, therefore, equals to:

$$F_d = F^{-1}(\phi(-0.7 * \beta_t)) \tag{5.5}$$

where ϕ is the cumulative distribution function of standard normal variable and β_t is the reliability target as prescribed in Table 5.2.

Translating Kinetic Energy to Reaction Force

As explained in Section 2.1.2, the kinetic energy can be translated to reaction force using the performance curve. Figure 5.3 shows the relation between kinetic energy

absorbed by a fender and reaction force it generates. This relationship was used in this thesis to derive the reaction force distribution (step 2 in Figure 5.2).

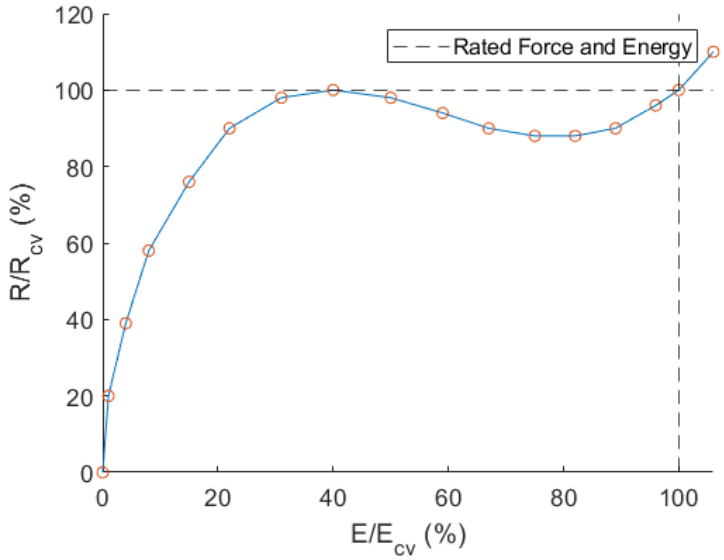

Figure 5.3: Energy-Reaction curve

Moreover, since the reaction force peaks twice (at 35% and 72% deflection), the rated force (R_{cv}) was used when the fender deflection is higher than 35%. Therefore, reaction force corresponding to the absorbed berthing energy could be computed using the following equation:

$$F = \begin{cases} R_{cv} & \text{if } \delta \geq 35\% \\ 2 * 10^{-7}E^5 - 5 * 10^{-5}E^4 + 0.0051E^3 - 0.288E^2 + 8.1465E + 7.08 & \text{if } \delta < 35\% \end{cases} \tag{5.6}$$

where E is the kinetic berthing energy absorbed by a fender (kNm) and δ is the fender deflection (%). In the case of multiple fender contact, one fender with the maximum reaction force was chosen as the representative for the fender system.

Furthermore, the actual reaction force is influenced by the surrounding temperature, production tolerance, velocity, and angle of berthing. Therefore, the influence factors must be applied to the computed reaction force:

$$F_{actual} = F * MF * VF * TF * AF \tag{5.7}$$

5.1.3 Reliability target

In the semi-probabilistic method, a structure is designed based on a certain acceptable probability of failure. One way to represent the acceptable failure probability is by using reliability target index. Table 5.1 presents target reliability indexes for different consequence classes proposed by a subgroup of PIANC WG211. The values in the table were derived based on ISO2394. It should, however, be noted that these reliability targets are not yet the final values.

Table 5.1: Annual reliability targets for different consequence classes proposed by a subgroup of PIANC WG211

Reference Period	1 year			
Consequence class	A	B	C	D
Failure consequence	Negligible	Some	Considerable	High
Beta target ($\beta_{t_{ref}=1year}$)	3.7	4.2	4.4	4.7

The failure probability corresponding to a certain target reliability index could be computed as:

$$P_f = \phi(-\beta_t) \tag{5.8}$$

where ϕ is the cumulative distribution function of the standard normal distribution.

Furthermore, one needs to be aware that a target reliability is always tied to a certain reference period. For instance, the reliability targets in Table 5.1 are specified for 1-year reference period. It is possible to convert the failure probability associated with a certain reference period, to different reference periods (e.g. 1-year or per single berthing event) using the following formula:

$$P_{f;t_{ref}} = 1 - (1 - P_{f;singlearrival})^n \tag{5.9}$$

where:

$P_{f;t_{ref}}$ = the probability of failure in the interval [o,t_{ref}]
$P_{f;singlearrival}$ = the probability of failure per single arrival
n = Number of events during the reference period

Figure 5.4 shows a relation between berthing frequency per year and its corresponding reliability target index.

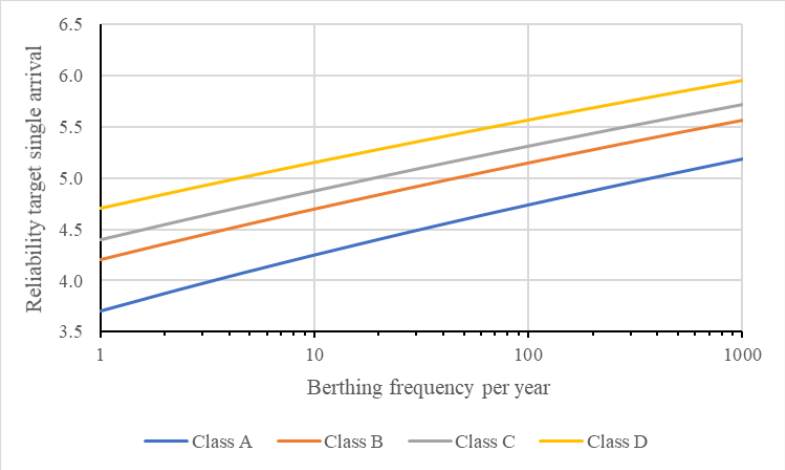

Figure 5.4: Reliability target index as a function of berthing events per year

Given that there are 100 berthing arrivals per year in a container berth in Port of Rotterdam, the reliability targets per single arrival corresponding to the annual reliability target (Table 5.1) are given in Table 5.2. These values will be used to derive the partial safety factor in this chapter.

Table 5.2: Reliability target (per berthing arrival) used for the calculation of partial safety factors

Class	Reliability target (β_t)	Probability of failure
A	4.75	$1.08*10^{-6}$
B	5.15	$1.33*10^{-7}$
C	5.32	$5.41*10^{-8}$
D	5.57	$1.30*10^{-8}$

5.2 DERIVATION OF PARTIAL SAFETY FACTORS FOR KINETIC ENERGY AND FENDER CAPACITY

This section presents the derivation of partial safety factors for the reliability targets specified in Table 5.2. In addition, the characteristic and design values are also given.

5.2.1 Design Values

The design values of the kinetic energy for the prescribed reliability targets are presented in Table 5.3. As explained in the previous section, the design values were determined based on the design points of the basic variables obtained from FORM analysis (see Appendix B for the complete results). The result shows that the design points for independent cases are significantly higher than the dependent cases, implying that larger fenders are needed when the load variables are independent of each other.

Table 5.3: Design values of kinetic energy for the prescribed target reliability

Cases	$E_{k,d}$ (kNm)			
	β_t =4.75	β_t =5.15	β_t =5.32	β_t =5.57
Single-Independent	3669	4382	4698	5214
Single-Dependent	1935	2319	2488	2756
Multiple-Independent	3171	3822	4113	4600
Multiple-Dependent	1521	1845	2005	2242

Table 5.4 displays the design values of the fender absorption capacity ($E_{Fender;d}$) as a function of the fender rated energy (E_{cv}). Recall that E_{cv} is a deterministic parameter and thus, does not influence the results of the partial safety factor. Therefore, it is better to write the design value as a function of E_{cv} rather than using its nominal value so it can be cancelled out later when deriving the partial safety factor (see Equation 5.2).

The design value of resistance usually decreases for a higher reliability target. However, a slight increase in design value is observed for the single-independent case. This increase can be explained by the fact that the fender capacity is influenced by the velocity factor, whose value is proportional to the berthing velocity. Therefore the design value of the fender capacity will increase as the design berthing velocity also increases for higher reliability targets.

Table 5.4: Design values of fender capacity for the prescribed target reliability

Cases	$E_{Fender;d}$ (kNm)			
	β_t=4.75	β_t=5.15	β_t=5.32	β_t=5.57
Single-Independent	1.07 E_{cv}	1.07 E_{cv}	1.07 E_{cv}	1.08 E_{cv}
Single-Dependent	1.07 E_{cv}	1.07 E_{cv}	1.07 E_{cv}	1.07 E_{cv}
Multiple-Independent	3.22 E_{cv}	3.19 E_{cv}	3.19 E_{cv}	3.18 E_{cv}
Multiple-Dependent	3.55 E_{cv}	3.48 E_{cv}	3.45 E_{cv}	3.42 E_{cv}

5.2.2 Characteristic Values

Eurocode defines characteristic value as a value with an intended probability of not being exceeded by a more extreme value during some specific reference period. In this thesis, the characteristic value of the variables and its associated exceedance probability are presented in Table 5.5. It should be noted that the exceedance probability specified in Table 5.5 corresponds to the exceedance probability per single arrival, which is proposed by a subgroup of PIANC WG211. Table B.5 lists the coefficients and influence factors associated with the characteristic values in Table 5.5.

Table 5.5: Description of the characteristic values

Variables	Exceedance Probability	Characteristic Value
Velocity*	0.2%	15.44 cm/s
Displacement**	0%	260,000 ton
Angle	5%	0.91^o
Manufacturing Tolerance	50%	1
Temperature	50%	15^oC

*)Corresponding to an exceedance probability of 2% during a reference period of 1 year

**)The displacement of the largest vessel

The characteristic kinetic energy ($E_{k;kar}$) and fender capacity ($E_{Fender;kar}$) were then computed based on the characteristic values of the random variables presented in Table 5.5. The results are:

$$
\begin{aligned}
E_{k,kar} &= 2460 \quad \text{kNm} \\
E_{Fender;kar} &= 1.08\ E_{cv} \quad \text{kNm} \quad \text{(For single fender contact)} \\
E_{Fender;kar} &= 3.30\ E_{cv} \quad \text{kNm} \quad \text{(For multiple fender contact)}
\end{aligned}
$$

The characteristic value of the fender capacity for single fender contact is different from the value for multiple fender contact. The difference is due to the contribution of energy multiplication factor ($n_{multiple}$).

5.2.3 Partial Safety Factors

Once the design and characteristic values obtained, the partial safety factors could be derived directly using Equation 5.2. Table 5.7 shows the computed partial safety factors for the kinetic energy. The result shows that the partial safety factors are significantly higher when the load variables are independent of each other compared to when they are negatively correlated. Partial safety factors lower than one are found for dependent cases, indicating that the design values of the kinetic energy are lower than the chosen characteristic values. Thus, lower characteristic values might be used when variables have negative dependence. In addition, it is found that the partial safety factors for multiple fender contact are slightly lower compared to those of single fender contact.

Table 5.7: Partial safety factors for kinetic energy

Consequence classes	β_t	γ_{E_k}			
		Single-Independent	Single-Dependent	Multiple-Independent	Multiple-Dependent
A	4.75	1.49	0.79	1.29	0.62
B	5.15	1.78	0.94	1.55	0.75
C	5.32	1.91	1.01	1.67	0.81
D	5.57	2.12	1.12	1.87	0.91

Table 5.8 shows the partial safety factors for fender capacity. The results show that $\gamma_{E_{Fender}}$ is in general close to 1, indicating that the uncertainty in fender capacity is much lower compared to the uncertainty of kinetic energy. Furthermore, partial safety factors lower than one are found for multiple-dependent case. This could be explained by the fact that the chosen characteristic berthing angle is higher than the design berthing angle. Consequently, the characteristic fender capacity is lower than the design fender capacity.

Table 5.8: Partial safety factors for fender resistance

Consequence classes	β_t	$\gamma_{E_{Fender}}$			
		Single-Independent	Single-Dependent	Multiple-Independent	Multiple-Dependent
A	4.75	1.01	1.01	1.02	0.93
B	5.15	1.01	1.01	1.03	0.95
C	5.32	1.01	1.01	1.03	0.96
D	5.57	1.00	1.01	1.04	0.96

Given the partial safety factors in Table 5.7 and Table 5.8, the necessary fender size and rated capacity needed to achieve the prescribed target reliability could then be determined.

5.3 SENSITIVITY FACTORS

Besides the partial safety factors, it is also essential to find the sensitivity factors (α) of the basic variables. Knowing α-values allows us to determine partial factors for reliability targets other than those specified in Table 5.1. Moreover, it could be used to differentiate the dominant variables with the non-dominant variables.The non-dominant variables then could be considered as deterministic when deriving partial safety factors.

Table 5.9 and Table 5.10 present the sensitivity factors of the design variables for single fender contact case. The first table presents the sensitivity factors for the independent case, whereas the second table for the dependent case. The result shows that berthing velocity and displacement are the only important variables in the event of single fender contact, indicated by a high α-value.

Table 5.9: Sensitivity factors (α) for single fender contact and independent case

Variables	α			
	β_t=4.75	β_t=5.15	β_t=5.32	β_t=5.57
Velocity	0.95	0.96	0.96	0.96
Displacement	0.31	0.30	0.29	0.28
Angle	0.0002	0.0002	0.0002	0.0002
MF	-0.020	-0.018	-0.018	-0.017
Temperature	0.0024	0.0022	0.002	0.002

It is worth noting that, for the dependent case, the sensitivity factor (α) does not reflect the importance of the design variables in the physical space but in the standard normal U-space. However, we should also recall that in FORM the design points are solved in the standard normal space. Therefore, the α-values are still relevant in this case.

Table 5.10: Sensitivity factors (α) for single fender contact and dependent case

Variables	α			
	β_t=4.75	β_t=5.15	β_t=5.32	β_t=5.57
Velocity	0.70	0.70	0.71	0.71
Displacement	0.71	0.71	0.70	0.70
Angle	0.0001	0.0001	0.0001	0.0001
MF	-0.066	-0.070	-0.072	-0.075
Temperature	0.018	0.019	0.019	0.019

Table 5.11 and Table 5.12 give the sensitivity factors for the multiple fender contact cases. It could be seen that the berthing angle now also has a fairly high sensitivity factor, indicating its substantial contribution to the uncertainty of the limit-state function.

Table 5.11: Sensitivity factors (α) for multiple fender contact and independent case

Variables	α			
	β_t=4.75	β_t=5.15	β_t=5.32	β_t= 5.57
Velocity	0.89	0.90	0.90	0.90
Displacement	0.28	0.27	0.27	0.26
Angle	0.35	0.33	0.33	0.32
MF	-0.065	-0.072	-0.074	-0.078
Temperature	0.017	0.019	0.019	0.02

Table 5.12: Sensitivity factors (α) for multiple fender contact and dependent case

Variables	α			
	β_t=4.75	β_t=5.15	β_t=5.32	β_t=5.57
Velocity	0.64	0.65	0.65	0.65
Displacement	0.63	0.63	0.63	0.63
Angle	0.43	0.42	0.41	0.41
MF	-0.058	-0.061	-0.063	-0.066
Temperature	0.015	0.016	0.016	0.017

The result shows that α-values of the design variables are relatively constant for different target reliability indexes, implying that the limit-state function is relatively linear in the region adjacent to the design points. Consequently, it is possible to use a single α-value for each design variable. This thesis used a weighted average method to determine the standardized α-values. Table 5.13 presents the standardized α-values for the dominant variables, which are defined as the variables with α-value higher than 0.1.

Table 5.13: Standardized α-values for dominant variables

Variable	Standardized α-values			
	Single-Independent	Single-Dependent	Multiple-Independent	Multiple-Dependent
Velocity	0.95	0.71	0.90	0.65
Displacement	0.29	0.71	0.27	0.63
Angle	-	-	0.33	0.42

5.4 DERIVATION OF PARTIAL SAFETY FACTORS FOR REACTION FORCE

This section presents the derivation of partial safety factors for reaction force for cone fenders, for which the procedure is explained in Section 5.1.2. These partial factors are essential for designers to determine the design value of the reaction force, which is generated by a single fender during berthing impact.

Table 5.14 presents the partial safety factors for different reliability targets. The R_{cv} used in this analysis corresponds to the E_{cv} which were obtained from the FORM analysis which was performed for the energy (see Appendix B). In addition, Figure 5.5 presents the distribution of reaction force, the characteristic value, and also the design value for the independent variables case.

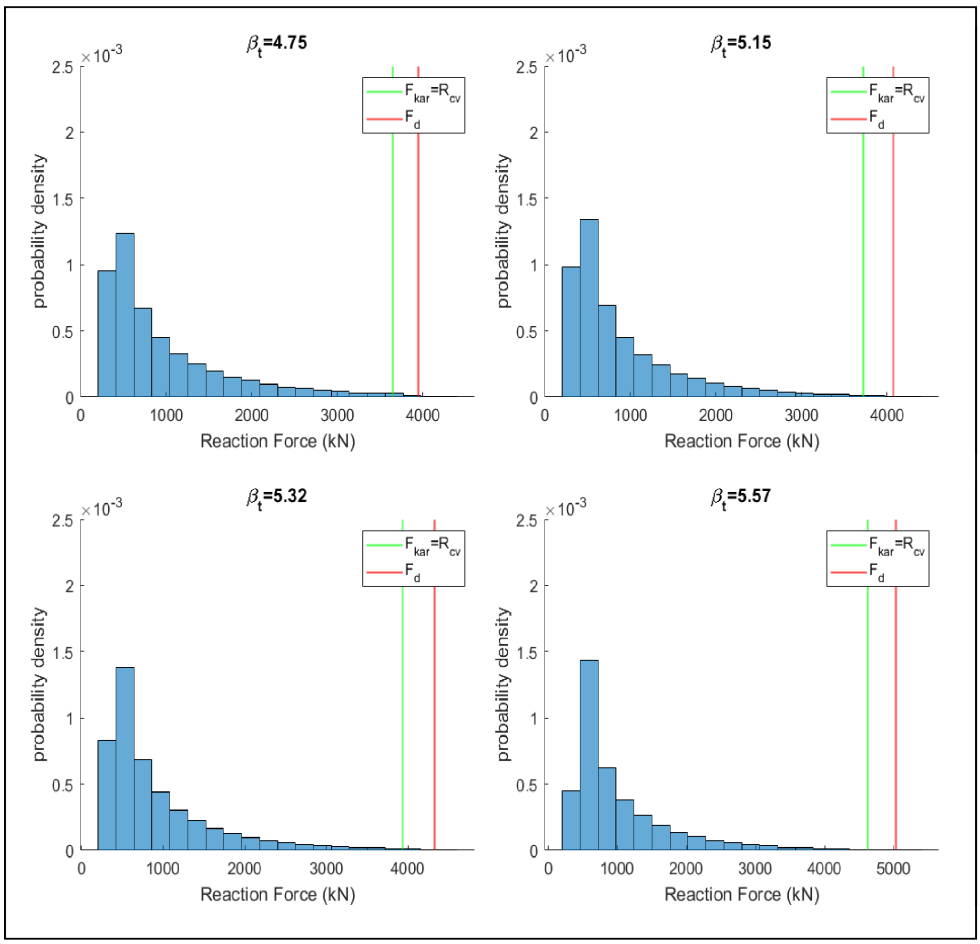

Figure 5.5: Partial safety factor for reaction force (Independent case)

The result shows that for cone fenders, the partial safety factors for independent variables case are in general, close to 1.1. Whereas, values slightly lower than 1 are found for the dependent variables case. The results therefore suggest that the uncertainty of the reaction force is lower compared to the kinetic energy. This finding could be explained by the fact that the uncertainty of reaction force is mainly influenced by the influence factors (e.g. temperature factor, velocity factor, manufacturing tolerance) and the exponential increase due to the exceedance of the rated deflection whose uncertainty is relatively low.

Table 5.14: Partial safety factors for reaction force (SCN Fender)

β_t	R_{cv}	TF(t_{kar})=6^{o}C	F_{kar} (kN)	Independent		Dependent	
				F_d (kN)	γ_F	F_d (kN)	γ_F
4.75	3568	1.02	3639	3947	1.08	3518	0.97
5.15	3640		3713	4067	1.10	3601	0.97
5.32	3850		3927	4321	1.10	3825	0.97
5.57	4523		4613	5134	1.11	4529	0.98

It should be noted that the partial factors in Table 5.14 were derived for cone fenders. The values of partial safety factors will be higher for cylindrical fenders. However, the partial factor for cylindrical fenders is outside of the scope of this thesis.

5.5 DISCUSSION

5.5.1 Evaluation of the Safety Factors of PIANC [2002]

This section evaluates the safety factors recommended by PIANC [2002] and compares them with the partial safety factors derived in this thesis. As explained in Section 3.3.2, PIANC [2002] introduces abnormal berthing coefficient (C_{ab}) as a global safety factor to be applied to the normal kinetic energy. PIANC recommends to assign a global safety factor of 1.5 for the largest container vessel and 2.0 for the smallest container vessel to the kinetic energy (see Table 2.1). Table 5.15 compares the abnormal berthing coefficient suggested by PIANC guideline and the partial safety factors for kinetic energy derived in this thesis for the independent variables cases. It could be seen that the values of γ_{E_k} are found to be in the similar range of the C_{ab} recommended by PIANC.

Table 5.15: Comparison between C_{ab} and γ_{E_k}

Consequence	C_{ab}	γ_{E_k}	
		Single-Independent	Multiple-Independent
Low	1.5-2.0	1.49	1.29
Some		1.78	1.55
Considerable		1.91	1.67
High		2.12	1.87

However, it should be noted that the design philosophy of PIANC [2002] is different from the partial safety factor method. In the PIANC guidelines, the safety factor is assigned to the 'normal kinetic energy', which is computed based on the deterministic values recommended in the guidelines. Whereas, the characteristic values are derived from the marginal distribution of the basic variables. The characteristic kinetic energy in this thesis is found to be higher than the 'normal kinetic energy' computed based on the PIANC guidelines (see Table 5.16); this is because the characteristic berthing velocity is far higher than the velocity recommended by Brolsma et al. [1977].

Table 5.16: Comparison between the 'Normal' kinetic energy computed based on the deterministic approach of PIANC [2002] and the characteristic kinetic energy derived in this thesis

Method	Displacement (ton)	Velocity (cm/s)	Angle (degree)	Kinetic Energy (kNm)	Remarks
Deterministic	260,000	10	1.5	1193	Table 3.3
Semi Probabilistic	260,000	15.5	0.9	2460	Table 5.5

Therefore, it is highly recommended to update the Brolsma's velocity curve, as also suggested by Roubos et al. [2016], such that the 'normal kinetic energy' matches the characteristic value. It is further recommended to implement the partial safety factor method in the new fender guideline as it has some advantages over the existing global safety factor. For instance, the use of partial safety factor allows engineers to allocate an appropriate partial factor according to the intended reliability target and design assumption (e.g. multiple fender contact) and therefore, an over-designed fender could be avoid.

5.5.2 Verification of the method used to find design values for the case of dependent variables

It has been explained in the previous in Section 2.9 that the design values could be approximated based on the sensitivity factors (α). This method, however, might be not accurate when variables are dependent on each other due to the non-linear iso-probabilistic transformation (e.g. Rosenblatt transformation). Therefore, this document aims to confirm whether the approximated failure probability determined using the α-values matches the intended reliability target (β_t).

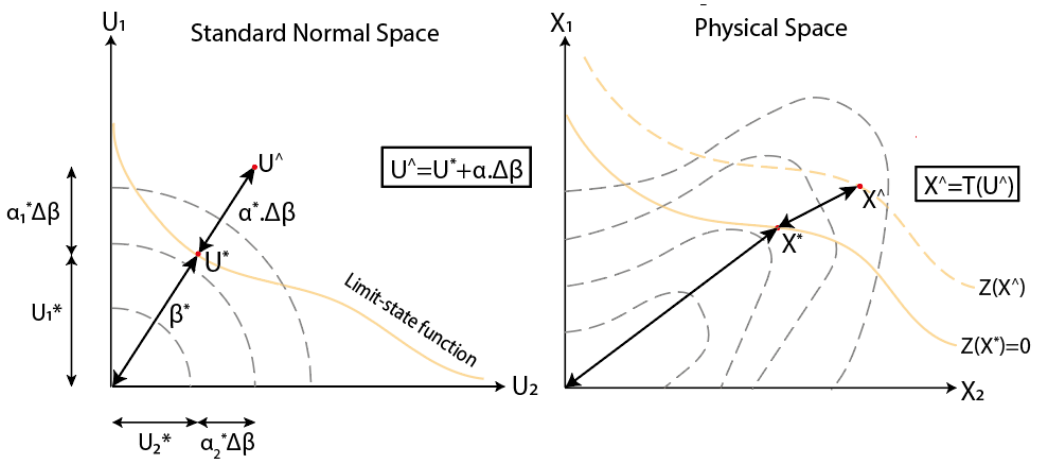

Figure 5.6: Conceptual illustration of the design points in the standard normal U-space and physical X-space for dependent variables (The author's illustration)

Figure 5.6 illustrates the verification process. A FORM analysis was performed for a fender (single-dependent case), resulting in $\beta^* = 4.75$ and the associated sensitivity factors ($\boldsymbol{\alpha}^*$) and design points ($\boldsymbol{X}^*$). Those results were then used to approximate the new design values for a different reliability target (e.g. $\hat{\beta} = 5.15$). The new design values were obtained using Equation 2.67, for which the results are presented in Table 5.17.

Table 5.17: The results of the calculation of the new design points ($\hat{\boldsymbol{X}}$)

Variables	α^*	$\alpha^*.(\hat{\beta} - \beta^*)$	U^*	$\hat{U}$	X^*	$\hat{X}$
Velocity	0.70	0.28	3.32	3.60	14.55 cm/s	15.68 cm/s
Mass	0.71	0.284	3.38	3.66	229,132 ton	236,047 ton
Angle	1.10^{-4}	4.10^{-5}	$5 * 10^{-4}$	$5 * 10^{-4}$	0.19^o	0.20^o
MF	-0.066	-0.028	-0.32	-0.34	0.99	0.99
Temperature	0.018	0.008	0.08	0.09	15.41^oC	15.45^oC

As illustrated in Table 5.17, the design values of velocity, displacement, and angle are higher for the new reliability target, implying that the loads have to be more extreme or unlikely to reach a failure condition. As these new design loads have a smaller exceedance probability, the failure probability will therefore also be lower.

However, the question was whether this failure probability is similar to the allowable maximum probability corresponding with the desired reliability target. One way to verify that is by analysing whether the following approximation holds:

$$P[Z < Z(\hat{X})] \cong \phi(-\hat{\beta}) \tag{5.10}$$

The new reliability level ($\hat{\beta}$) represents the exceedance probability of the new limit-state function Z=Z($\hat{X}$), as illustrated in Figure 5.7. It could be seen from the figure that the new exceedance probability is smaller than the original failure probability.

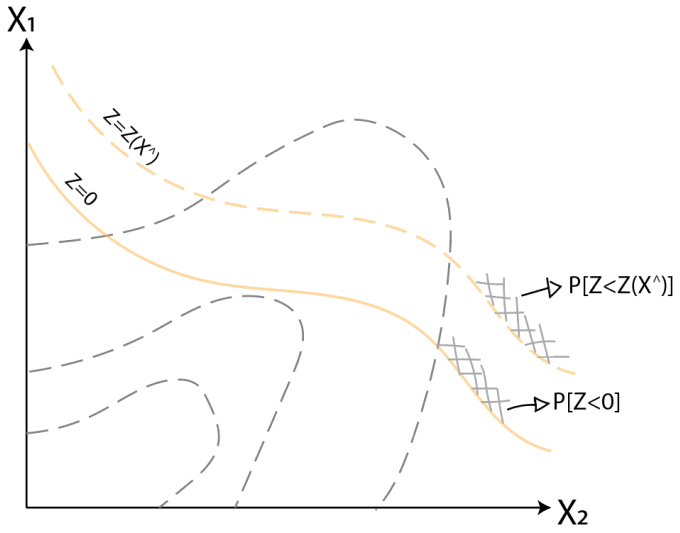

Figure 5.7: The exceedance probability of the new limit-state function Z=Z($\hat{X}$) (The author's illustration)

The value Z($\hat{X}$) was computed according to the new design points ($\hat{\boldsymbol{X}}$) given in Table 5.17, for which the result is -381 kNm. The exceedance probability of the new limit state function P[Z<Z($\hat{X}$)] was then determined by means of Monte Carlo and FORM, for which the results are given in Table 5.18.

Table 5.18: The exceedance probability of the new limit-state function

$\hat{\beta}$	$\phi(-\hat{\beta})$	FORM	Monte Carlo*	
		$P[Z < Z(\hat{X})]$	$P[Z < Z(\hat{X})]$	c.o.v
5.15	$1.30*10^{-7}$	$1.26*10^{-7}$	$5.06*10^{-8}$	0.09

*) Monte Carlo was performed using 1 million samples

The results show that the exceedance probability obtained from FORM is close to the intended target reliability, whereas the exceedance probability computed using Monte Carlo is slightly smaller. The difference between the result of Monte Carlo and the target failure probability is due to the non-linear transformation of the dependent variables, however, this difference is fairly small and still acceptable.

Figure 5.8 shows the exceedance probability of the new limit-state function obtained from the Monte Carlo simulation and its associated confidence interval, and the desired failure probability. The result shows that the uncertainty of the Monte Carlo's failure probability is much smaller compared to its difference with the intended target reliability, indicating the convergence of the Monte Carlo result.

Based on the analysis results, it could be concluded that it is safe to use α-values to derive design values for dependent variable cases.

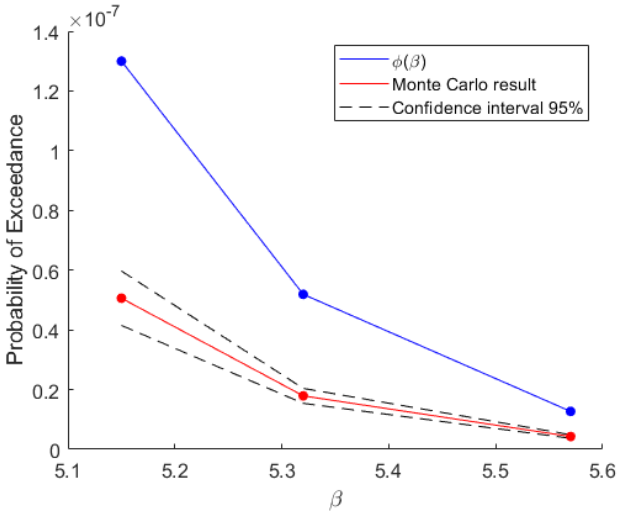

Figure 5.8: The difference between the target failure probability and the actual exceedance probability for different reliability targets

5.6 CONCLUSION

The following points give the key takeaways of this chapter:

- The existing fender design guideline published by PIANC does not specify the expected reliability associated with the given abnormal berthing coefficient (C_{ab}). Moreover, it also does not take into account the influence of berthing frequency. Therefore, the reliability of the resulted fender design could not be quantified.
- The values of partial safety factor are mainly influenced by the prescribed reliability target, the uncertainty of the basic variables, and the berthing frequency. It is also found that partial safety factors are higher for the kinetic energy (1.29-2.12) than the partial factors for fender capacity (approximately 1). On the other hand, partial safety factors are close to 1.1 for the reaction force. The results could be found in Table 5.7, Table 5.8, and Table 5.14.
- It is recommended to implement the partial safety factors method in the new PIANC design guidelines as this method gives a clearer definition regarding the reliability level of the associated fender design. This method could be implemented by introducing the 'characteristic value' and 'design value' terms as a substitute for the 'normal' and 'abnormal kinetic energy' which are currently used in PIANC [2002]. Also, it is found that the characteristic value of the berthing velocity (see Table 5.5) is higher than those recommended by Brolsma et al. [1977]. This finding is aligned with the findings of the PIANC committee of WG145 [2020].
- Although, the partial safety factors method is recommended for the new design guidelines; however, caution should be exercised when using the partial factors for dependent variables. This is because the partial factor for dependent variables highly depends on the local conditions. Therefore, the general applicability of the **partial factor values** for the case of dependent variable is still questionable.

6 ECONOMIC OPTIMISATION

"How safe is safe enough?" is one of the fundamental questions that every engineer should have an answer to before designing a structure. Engineers can make a highly safe structure which obviously will lead to a reasonably high cost of investment, or they can also create a cheaper design at the expense of the reliability of the structure. Engineers and the project owner hence will always encounter this dilemma when they decide to build a structure. In essence, the appropriate reliability level of a structure depends on the efficiency of the safety measure and the failure consequence of the structure.

In practice, structures are usually designed to meet a certain safety level, as prescribed in the relevant codes or standards. For instance, engineers in Europe usually create their design following the Eurocode. However, the existing codes are mainly derived for buildings. It is thus unclear whether or not the prescribed reliability targets in the standard are still relevant for structures with different risk-profile. The goal of this chapter is to derive the optimum reliability target for fender structure based on the economical optimisation.

6.1 PROCEDURE

Figure 6.1 shows the flow-chart of the analysis used for finding the most appropriate reliability target for fender structure. Besides the economic optimization, sensitivity analysis will also be conducted to determine which parameter has a dominant influence on the fender's optimum reliability. In this analysis, the optimum reliability level will be derived for the case of single fender contact with independent parameters.

The first step of the analysis is to determine the value of input parameters used for the calculation, such as interest rate, failure cost, investment cost, and the lifetime period of a fender structure. This study collects relevant data from various sources. For example, this study used the fender's price provided by Trelleborg, while the study of Roubos et al. [2019] was used to estimate the failure cost. When all of the necessary inputs are defined, one can determine the optimum reliability target by minimizing Equation 2.71. Readers can also find a more detailed elaboration on the concept of economic optimization in Section 2.10.

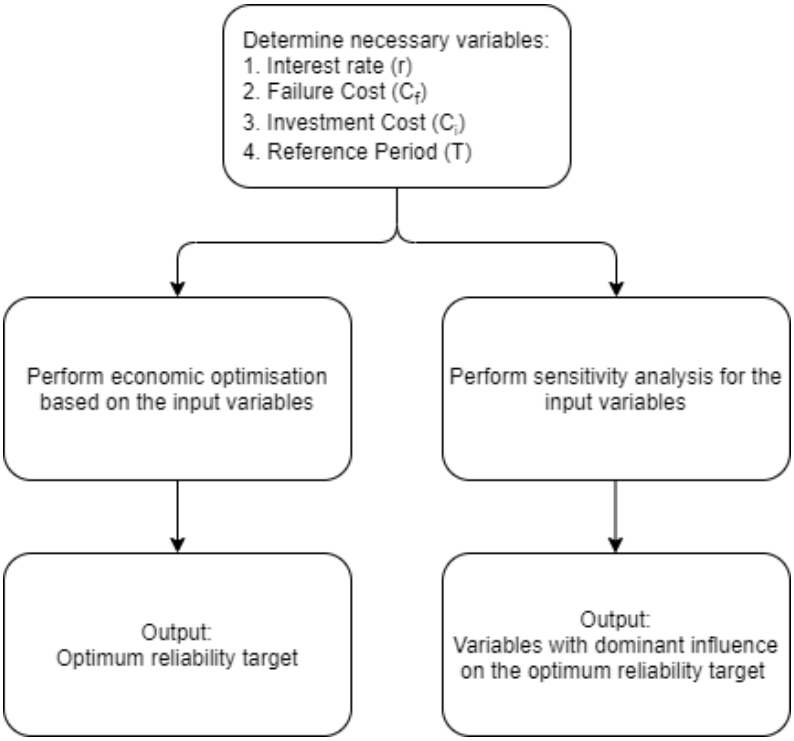

Figure 6.1: Flowchart of the economic optimization analysis

6.2 RESULT OF ECONOMIC OPTIMISATION

6.2.1 Data Analysis

In the economic optimization method, the investment cost (C_i) and capitalized risk cost (C_R) are defined as a function of the system's reliability level. One could obtain the relationship between fender's reliability level with the investment cost by performing reliability analysis, either Monte Carlo or FORM, for several fenders whose rated energy capacity and price have already known. Normally, the fender's rated energy is proportional to the reliability level.

Figure 6.2 presents the price of super cone fender (SCN) and cylindrical fender (CYL) as a function of the fender's reliability level per single arrival. It is clear from the figure that the fender's price increases as the reliability level increases. In addition to that, the price of the CYL type of fender is higher than the SCN one, and thus, we can compare the influence of the fender's price on the optimum reliability level. With polynomial regression, the price of the fender is approximated using a quadratic function. Equation 6.1 and Equation 6.2 are used to approximate the cost of investment for the SCN and CYL type of fender, respectively.

$$C_i = 2386 * \beta^2 + 146 * \beta + 6118 \tag{6.1}$$

$$C_i = 6268 * \beta^2 - 7395 * \beta + 11655 \tag{6.2}$$

Roubos et al. [2019] studied the optimum reliability target indices for the quay wall. In his study, he tried to examine the failure consequence of a quay wall by gathering expert's opinions on the qualitative and quantitative estimate of the failure consequences. He found that most experts agree that structural failure will not likely cause significant economic repercussions in large ports. However, a structural failure may harm the ports' reputation, and thus, mitigation measures are essential

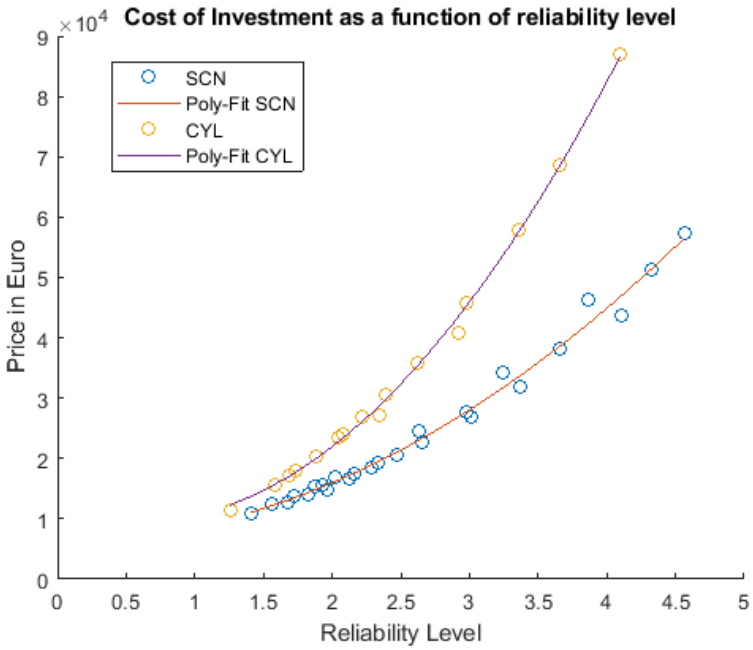

Figure 6.2: Prices of fender as a function of reliability level per arrival (Source:Trelleborg internal document)

to prevent failures. The majority of the experts also agree that the failure costs associated with structural failure of a commercial quay wall are in the ranges of €1-5 million.

It is not likely that the failure of a single fender will directly lead to marine structure failure. Therefore, the failure costs of the fender are most likely lower than the quay wall. Hence, in this thesis, it is assumed that a fender failure's consequence cost is $\leq$ €1 million. It is further assumed that the probability of fatality caused by a single fender failure is extremely small. The influence of failure costs on the optimum reliability level will be taken into account in the sensitivity analysis section.

Other parameters whose values need to be defined are interest rate and the design life-span of a fender. In practice, the design lifetime of a fender is 25 years. As for the interest rate, according to Miller [2020], the fixed 20-years fixed mortgage in the Netherlands is approximately 2.65-3.4% while Roubos et al. [2019] assumed interest rate of 3% in his study. In this thesis, 3% interest rate thus was also assumed.

6.2.2 Optimum Annual Reliability Level

Figure 6.3 presents the economic optimization results for the super cone fender and cylindrical fender. It could be seen that the optimum annual reliability index for the super cone fender is 3.47. On the other hand, the cylindrical fender's optimum reliability index is slightly lower, which is 3.24. The optimum reliability index will decrease when the cost of investment increases.

It is also observed from the figure that the steepness of the total cost curve is asymmetrical. The steepness on the left side of the graph is mainly influenced by the capitalized risk cost (the red line), while the steepness on the right side is influenced by the investment cost (the blue line). The efficiency of safety investment becomes less when the reliability level is already larger than 3.2, which means that spending more in the safety measure will not significantly reduce the probability of failure anymore. In the next section, the influence of the parameters on the optimum reliability level will be examined.

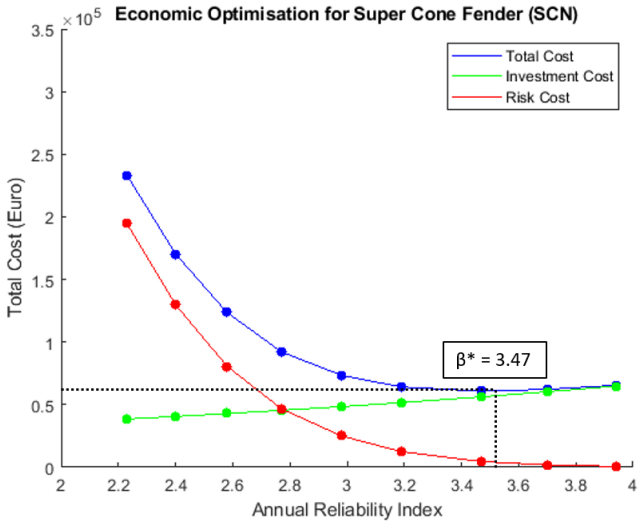

(a)

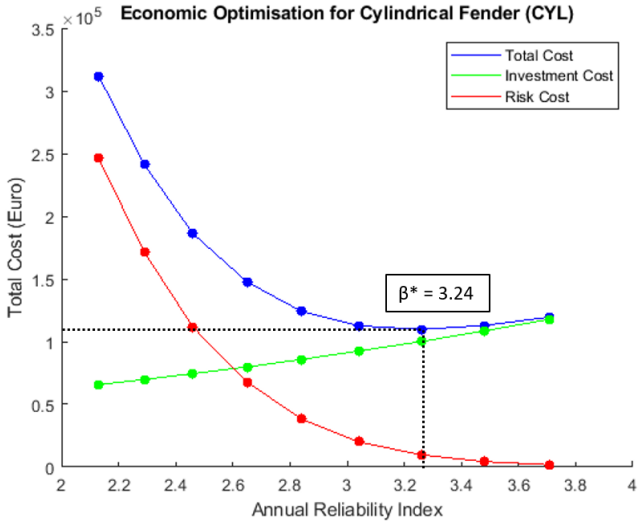

(b)

Figure 6.3: Optimum annual reliability index t_{ref}=25 years, r = 3%, C_f= €1 mil for (a) Super Cone Fender (b) Cylindrical Fender

6.3 RESULT OF SENSITIVITY ANALYSIS

The purpose of sensitivity analysis is to find which parameter that has a significant influence on the optimum safety level of a fender. We will perform sensitivity analysis for interest rate (r), failure cost (C_f), reference period (T), and the number of berthing arrivals per year. The sensitivity analysis was done by changing one parameter of interest while keeping the other parameters constant.

Figure 6.4 presents the results of the sensitivity analysis. As expected, the optimum reliability level goes up as the failure costs increase. The optimum reliability level increases exponentially for the low failure cost ($\leq$ €5 million). The increase is gentler for the higher failure cost. On the other hand, the interest rate has an opposite effect on the optimum reliability index than the failure cost. The optimum reliability level will decrease when the interest rate increases, which can be explained by the fact that the present value of the risk cost will be less for higher interest rates. The more extended reference period leads to a higher optimum reliability index. However, the optimum reliability index tends to be constant for a reference period longer than 30 years. This is because the capitalized risk cost is

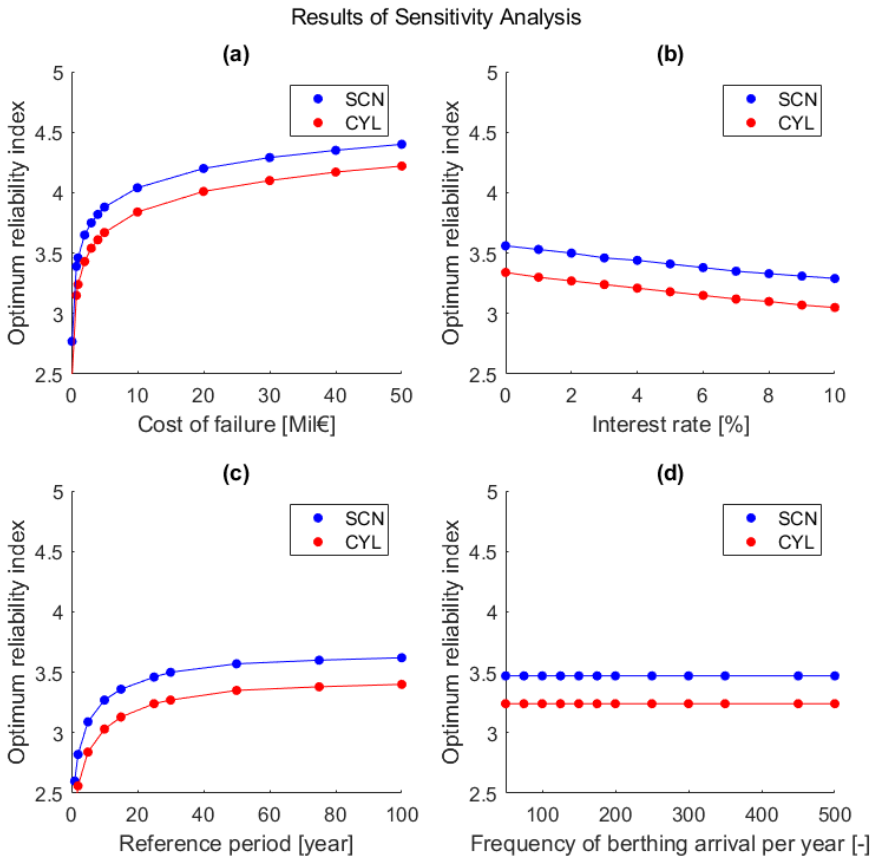

Figure 6.4: Influence of (a) cost of failure, (b) interest rate, (c) reference period, (d) berthing frequency per year on the annual reliability index for C_f= €1 mil, berthing frequency=100 arrivals/year, r=3%, T=25 years

mainly governed by the present value of the consequence cost in the near future. Lastly, the frequency of berthing arrival does not influence the optimum annual reliability index, but it will slightly influence the optimum reliability index of a single arrival.

6.4 DISCUSSION

6.4.1 Evaluation of the reliability target indices proposed by PIANC WG211

As explained in the previous chapter (see Figure 5.4), a sub-group of PIANC WG211 has proposed several reliability targets for different failure consequences, which are adopted from ISO2394 (2015). In this section, those proposed reliability targets are compared to the optimum reliability targets derived from the cost-benefit analysis, as presented in Table 6.1. The results of the cost-benefit analysis show that the proposed reliability targets are aligned with the optimum reliability targets derived for the Cylindrical fenders. Whereas, the optimum reliability targets for the Cone fenders are slightly higher due to the lower marginal cost. Therefore, based on the results of the economic optimisation, it could be concluded that the reliability targets proposed by the PIANC WG211 are already optimum.

However, it should be noted that the optimum reliability targets derived in this thesis do not take into account the fatalities and environmental consequences. There-

fore, a higher reliability target should be imposed where the failure of a fender system leads to fatalities or severe environmental damages.

Table 6.1: The annual reliability targets proposed by PIANC WG211 and the optimum reliability targets derived in this thesis for different failure consequences

Class	Consequence	Failure cost (million €)	$\beta_{t_{ref}=1year}$		
			PIANC WG211	SCN Fenders	CYL Fenders
A	Low	≤8	3.7	4.0	3.8
B	Some	≤50	4.2	4.4	4.2
C	Considerable	≤200	4.4	4.7	4.5
D	High	≤1500	4.7	5.1	4.9

6.5 CONCLUSION

Some important findings of this chapter are:

- The optimum annual reliability target indices is largely influenced by the failure cost and also, the cost of investment. Higher consequence cost will result in the higher optimum reliability target. On the other hand, the optimum reliability target will become lower when the investment cost is more expensive.
- The optimum reliability target for cylindrical fender is slightly lower than the super cone fender, as it has a higher investment cost (see Figure 6.3).
- Given that the failure cost of a single fender is €1 million, 100 berthing arrivals per year and that the design lifetime of the fender is 25 years, the annual optimum reliability of a super cone fender and cylindrical fender are 3.47 and 3.24, respectively.
- The optimum annual reliability target suggested by PIANC WG121 is aligned with the optimum reliability target found from the economic optimisation as the analysis shows that the optimum reliability target should be in the range of 3.5-4.5 depending on the failure consequences.

7 CONCLUSION AND RECOMMENDATION

This thesis has addressed some critical aspects related to the reliability of a fender system. The First Order Reliability Method (FORM) and Monte Carlo simulation were performed to assess the reliability level of the fenders selected using PIANC [2002] while taking into account the influence of multiple fender contact and negative dependence between the load variables. This thesis is the first study that takes the effect of multiple fender contact and negative dependence into consideration since the previous studies by Ueda et al. [2003], Yamase et al. [2010], and Versteegt [2013], assumed a single fender contact and independent variables. Furthermore, this thesis shows how partial safety factors could be derived using the results of the level-II probabilistic analysis (FORM). In the last chapter, the optimum reliability target index was determined through a cost-benefit analysis. During this study, some novel insights related to fender design have been acquired. It is highly recommended that these aspects be discussed in future PIANC working groups.

7.1 CONCLUSION

This section presents the answer to the sub-questions and also the main research questions formulated in Chapter 1 based on the results of the reliability-based assessment performed in this thesis which also summarises the main findings of this thesis.

1. **What are the reliability levels of the fender systems designed using the current PIANC fender design guidelines?**

   The answer to this question is given in Section 4.5 and discussed specifically in Section 4.7.1. The result shows that for the single fender contact berthing procedure, the reliability levels of the fender selected based on PIANC [2002] are 3.70 and 5.06 for independent and dependent variables cases, respectively. Whereas, much higher reliability levels are found for the multiple fender contact berthing procedure. The reliability level of the fender system is 5.20 for the independent variables and 6.88 for the dependent load variables, respectively.

2. **Do those fender designs meet the reliability targets proposed by PIANC WG211?**

   If we compare the reliability level of the fenders to the reliability targets proposed by PIANC WG211, it is found that the reliability level for the single-independent case (β = 3.70) is below the proposed reliability target. A higher characteristic berthing velocity, therefore, is recommended to be used for the design calculation. On the other hand, the reliability-based assessment result shows that for the multiple fender contact type of berthing, the reliability of the fender design is in the range of the reliability target proposed by PIANC WG211. However, it should be noted that for the multiple fender contact, 3-fender contact was assumed (Figure 3.5). Hence, it could be concluded that the existing design method is suitable for the multiple fender contact type of berthing.

3. **How could the dependence between the load variables be modelled?**

A dependence analysis was performed for the container terminal data-set in Port of Rotterdam to answer the question above. It is found that the vessel size has a negative correlation with berthing velocity ($\rho = -0.61$) and berthing angle ($\rho = -0.54$). Furthermore, the result of Kendall's tau independence test also confirms the dependence between those load variables. A Vine-copula was then used to model the dependence structure between those variables and included in FORM analysis using the algorithm proposed by Jiang et al. [2015].

4. **What influence does dependence have on the reliability of a fender system?**

   The reliability assessment results further show that the negative dependence between the load variables could significantly reduce the calculated failure probability of a fender system, enhancing the calculated reliability of the fender system. This decrease in the failure probability is because the large vessels will tend to have lower berthing angle and velocity when they are negatively correlated. Therefore, the occurrence probability of extreme kinetic energy will become smaller. Neglecting this negative dependence might lead to an oversized fender design.

5. **How could the influence of multiple fender contact be included in the limit-state function?**

   In the event of multiple fender contact berthing procedure, the kinetic energy exerted by the vessel is absorbed by multiple fenders that are in contact with the vessel. The proportion of the energy absorbed by those fenders depends on the deflection of each fender. To account for the contribution from several fenders in contact the energy multiplication factor $n_{multiple}$ is introduced. This factor depends on the geometry of the vessels and the spacing between fenders and can be determined based on geometrical analysis or more advanced simulation (see Section 4.1.2). For relatively low berthing angles, $n_{multiple}$ is mainly influenced by the vessel length. On the other hand, for high berthing angles, $n_{multiple}$ is governed by the bow radius.

6. **How significant is the influence of the multiple fender contact on the reliability of a fender system?**

   The multiple fender contact has a favourable influence on the reliability of a fender system, which is similar to the effect of the negative dependence between the load variables. When the influence of multiple fender contact is taken into account, the calculated failure probability of a fender system becomes significantly lower. Therefore, it is essential to take this favourable effect of the reasonably low berthing angle and multiple fender contact into account in the design of a fender system; otherwise, the design might become too conservative.

7. **Which random variable has the most dominant influence on the failure of a fender system?**

   This thesis confirms that the uncertainty of berthing velocity has the largest contribution to the failure of the fender system. This finding is aligned with the findings of Ueda et al. [2003], Yamase et al. [2010], and Versteegt [2013]. Besides the berthing velocity, another variable whose uncertainty has a substantial influence on the variance of the limit-state function is the vessel displacement. Whereas, the contribution of berthing angle becomes significant in the event of multiple fender contact.

8. **What are the optimum reliability target (β_t) for a fender system?**

   The cost-benefit analysis result shows that the optimum annual reliability target is aligned with those proposed by the sub-group of PIANC WG211, which is in the range of 3.5-4.5 (depending on the failure consequence). It is also

found that the optimum reliability target is mainly influenced by the safety measure cost, the cost of failure consequence, and the reference period.

9. **What is the appropriate partial safety factors for the kinetic energy, fender capacity, and reaction force?**

   Chapter 5 shows how the partial safety factors were derived based on the results of FORM analysis. In essence, the design points obtained from the FORM analysis were used as the design values for determining the partial safety factors. It is found that a higher safety factor (1.2-2.2) needs to be assigned to the kinetic energy as its uncertainty dominates the failure of a fender system. Whereas, in general, it is found that the partial safety factors for fender capacity are approximately 1. On the other hand, the partial safety factors for reaction force for cone fenders in general equals 1.1.

Finally, the main research question below could be answered:

"How can the existing fender design approach be improved using the reliability-based design approach and what aspects need to be considered?"

Most of the existing fender design guidelines adopt the deterministic approach in which the reliability related to fender engineering is not taken into account. This thesis shows how those uncertainties could be incorporated into design consideration in order to produce a sufficiently safe fender design. One way to improve the existing design approach is by implementing the partial safety factor method to update the current deterministic approach. In the partial safety factor method, the uncertainties of the load variables (e.g. berthing velocity, berthing angle, and displacement) are taken into account via the characteristic and design values. Furthermore, this method allows fender designers to allocate an appropriate partial factor according to the intended failure consequence and design assumption (e.g. single/multiple fender contact) and thus, avoiding an oversize fender design. The berthing frequency is also taken into account into the design consideration through the reliability target per berthing arrival.

This thesis has several contributions to both academic research and industrial applications. In terms of academic contribution, this thesis shows a practical application of the Vine Copula FORM algorithm developed by Jiang et al. [2015]. This thesis further demonstrates how the design points could be determined using the Rosenblatt transformation in the event of dependent variables is modelled using Vine copula. The methods were then verified in Section 5.5.2. Whereas, for the industrial contributions, this thesis manages to show how the influence of multiple fender contact and dependence between the load variables could be integrated into the design of a fender system. In the earlier studies (e.g. Yamase et al. [2010], Ueda et al. [2003], Versteegt [2013]), the effects of the negative dependence and multiple fender contact were not considered. The results of this thesis show how those effects have a very dominant influence on the reliability of a fender system. Therefore, this thesis could be used by PIANC WG 211 to update the existing design approach of fender systems and help to interpret the berthing records analyzed by PIANC WG145.

7.2 RECOMMENDATIONS

The following recommendations are recommended for future research and the formulation of new fender design guidelines:

1. It is recommended to take into account the favourable effects of multiple fender contact and relatively low berthing angles in the design guidelines for

the fender system in order to create a more cost-effective fender design. PIANC should develop design guidance for parallel berthing as it is still lacking in the existing guidelines.

2. Although PIANC WG145 has collected many data, the available amount of berthing operation records is still limited. Consequently, it is recommended to collect new data to confirm correlations between berthing velocity and other design variables.

3. PIANC WG211 should take the effect of negative dependence between the load variables into fender design consideration as it could significantly reduce the required fender size. For instance, we could apply a correction factor to the characteristic kinetic energy in order to account for the effect of the dependence. However, since the dependence between the variables depends heavily on the local port conditions, it is not easy to formulate a value that could be used for general practice. In fact, consideration of negative dependence between load variables may lead to an inadequate fender design if incorporated without proper justification from site-specific data.

4. In order to improve the results of the reliability-based assessment, it is recommended to perform the Second-Order Reliability Method (SORM) to assess the reliability of the fender system. This is because results of FORM might not be accurate when the limit-state function is strongly non-linear, and when the dependency between variables is non-linear.

5. Finally, it is recommended to improve the multiple fender contact simulation which was used in this thesis. For future research, more variables could be incorporated into the simulation model (e.g. fender pitch, fender size) in order to gain more insight into what factors determine the contribution of multiple fender contact.

BIBLIOGRAPHY

Bedford, T. and Cooke, R. (2001). *Probabilistic Risk Analysis: Foundations and Methods*. Cambridge, Cambridge.

Brolsma, J., Hirs, J., and Langeveld, J. (1977). Paper of fender design and berthing velocities. *PIANC World Congress*.

Coastal Development Institute of Technology, . (2019). *Guidelines for Design and Testing of Rubber Fender System*. Japan.

Cooke, R. (1997). Markov and entropy properties of tree- and vine-dependent variables. *American Statistical Association - Proceedings of the Section on Bayesian Statistical Science*.

Genest, C. and Favre, A.-C. (2007). Everything you always wanted to know about copula modeling but were afraid to ask. *Journal of Hydrologic Engineering (ASCE)*.

Gräler, B., van den Berg, M. J., Vandenberghe, S., Petroselli, A., Grimaldi, S., De Baets, B., and Verhoest, N. E. C. (2013). Multivariate return periods in hydrology: a critical and practical review focusing on synthetic design hydrograph estimation. *Hydrology and Earth System Sciences*.

Hein, C. (2014). Berthing velocity of large container ships. *PIANC World Congress*.

Iversen, R, P., W, Bruin, P., B, Phan, P., and J, Pyun, S. (2019). A proposed rational approach to design of fenders and supporting structures in the united states. *LRFD*.

Jiang, C., Han, X., Zhang, W., and Ni, B. (2015). A vine-copula-based reliability analysis method for structures with multidimensional correlation. *Journal in Mechanical Design*.

Jianping, L., Dengsheng, W., Xioqian, Z., and Young, S. (2015). On the aggregation of credit, market and operational risks. *Review of Quantitative Finance and Accounting*.

Jonkman, S., Steenbergen, R., Morales-Napoles, O., Vrijling, J., and Vrouwenvelder, A. (2017). *Probabilistic Design: Risk and Reliability Analysis in Civil Engineering*. Department of Hydraulic Engineering, Faculty of Civil Engineering and Geosciences, TU Delft, Delft.

Kiureghian, A. D. (2005). First- and second-order reliability methods. In Nikolaidis, E., M. Ghiocel, D., and Singhal, S., editors, *Engineering Design Reliability handbook*, chapter 14. CRC Press.

Kooij, L. V. D. (2020). Extreme value analysis if complex wave systems. Master's thesis, Delft University of Technology, Delft.

Kurowicka, D. and Cooke, R. (2006). *Uncertainty Analysis with High Dimensional Dependence Modelling*. Wiley Series in Probability and Statistics, Delft.

Lebrun, R. and Dutfoy, A. (2009). Do rosenblatt and nataf isoprobabilistic transformations really differ? *Probabilistic Engineering Mechanics*.

Lemaire, M. (2005). *Structural Reliability*. John Wiley & Sons, Inc., London.

Miller, I. (2020). Mortgages in the netherlands. https://www.expatica.com/nl/housing/buying/your-guide-to-dutch-mortgages-101837/. Accessed: 2020-06-10.

Moss, R. E. S. (2020). *Applied Civil Engineering Risk Analysis 2nd ed*. Springer, Cham, Switzerland.

PIANC (2002). *Guidelines for the design of fender system:2002*.

Roubos, A., Groenewegen, L., and Peters, D. J. (2016). Berthing velocity of large seagoing vessels in port of rotterdam. *Marine Structures*, 51:202–219.

Roubos, A., Groenewegen, L., Peters, D. J., and Steenbergen, R. (2018). Partial safety factors for berthing velocity and loads on matrine structures. *Marine Structures*, 58:73–91.

Roubos, A., Schweckendiek, T., Brinkgreve, R., Steenbergen, R. D. J. M., and Jonkman, S. (2019). Finite element-based reliability assessment of quay walls. *Georisk:Assessment and Management of Risk for Engineered Systems and Geohazards*.

Shibata (2017). *Fender Design Manual*.

Trelleborg (2018). *Fender Application Design Manual*.

Ueda, S., Nagao, T., and Okada, T. (2003). Study on reliability-base design method for fenders based on form. *Proc. of Annual Journal of Civil Engineering in the Ocean, JSCE*.

Valls, S. S. (2019). A vine-based approach for defining critical infrastructure loads. Master's thesis, Delft University of Technology, Delft.

Versteegt, G. (2013). Berthing loads in structural design (validation of partial factor. Master thesis, Delft University of Technology.

Vrijburcht, A. (1991). *Loads on fender structures and dolphins by sailing ships*. Rijkswaterstaat, the Hague.

WG145, P. (2020). Berthing velocity analysis of seagoing vessels over 30,000 dwt. Technical report, PIANC.

Yamase, S., Ueda, S., and Okada, T. (2010). Reliability design of fender system for berthing ships. *PIANC MMX Congress Liverpool UK*.

A VINE COPULA GOODNESS-OF-FIT

A.1 SEMI-CORRELATION

The semi-correlation analysis was performed to see how well the selected copulas fit the empirical copula in a specific quadrant of interest. Figure A.1 shows that there is a strong dependence between displacement and berthing velocity in the north-west quadrant, indicating that small vessels have a strong tendency to have higher berthing velocities. One could also see from the figure that the Gumbel rotated copula can adequately model this dependence structure.

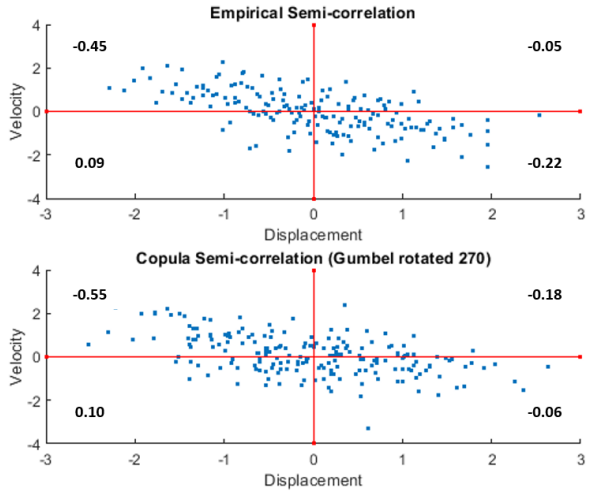

Figure A.1: Semi-Correlation plot between Displacement and Velocity

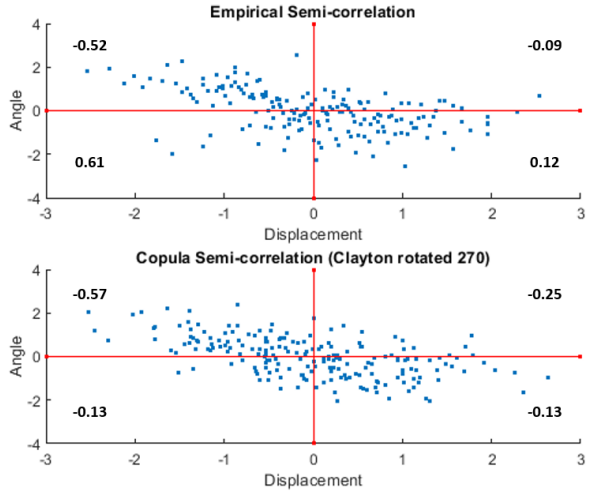

Figure A.2: Semi-Correlation plot between Displacement and Angle

The dependence between displacement and berthing angle has a similar structure to that of displacement and berthing velocity. As can be seen in Figure A.2, displace-

ment and berthing angle seems to show a relatively strong negative correlation in the north-west quadrant. Moreover, the figure shows that the Clayton copula fits the empirical copula sufficiently well in the north-west quadrant.

Figure A.3 compares the semi-correlation plot of the empirical and theoretical copula for berthing angle and berthing velocity. An apparent positive correlation is observed in the north-east quadrant. Although it describes the data well, Frank copula over-estimates the correlation in the north-east quadrant. In general, the selected theoretical copula seems to be sufficiently accurate to model the dependency structures.

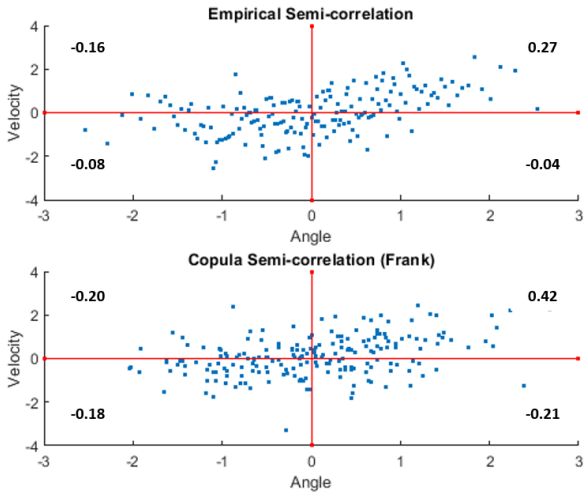

Figure A.3: Semi-Correlation plot between Angle and Velocity

A.2 CRAMER-VON MISES

Besides the semi-correlation, the Cramer-von Mises statistic was also performed to see how similar the cumulative density of the theoretical copula compared to the empirical copula. The result is shown in Table A.1. It is found that in general, the selected Vine copula structure has a small difference with the empirical copula. However, a substantial difference is found between the empirical and theoretical copulas that describe the dependence between berthing velocity and berthing angle. This is probably caused by the use of conditional distribution, since in Vine copula the joint cumulative distribution between berthing velocity and angle is conditional to the displacement.

Table A.1: Cramer-von Mises of Vine Copula

Variables	Copula	CvM
Displacement-Angle	Clayton 270°	68.16
Velocity-Displacement	Gumbel 270°	48.38
Velocity-Angle| Displacement	Frank	408.55

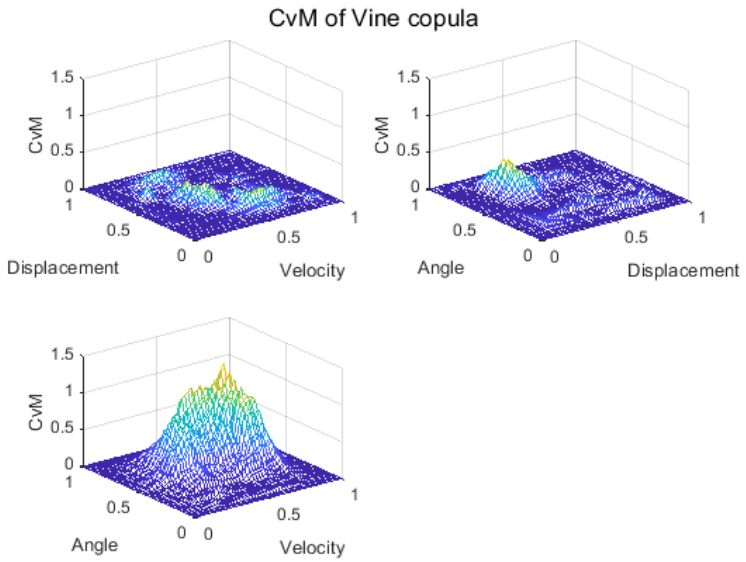

Figure A.4: Cramer-von Mises for Vine Copula

A.3 PLOT OF SIMULATED RANDOM VARIABLES

Another way to evaluate our copula model's quality is by plotting the empirical copula together with the theoretical copula, as shown in Figure A.5. It could be observed visually that the simulated data sufficiently fits the empirical data.

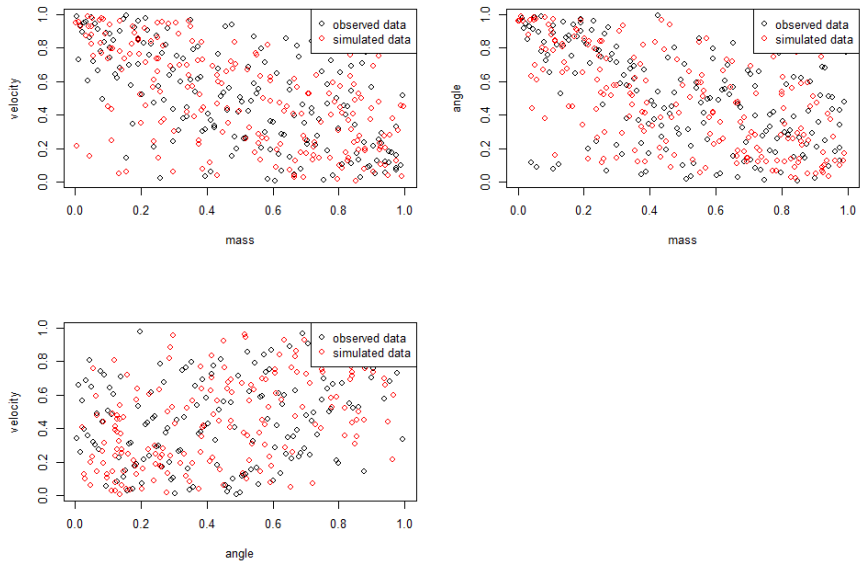

Figure A.5: Simulated copula plotted with the empirical copula

The Vine-Copula simulated random variables in the original space is going to be used for Monte Carlo analysis and thus, it is important to compare the simulated values with the empirical data. The value could be obtained by applying inverse of the marginal cumulative distribution function for each variable to the standard uniform value which is generated from the Copula. The result are shown in Figure A.6.

For comparison, the randomly generated variables in case of independence are shown in Figure A.7. It could be seen then that the samples generated from the Vine

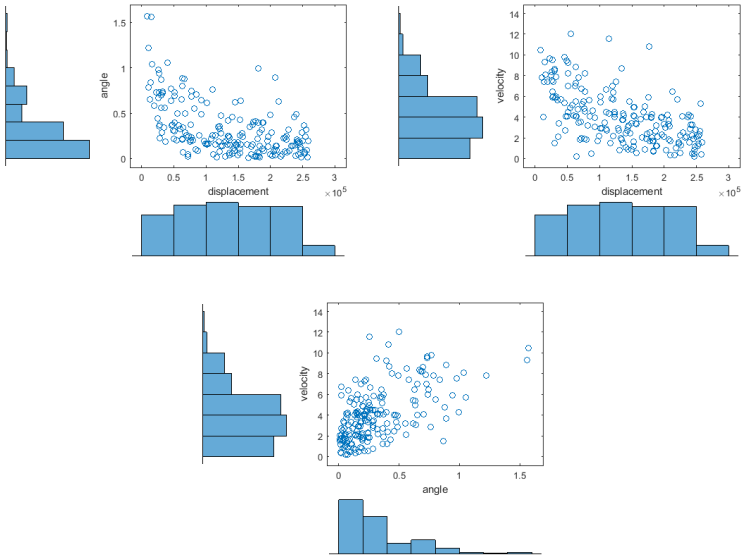

Figure A.6: The simulated dependent random variables

copula shown in Figure A.6 is much more similar to the observed data in Figure 4.7. Hence, it is crucial to incorporate the variables' dependencies into the reliability calculation to have a realistic estimate of the probability of failure. However, there will be some differences in our simulated data compared to the original one since we assume the displacement has uniform distribution while it is not.

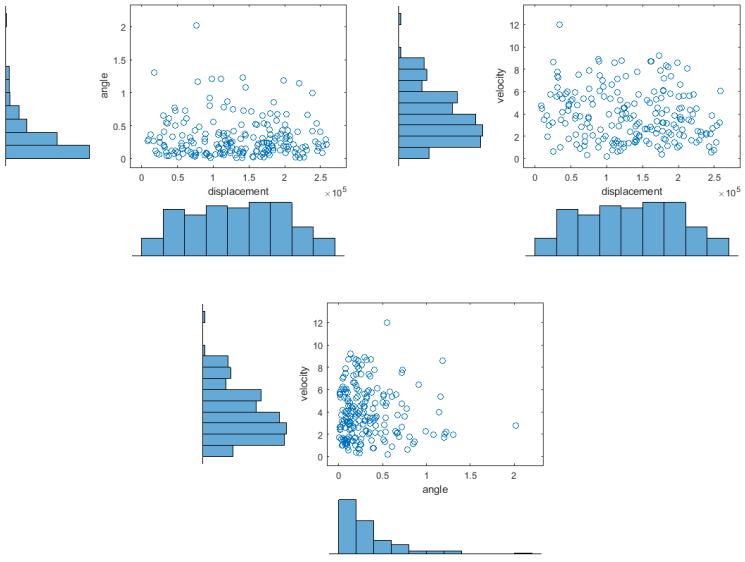

Figure A.7: The simulated independent random variables

B DESIGN AND CHARACTERISTIC VALUES OF THE PARAMETERS

This appendix gives the design values used for computing partial safety factors in Chapter 5.

Table B.1: Design values of the parameters for β=4.75

Parameters	Unit	Design values for β=4.75			
		Single-Independent	Single-Dependent	Multiple-Independent	Multiple-Dependent
E_{cv}	kNm	3430	1820	975	428
Velocity	cm/s	19.52	14.55	18.31	13.43
Displacement	ton	241,625	229,132	237,488	210,729
Angle	deg	0.24	0.20	0.91	0.71
MF	-	1.00	0.99	0.99	0.99
Temperature	^{o}C	15.06	15.41	15.42	15.36
C_m	-	1.74	1.75	1.74	1.76
C_e	-	0.46	0.46	0.46	0.46
TF	-	1.00	1.00	1.00	1.00
VF	-	1.07	1.08	1.09	1.07
$n_{multiple}$	-	1.00	1.00	2.99	3.35
E_k	kNm	3669	1935	3171	1521
E_{Fender}	kNm	1.07 E_{cv}	1.07 E_{cv}	3.22 E_{cv}	3.55 E_{cv}

Table B.2: Design values of the parameters for β=5.15

Parameters	Unit	Design values for β=5.15			
		Single-Independent	Single-Dependent	Multiple-Independent	Multiple-Dependent
E_{cv}	kNm	4080	2175	1195	530
Velocity	cm/s	21.25	15.80	20.00	14.57
Displacement	ton	243,787	232,986	240,060	217,519
Angle	deg	0.24	0.19	0.94	0.74
MF	-	1.00	0.99	0.99	0.99
Temperature	^{o}C	15.05	15.48	15.48	15.41
C_m	-	1.74	1.75	1.74	1.75
C_e	-	0.46	0.46	0.46	0.46
TF	-	1.00	1.00	1.00	1.00
VF	-	1.08	1.08	1.09	1.08
$n_{multiple}$	-	1.00	1.00	2.96	3.27
E_k	kNm	4382	2319	3822	1845
E_{Fender}	kNm	1.07 E_{cv}	1.07 E_{cv}	3.19 E_{cv}	3.48 E_{cv}

Table B.3: Design values of the parameters for β=5.32

Parameters	Unit	Design values for β=5.32			
		Single-Independent	Single-Dependent	Multiple-Independent	Multiple-Dependent
E_{cv}	kNm	4365	2330	1290	580

Table B.3 continued from previous page

Parameters	Unit	Design values for β=5.32			
		Single-Independent	Single-Dependent	Multiple-Independent	Multiple-Dependent
Velocity	cm/s	21.96	16.32	20.72	15.1
Displacement	ton	244,568	234,356	241,016	220,147
Angle	deg	0.24	0.19	0.96	0.75
MF	-	1.00	0.99	0.99	0.99
Temperature	^{o}C	15.05	15.50	15.52	15.44
C_m	-	1.74	1.75	1.74	1.75
C_e	-	0.46	0.46	0.46	0.46
TF	-	1.00	1.00	1.00	1.00
VF	-	1.08	1.08	1.10	1.08
$n_{multiple}$	-	1.00	1.00	2.95	3.24
E_k	kNm	4698	2488	4114	2005
E_{Fender}	kNm	1.07 E_{cv}	1.07 E_{cv}	3.19 E_{cv}	3.45 E_{cv}

Table B.4: Design values of the parameters for β=5.57

Parameters	Unit	Design values for β=5.57			
		Single-Independent	Single-Dependent	Multiple-Independent	Multiple-Dependent
E_{cv}	kNm	4840	2580	1447	655
Velocity	cm/s	23.10	17.11	21.85	15.86
Displacement	ton	245,700	236,269	242,383	223,476
Angle	deg	0.24	0.19	0.97	0.77
MF	-	1.00	0.99	0.99	0.99
Temperature	^{o}C	15.05	15.54	15.56	15.48
C_m	-	1.74	1.74	1.74	1.75
C_e	-	0.46	0.46	0.46	0.46
TF	-	1.00	1.00	1.00	1.00
VF	-	1.08	1.08	1.10	1.08
$n_{multiple}$	-	1.00	1.00	2.94	3.21
E_k	kNm	5214	2756	4600	2242
E_{Fender}	kNm	1.08 E_{cv}	1.07 E_{cv}	3.18 E_{cv}	3.42 E_{cv}

Table B.5: Characteristic values of the parameters

Parameters	Unit	Characteristic Values	
		Single Fender Contact	Multiple Fender Contact
Velocity	cm/s	15.44	
Displacement	ton	260,000	
Angle	deg	0.91	
MF	-	1	
Temp	^{o}C	15	
C_m	-	1.73	
C_e	-	0.46	
TF	-	1.00	
VF	-	1.08	
$n_{multiple}$	-	1.00	3.06
E_k	kNm	2460.92	
E_{Fender}	kNm	1.08 E_{cv}	3.30 E_{cv}

C FIND DESIGN POINTS FOR DEPENDENT CASE

Using the example of single fender dependent case class A, where it is given that:

- $\alpha_{velocity}$ = 0.7
- $\alpha_{displacement}$ = 0.71
- β_t = 4.75
- Velocity distribution = Weibull (4.38, 1.7)
- Displacement distribution = Uniform (8000, 260000)
- Bivariate Copula of velocity and displacement is Rotated Gumbel (270^o) with parameter 1.69.

The design values in the original space for the velocity (x1) and displacement (x2) are going to be calculated. The steps are given below:

1. $F_1(x_1) = \phi(\alpha_{velocity} * \beta_t) = \phi(0.7 * 4.75) \longrightarrow 0.999547$
2. $x_1 = F_1^{-1}(F_1(x_1)) = (4.38*(-\log(1-0.999547))^{\frac{1}{1.7}} \longrightarrow 14.64$ cm/s
3. $F_{2|1}(x_2|x_1) = \phi(\alpha_{displacement} * \beta_t) = \phi(0.71 * 4.75) \longrightarrow 0.999618$
4. Solve the inverse h-function below for $F_2(x_2)$:
   $F_{2|1}(x_2|x_1) = exp(-((-ln(1-F_1(x_1))^{1.69}) + (-ln(F_2(x_2))^{1.69}))^{1/1.69}) \frac{1}{(F_2(x_2))} (-log(F_2(x_2)))^{1.69-1} ((-log(1-F_1(x_1))^{1.69}) + (-log(F_2(x_2))^{1.69}))^{1/1.69-1} \longrightarrow F_2(x_2) = 0.8725$
5. $x_2 = F_2^{-1}(F_2(x_2)) = 0.8725*(260000-8000)+8000 = 227864$ ton

It is thus found that the design points for the velocity and displacement are 14.64 cm/s and 227864 ton respectively. Using the same method, the design point for berthing angle could also be computed.

D STANDARD DIMENSIONS OF CONTAINER VESSELS

The table below shows the standard dimension of container vessels published by PIANC WG121. The dimensions were used in this thesis for the multiple fender contact simulation and also to determine the eccentricity and additional mass factors.

Table D.1: Standard dimensions of the container vessels, the actual dimensions may vary up to 10% depending on construction and country of origin (Source: PIANC WG121 document)

Type	DWT (ton)	Displacement (ton)	LOA (m)	LPP (m)	B (m)	Draft (m)	C_B	Approximate Capacity (TEU)
Container Ships (Post-Panamax) TEU	245,000	340,000	470	446	60	18	0.69	22,000
	200,000	260,000	400	385	59	16.5	0.68	18,000
	195,000	250,000	418	395	56.4	16	0.68	14,500
	165,000	215,000	398	376	56.4	15	0.66	12,200
	125,000	174,000	370	351	45.8	15	0.7	10,000
	120,000	158,000	352	335	45.6	14.8	0.68	9,000
	110,000	145,000	340	323	43.2	14.5	0.7	8,000
	100,000	140,000	326	310	42.8	14.5	0.71	7,500
	90,000	126,000	313	298	42.8	14.5	0.66	7,000
	80,000	112,000	300	284	40.3	14.5	0.66	6,500
	70,000	100,000	280	266	41.8	13.8	0.64	6,000
	65,000	92,000	274	260	41.2	13.5	0.62	5,600
	60,000	84,000	268	255	39.8	13.2	0.61	5,200
	55,000	76,500	261	248	38.3	12.8	0.61	4,800
Container Ships (Panamax) TEU	60,000	83,000	290	275	32.2	13.2	0.69	5,000
	55,000	75,500	278	264	32.2	12.8	0.68	4,500
	50,000	68,000	267	253	32.2	12.5	0.65	4,000
	45,000	61,000	255	242	32.2	12.2	0.63	3,500
	40,000	54,000	237	225	32.2	11.7	0.62	3,000
	35,000	47,500	222	211	32.2	11.1	0.61	2,600
	30,000	40,500	210	200	30	10.7	0.62	2,200
	25,000	33,500	195	185	28.5	10.1	0.61	1,800
	20,000	27,000	174	165	26.2	9.2	0.66	1,500
	15,000	20,000	152	144	23.7	8.5	0.67	1,100
	10,000	13,500	130	124	21.2	7.3	0.69	750

E | CODES

The R-codes which were used to perform FORM reliability analysis and also the MATLAB code for the multiple fender contact simulation could be found in:
https://github.com/FelixOrlin/R-Code–FORM-

COLOPHON

This document was typeset using LaTeX. The document layout was generated using the arsclassica package by Lorenzo Pantieri, which is an adaption of the original classicthesis package from André Miede.


SRI LANKA PORTS AUTHORITY
CONTAINER CRANE J-13
HYUNDAI
MITSUI - PACECO
EVERGREEN

TU Delft